



**THÈSE DE DOCTORAT**  
**DE L'UNIVERSITÉ PSL**

Préparée à l'Observatoire de Paris

**Analytical representation for ephemeris  
with short time span:  
Application to the longitude of Titan**

Soutenue par  
**XiaoJin XI**  
Le 17 12 2018

Ecole doctorale n° 127  
**Astronomie et astrophysique  
d'Île-de-France**

Spécialité  
**Astronomie et Astrophysique**

Composition du jury :

Jean, SCOUCHAY Observatoire de Paris	<i>Président</i>
Anne, LEMAITRE Université de Namur	<i>Rapporteur</i>
Yan Ning, FU Observatoire de la Montagne Pourpre, CAS	<i>Rapporteur</i>
Qing Yu, PENG JI-NAN Université	<i>Examineur</i>
Alain, VIENNE Observatoire de Paris	<i>Directeur de thèse</i>
RongChuan, QIAO National Time Service Centre, CAS	<i>Directeur de thèse</i>



Analytical representation for ephemeris with short  
time span:  
Application to the longitude of Titan

XIAOJIN XI



For my parents



# Remerciements

Traditionnellement, pour une thèse rédigée en anglais, les remerciements doivent être aussi rédigés en anglais. Néanmoins, je voudrais adresser mes remerciements en français, comme la plupart des personnes qui m'ont offert tant de chaleur et tant d'aide ne parlent que français. Ce n'est peut-être pas très facile pour quelques-uns d'entre eux de comprendre ce que j'ai fait pendant ma thèse. Mais j'espère vraiment de leur exprimer mes remerciements les plus sincères du fond de mon cœur.

Il y a tant de personnes qui m'ont soutenue et encouragée que je ne peut-être arrive pas à énumérer leur nom un par un.

Merci beaucoup à Madame BALLENGHIEN pour votre gentillesse, qui me fait sentir comme entourée de la famille malgré la grande distance entre mon pays natal et moi.

Je voudrais aussi remercier Mademoiselle Delphine THOMASSON, maintenant Dr. THOMASSON, qui m'a tout expliqué (comme les documents, les messages, les emails...) en des milliers d'occasions. C'est probablement l'aide la plus efficace pour une étrangère.

Je tiens à remercier vivement à Madame Anne LEMAITRE, qui m'a donné beaucoup de conseils et de suggestions sur la rédaction de mon manuscrit.

Je remercie les dames et les messieurs à l'Association Jonckheere et tous mes collègues à l'Observatoire de Lille et à IMCCE.

Je remercie également tous mes amis. Merci à Yuan-Yuan YAN, Wei WANG, Yang HANG, Mei-Zi WANG, Yu-Fei CHEN, Shan-na LI.

Enfin, je voudrais exprimer mes plus grands remerciements et ma sincère reconnaissance à mon directeur, Monsieur Alain VIENNE, qui est patient, sympathique, gentil et sage. Il est le meilleur mentor que l'on pourrait rêver de rencontrer. Merci beaucoup de tout de son guidance et de son énergie consacrée pendant les quatre années. Bien que mon travail soit comme une faible étincelle, toute la brillance lui appartient.





# Abstract

The ephemerides resulting from numerical integration, which are convenient to download from online service of IMCCE or Horizons of the JPL, have a very good precision on the fitting to recent observations. Meanwhile, analytical ephemerides like TASS describe in detail the dynamical system by a representation based on a combination of the proper frequencies.

We plan to use these two types of ephemerides in order to study the rotation of the natural satellites. It requires to rebuild a long-lasting and high precision ephemeris with proper frequencies based on the numerical integration ephemeris. The main difficulty is to avoid the shortcoming of the limited interval of the numerical ephemeris.

In our work, we use the representation of the orbital elements of Titan from the TASS ephemeris analyzed over 10,000 years as a reference example. We experiment to obtain the proper frequencies with the TASS ephemeris over 1,000 years only, and then to get the analytical representation of the mean longitude of Titan in this limited interval. Due to this 1000 years time span, we use the least squares method instead of the frequency analysis, especially for the long period terms.

The efficiency and exactness of the whole method are verified by comparing TASS representation of the mean longitude of Titan obtained by the least squares method with the 10,000 years reference example.

Finally and most importantly, we get the representation of the mean longitude of Titan from JPL ephemeris over 1,000 years. Between the solution of JPL and the representation of TASS, it exists a 60 km difference in the amplitude of the major component. This difference is considered as a system difference. The limited interval of the ephemeris modifies the proper frequencies, which leads to the error in the long period terms such as the one from the node of Titan. For almost all other components, their amplitudes and phases are similar to the relative terms from TASS. The error in our representation is less than 100 kilometers over 1,000 years and the standard deviation is about 26 kilometers.



# Contents

<b>1</b>	<b>Introduction and aims</b>	<b>9</b>
1.1	Context and aims . . . . .	10
1.2	Notations . . . . .	12
1.3	The manuscript . . . . .	14
<b>2</b>	<b>Ephemeris</b>	<b>17</b>
2.1	The different kinds of ephemerides . . . . .	18
2.1.1	Numerical integrations . . . . .	18
2.1.2	Analytical theories . . . . .	18
2.1.3	Synthetic representations . . . . .	19
2.2	Numerical ephemerides . . . . .	19
2.2.1	Generalities (Lainey et al. 2014) . . . . .	19
2.2.2	Ephemeris from JPL and NOE . . . . .	21
2.3	The ephemeris TASS . . . . .	23
2.3.1	The theory . . . . .	23
2.3.2	Representation of TASS . . . . .	25
2.4	Use of theses ephemerides . . . . .	27
<b>3</b>	<b>Frequencies and synthetic representation of motion</b>	<b>29</b>
3.1	Integrable system, quasi-periodics series and proper frequencies	30
3.2	The D'Alembert rule . . . . .	31
3.3	FA: the frequency analysis . . . . .	35
<b>4</b>	<b>Context and difficulties of the realization</b>	<b>41</b>
4.1	Comparison in positions and elements between TASS and JPL ephemerides . . . . .	42
4.1.1	Comparison in positions . . . . .	42
4.1.2	Comparison in elements . . . . .	45
4.2	The main slope in mean longitude : $N$ and $\lambda_0$ . . . . .	50
4.3	Comparison in $r$ between TASS and JPL . . . . .	52
4.3.1	The periodic part $r = \lambda - Nt - \lambda_0$ . . . . .	52
4.3.2	The comparison . . . . .	54
4.4	Correlation of $\lambda_0$ with the time span . . . . .	56

4.4.1	$\lambda_0$ of TASS . . . . .	56
4.4.2	$\lambda_0$ of JPL . . . . .	57
4.5	Conclusion . . . . .	59
<b>5</b>	<b>Extension of the frequency analysis by the least squares method</b>	<b>61</b>
5.1	The least squares method, term by term . . . . .	62
5.2	Reference plane and transformation error . . . . .	64
5.3	The least squares method for several terms . . . . .	67
<b>6</b>	<b>Test of the method with TASS over 1,000 years</b>	<b>71</b>
6.1	Proper frequencies . . . . .	71
6.2	Determination of the short period and semi-long period terms	78
6.3	Determination of the long period terms . . . . .	80
6.4	Conclusion . . . . .	84
<b>7</b>	<b>Results for the mean longitude of Titan</b>	<b>85</b>
7.1	Proper frequencies in the JPL ephemeris . . . . .	85
7.2	Determination of the short period and semi-long period terms	92
7.3	Determination of the long period terms . . . . .	94
7.4	Conclusion . . . . .	99
<b>8</b>	<b>Digitization and reduction of old astronomical plates of natural satellites</b>	<b>101</b>
8.1	Background . . . . .	101
8.2	Plates . . . . .	102
8.3	Digitization . . . . .	102
8.3.1	Scanner . . . . .	102
8.4	Reduction . . . . .	105
8.5	New observed satellite astrometric positions . . . . .	107
8.6	Comparison with theory . . . . .	107
8.7	Conclusion . . . . .	109
<b>9</b>	<b>Conclusion</b>	<b>111</b>
<b>10</b>	<b>Appendix</b>	<b>113</b>
10.1	Appendix 1 . . . . .	113

# Chapter 1

## Introduction and aims

The discovery of the Saturn system by humans has never stopped. Ancient Chinese selected 28 groups of stars near the equator, which were called the Twenty-eight mansions, as relative markers for measuring the positions of the Sun, the Moon, and the five major planets in the Solar System (Mercury, Venus, Mars, Jupiter, and Saturn). The first record of the twenty-eight lunar mansions in China was found in the tomb of Marquis Yi of ZENG. The tomb is considered to be built around 443 BC. The Saturnian orbital period is about 29.657 years, making Saturn enter a new constellation every year. In ancient China, Saturn was a star that represented the regular pattern and morality, further extended as a sign for the stability of kingdom.

In 1610, Galileo turned his telescope towards the planet Saturn to observe its beautiful “ears”, which were finally identified as planetary rings about 50 years later, and he was confused about the disappearance and re-appearance of the mysterious “ears”. Since then, the Saturn system has interested us so much, not only for the planet itself but also for its rings and its complex satellite system. Titan was found in 1655 by Huygens, as the largest satellite. Subsequently, Cassini discovered Iapetus (1671), Rhea (1672), Dione and Tethys (1684). Almost one century later, in 1789, W.Herschel discovered Mimas and Enceladus. Untill 1848, when Bond and Lassell found Hyperion, humans had found all the eight principal satellites. In the increasing order of their distances to Saturn, they are:

(1) Mimas, (2) Enceladus, (3) Tethys, (4) Dione, (5) Rhea, (6) Titan, (7) Hyperion, (8) Iapetus

The dynamics of these eight satellites is characterized by several mean motion resonance relations:

- resonance 2 : 4 between Mimas and Tethys
- resonance 1 : 2 between Enceladus and Dione
- resonance 3 : 4 between Titan and Hyperion

For example, while Dione turns once around Saturn, Enceladus makes two revolutions.

These resonances behave as faint gravitational perturbations among the satellites. The consequences are oscillations of the conjunction between each pair of satellites around a reference direction. Furthermore, this direction slowly precesses because of the oblateness of Saturn.

The Saturnian System also includes some other small satellites, associated with numerous mutual phenomena. However, they are not the focus of this thesis. In our work, we paid all our attention to the dynamics of the 8 major satellites.

## 1.1 Context and aims

It is convenient to download ephemerides from the on line service of IMCCE [1] or Horizons of JPL [2]. Such kind of ephemeris, based on the recent observations, has very good precision. For example, the precision of NOE (Numerical Orbits and Ephemerides) from IMCCE (Lainey.V et al. 2004a [3] and Lainey.V et al. 2004b [4]) of the 5 major satellites in the Saturn system is about 10km during 1990-2017. The situation of Titan, Hyperion and Iapetus, is a bit different. Their precision is about 100km. Hyperion and Iapetus are influenced by the lack of observations from Cassini and the difficulty to determine the mass center of the object. For Titan, we can not reach a precision as good as for the others, since there is no observation data from Cassini, and the flyby data of Radio-Science [5] has not been used in the calculations.

Meanwhile, there is another sort of ephemeris, the analytical theories of motion, like TASS (Theorie Analytique des Satellites de Saturne) (Vienne.A and Duriez.L 1995 [6]). We made use of TASS version 1.7 in our calculations, for the positions and velocities of the satellites Rhea, Titan, and Iapetus referred to the center of Saturn of the mean ecliptic and mean equinox at J2000.0 epoch (with a precision of 100km over the recent 100 years). Based on an analytical description of the system and a numerical integration method, TASS shows the details of the system motion in a representation using the proper frequencies. It has benefited us to study the influences between the different satellites in the Saturn system. However, TASS also has its shortcoming. It is not as good as NOE and JPL in precision.

In our work, we propose to find a method with both advantages: a good precision and a representation with the proper frequencies. Such method will be tremendous usefulness, for example, in the study of the rotation of Titan and other satellites.

In these studies of the rotation, great attention is given in the representation of the true longitude. Table 1.1 comes from a study of the librational response of a deformed 3-layer Titan perturbed by non-Keplerian orbit and atmospheric couplings. (Richard.A et al., 2014 [7]). Since it is the result of Andy Richard, we keep the original expressions even if it has different units,

Table 1.1: Representation of the difference between the true longitude and the true anomaly of Titan from Richard.A (Richard.A et al. 2014 [7]). We keep the notation of the original publication even though the identification does not use the proper arguments.

Freq. rad/day	Periods days	Magnitude "	Phase degree	Identification
0.394018	15.9464	11899.3237	163.3693	$\lambda_6 - \varpi_6$
0.788036	7.9732	212.5868	-32.7941	$2\lambda_6 - 2\varpi_6$
0.394081	15.9439	56.6941	-68.1211	$\lambda_6 - 2\varpi_8 + 2\Omega_6$
0.001169	5376.6331	43.7313	-66.0428	$2\lambda_s$
0.00584	10750.3648	37.5508	138.4821	$\lambda_s$
0.392897	15.9919	31.5673	10.8789	$\lambda_6 + \Omega_6 - \lambda_s$
0.001753	3583.9304	5.6147	250.1412	$3\lambda_s$
0.009810	640.4892	1.4983	-77.2905	-

marks and abbreviations of physical quantities. Furthermore the identification does not use the proper arguments<sup>I</sup>.

In this Table, the notations for the fundamental frequencies  $\omega_j^*$  are :

$\Omega$  longitude of the ascending node

$\varpi$  longitude of the perihelion

$\lambda$  mean longitude

The subscript 6 is for Titan and  $s$  means the Sun (motion around Saturn). The Table has to be read as :

$$\nu - M - \phi_0 = \sum_{i=1}^n A_i \sin(\omega_i t + \phi_i) \quad (1.1.1)$$

where  $\omega_i$ ,  $A_i$  and  $\phi_i$  are respectively the first, the third and the fourth column.

The last column gives the identification of the frequency  $\omega_i$  as an integer combination of the  $m$  fundamental frequencies  $\omega_j^*$  of the system.

$$\omega_i = \sum_{j=1}^m k_{i,j} \omega_j^* \quad (1.1.2)$$

Table 1.1 describes the simple representation of the difference between the true longitude  $\nu_6$  and the mean anomaly  $M_6$  of Titan in JPL ephemeris, in which  $\phi_0$  is the initial value of the satellite rotation angle measured from the line of the ascending node,  $A_i$  is the magnitude of every component,  $k_i$  is a constant parameter in the combination,  $\omega_i$  is the frequency of every component, and  $\phi_i$  is its phase.

<sup>I</sup>See Chapter 3 for a correct definition of the fundamental frequencies

In Table 1.1, the influence of the mean longitude of the Sun is obviously found as  $L_S, 2L_S, 3L_S$ , which come from the true longitude of Titan  $\nu_6$ , instead of the components of the mean anomaly  $M$ . Therefore, it is not the best method to study the rotation by the difference between the true longitude and the mean anomaly. In contrast to the expression above, we will see in Table 3.1 a representation of the difference between the true longitude and the mean longitude. The advantage of our representation is to reduce the major influences outside the Saturn system and to remove the most obvious terms with large amplitudes.

Meanwhile, in Table 1.1, there are some incorrect identifications, such as the one of the frequency value 0.394081 rad/day, which is identified as  $L_6 - 2\varpi_8 + 2\Omega_6$ . It is unfitted to the D'Alembert rule<sup>II</sup>. The reason for such problem, may not be a real mistake, but is probably the omission of some long-period proper frequencies. Besides, we can only find 5 other different frequencies in their result. However, it is still too far away from what we should obtain in our research. The problem of the above result comes from the limited time span (400 years) of JPL ephemeris used. It is impossible to get more details of the representation in such a short time span. Note also that R.M. Baland and collaborators ( R.M.Baland et al. 2014 [8]) mentioned the need for a formula for the mean longitude of Titan for their study of its rotation.

## 1.2 Notations

In my thesis,  $a, e, i, \Omega, \varpi$  and  $\lambda$  are marked as the classical elliptical osculating elements. They are referred to the center of Saturn. The horizontal plane is the equatorial plane of Saturn. The origin on this plane corresponds to the node with the mean ecliptic J2000.

We also note  $n$  the osculating mean motion :

$a$	semi-major axis
$e$	eccentricity
$i$	inclination
$\Omega$	longitude of the ascending node
$\varpi$	longitude of perihelion
$\lambda$	mean longitude
$n$	mean motion

It is also convenient to use  $p, q, z$  and  $\zeta$  :

---

<sup>II</sup>To fit the D'Alembert rule, we have to consider some elements of the Sun, which lead to a high degree in eccentricity and inclination.



$$\begin{aligned}
a &= A(1+p)^{-2/3} \iff n = N(1+p) \\
\lambda &= \int n dt + \epsilon = Nt - \sqrt{-1}q \\
z &= e \exp \sqrt{-1}\varpi \\
\zeta &= \sin \frac{i}{2} \exp \sqrt{-1}\Omega
\end{aligned} \tag{1.2.1}$$

where  $N$  is the mean mean motion in such way that  $q$  has no linear part in time (and only a quasi-periodic part).

The variable  $p$  is real,  $q$  is purely imaginary,  $z$  and  $\zeta$  are complex and their conjugates are noted as  $\bar{z}$  and  $\bar{\zeta}$ .  $A$  is deduced from  $N$  by the third law of Kepler:  $N^2 A^3 = n^2 a^3 = GM_s(1+m)$ , where  $G$  is the constant of gravitation,  $M_s$  is the mass of Saturn, and  $m$  is the mass of the considered satellite.

Each satellite is distinguished by a subscript increasing with the distance to Saturn (from 1 for Mimas to 8 for Iapetus). We take  $s$  for the Sun, and  $S$  in capital letter for Saturn. For example,  $\lambda_6$  is the mean longitude of Titan and  $\Omega_8$  is the longitude of the ascending node of Iapetus. In addition we have:

$M$	mean anomaly
$\nu$	true anomaly
$r$	$= \lambda - N \times t - \lambda_0$
$s$	the Sun
$S$	Saturn
$J$	Jupiter

Here, we also give several parameters of the Saturn system which are used in our calculations (both in JPL and TASS). We have:

$a_5 = 527068$ km	semi-major axis of Rhea
$a_6 = 1221870$ km	semi-major axis of Titan
$a_8 = 3560820$ km	semi-major axis of Iapetus
$e_6 = 0.0288$	eccentricity of Titan
$e_8 = 0.0293$	eccentricity of Iapetus
$i_6 = 0.306$ degree	inclination of Titan
$i_8 = 8.298$ degree	inclination of Iapetus

At last, very often in the manuscript, angles are referred in the ring plane. They are defined as:

$$\begin{aligned}
\Omega_a &= 169.5291^\circ \\
i_a &= 28.0512^\circ
\end{aligned}$$

### 1.3 The manuscript

The numerical integration ephemerides have very good precision fitting on the recent observations. Meanwhile, the analytical ephemerides, like TASS, describe the system motion in detail by a representation using the proper frequencies. We envision to make a connection between these two different kinds of ephemerides, then it will benefit us to study the rotation of the natural satellites with a high precision ephemeris and to have system characteristics like the proper frequencies. For this aim, we have to avoid the shortcoming of the limited interval of ephemeris of JPL.

First, we introduce the system characteristics of the theoretical ephemeris and the numerical ephemeris in Chapter 2. We have an understanding of these two sorts of ephemerides. For JPL, which is a numerical integration ephemeris fitted on the observations, the equations of motion can achieve such accurate description of the motion with all the known perturbations so that it has a very good precision in a limited period (1,000 years).

On the other hand, the analytic models make it possible to understand the details of the dynamics of the system, by explicitly taking the perturbations into account. In the case of the orbital motion, we can develop the perturbing function according to the osculating elements, in order to make use of the Lagrange equations or their equivalents in Hamiltonian form. Depending on the expansion of the osculating elements (list of amplitudes, frequencies, phases, etc.), the theoretical ephemeris is compatible with precision requirements. However, complex physical systems always seek to simplify the problem for an explicit solution that is more difficult to handle. Likewise, it can not have the same precision as the numerical integration method. We give a detailed explanation of both ephemerides in Chapter 2.

In Chapter 3, we discuss the frequencies and the synthetic representation of a motion. We need to explain the integrable Hamiltonian systems as the background of our work. Most of the equations in celestial mechanics can be written in Hamiltonian forms which only depend on the initial value of their coordinates and momenta. Hence, we can describe a Hamiltonian system based only on their initial conditions and its action-angle variables, whose the first derivatives of time are the proper frequencies. Moreover, from the research of J.Laskar, we can make an analysis of an approaching motion to get the proper frequencies of a more complicated system, like the Saturnian System. Our work is able to obtain the proper frequencies from a numerical ephemeris. Additionally, we talk about the principle of the method noted Frequency Analysis (or FA) which is used to discriminate the proper frequencies in our work.

Based on this understanding of the ephemerides and the proper frequencies, we can make a full comparison between JPL and TASS in Chapter 4. We take the ephemeris of Titan as an example. We compare their osculating elements, their velocities, and instantaneous positions to get a more intui-

tive understanding of the resemblances and the differences between them. In this part, we make also a calculation of the mean mean motion of Titan with each ephemeris in different time span. For TASS, their mean mean motion and phase can be obtained over 10,000 years and over 1,000 years. For JPL, we only have the mean mean motion and phase over 1,000 years. So we can give a preliminary conclusion that the short time span makes no influence on the mean mean motion. However, it influences their phase. Then, we have to make a choice, not only for TASS, but also for JPL. In our following work, we take the phase from 10,000-year TASS ephemeris for the following use (JPL and TASS over 1,000 years).

Chapter 5 specifically describes our method to get the proper frequencies and to get the representation by a least squares method with a limited interval. Moreover, we make an experiment on the ascending node of Iapetus, which has a period of more than 3,000 years so that it can not finish a first cycle after 1,000 years (time span for JPL). We get a rough amplitude and phase by using all the proper frequencies of TASS and the ephemeris of JPL. In this way, we prove that it is possible to obtain the proper frequency of the long-period motion, which is much longer than the time span of the JPL ephemeris.

In Chapter 6, we take the representation of the mean longitude of Titan of TASS over 10,000 years as a template. We experiment to obtain the proper frequencies involved in the mean longitude of Titan with 1,000 years TASS ephemeris by a frequency analysis. With these two series of proper frequencies, we are aware about the effects of a limited interval ephemeris on the proper frequency. Moreover, according to the accuracy of such proper frequency, we can make a choice of the values used in the least squares method to seek the representation of the mean longitude of Titan, and then, to verify the effectiveness and exactness of the least squares method in rebuilding the representation. Finally and most importantly, we obtained the representation of Titan with 1,000 years TASS ephemeris.

It is shown in Chapter 7, that we can repeat all our previous work with JPL ephemeris. We obtain the proper frequencies of JPL along with the representation of the mean longitude of Titan with 1,000 years JPL ephemeris. It is then possible to give the final table of the mean longitude of Titan with JPL ephemeris. We discuss the residuals and the precision of our representation. Once this method is completed and proven effective for Titan and other satellites of Saturn, it will be easy to apply it to other planetary systems.

In Chapter 8, I present a collaborative work with my colleagues in China during the preparation of my thesis. It concerns the digitalization of the old plates and new observations reduction using the GAIA catalog.



## Chapter 2

# Ephemeris

Often presented as a miniature planetary system, natural satellites systems present an important difference, the close relationship by the scale times of there evolution. Tidal perturbation is proved as the major mechanism in their longtime evolution, which makes the study of natural satellites systems privileged to better understand the exoplanetary systems. To characterize the best orbit, it is necessary to consider the mass and form in the calculations. This kind of system usually involves resonances in mean motion. Hence, the following researcher is required to develop analytic theory specific to the various system, to take into account the diverse orbital resonances.

Today, the numerical methods allow us to study all these systems with the same tool, thus enabling an exhaustive approach more efficient and rapid. The integration of the equation of motion is the main difficulty in the expansion of planetary satellites. Even if the recent gravitational fields of the giant planets are given with a high precision, it still remains a lack of understanding in temporal variation. Meanwhile, the presence of chaos, in some satellites, which are near to their planets, needs technique adaptations to predict their positions with a minimum of confidence.

In order to deal with these difficulties, on the borderline of our current physical knowledges, the development of a precise ephemeris of the natural satellites in the solar system needs a considerable upstream research works. These works benefit from the adapted numerical integration methods and the most diverse observations, from the ancient observations which were made at the end of 19th century, to the space observations. They were obtained by the most recent space probes such as Cassini and Mars Express.

In this chapter, we first present the numerical ephemerides (JPL and NOE) and then in the next sections, the analytic model (TASS) in an articulated way. We emphasize the form of the representation of TASS because our aim is to write the numerical ephemeris in a similar form.

## 2.1 The different kinds of ephemerides

### 2.1.1 Numerical integrations

We are very interested in a highly precise ephemeris; so its users can plan their observations, or the spacecraft flyby. A numerical integration of the equation of motion could achieve such an accurate description of the motion with all the known perturbations. On the other hand, the prediction of ephemeris could not keep its precision very long. For example, it can barely last any longer than a few hundred years. The loss of precision is due to the uncertainty in the initial conditions, the incompleteness of the model and the accumulation error from the numerical integration, which does not keep the system properties. The numerical integration also could be used in describing the general motion over a huge time scale, from a few thousand to billion years, only considering secular phenomena. In both situations, we could obtain the evolution of the system over time, without any information neither on the influence from different origins, nor on the dynamic characteristics of the trajectories.

### 2.1.2 Analytical theories

An analytic model aims to understand the details of the dynamics of the system, by explicitly taking into account the perturbations. In case of the orbital motion, we can develop the perturbing function according to the osculating elements, in order to use the Lagrange equations or their equivalent in Hamiltonian form. There are different methods to solve these equations: successive approximations, Lie series, and so on. Concretely, we obtain an expansion of the osculating elements in trigonometric series, that means an analytic expression depending on time for the evolution of the system (list of amplitudes, frequencies and phases). Such expansion leads to a large quantity of terms (a priori infinite), which inevitably leads to a truncation at a certain level of amplitude or frequency compatible with the required precision. In addition, in order to obtain an explicit solution, theoretical studies always want to simplify the complex physical systems. Therefore, the analytic theories, which are considered to be more complicated, are difficult to handle and need more work to achieve a same precision as the numerical integration method. In other words, it informs directly on the mechanisms of the dynamics, and then, it has a much wider scope: overall evolution well described over a very long time scales, preservation of the properties of the system, methods useful for other similar systems, etc  
...

### 2.1.3 Synthetic representations

A compromise exists for both methods above: it is possible to rewrite the numerical integration solution into the form of an analytics one. In fact, if the system is integrable, there are action-angle variables, in which the dynamics should become very simple, and these coordinates can be obtained from a frequency analysis (Laskar.J 1993 [9]). Thus, the frequency analysis of the "true" solution gives the amplitudes and frequencies in a numerical series equivalent to the analytical expansions. Therefore, the different perturbations can be identified (integer combinations of proper frequencies), and the obtained series are suitable for providing ephemeris. A more detailed discussion will be given in Chapter 3.

## 2.2 Numerical ephemerides

### 2.2.1 Generalities (Lainey et al. 2014)

Numerical methods are used to produce the ephemerides of natural satellites. They are very similar to those used in space geodesy for the artificial satellites and space probes. First, they are appropriate to make an exhaustive assessment (within the bound of our knowledge) of the dynamic perturbations, which disturb the motion of the satellites, for the given precision of observations (Lainey.V et al. 2004a [3] and Lainey.V et al. 2004b [4]).

It is essential to have a safety margin, which is more than one order of magnitude (ideally two), between the precision of the observations and the post-adjustment influence of the perturbations. Indeed, most of the perturbations only provide a secular deviation on the angular variables, which is easy to absorb with a minimal modification of the initial conditions.

The model is different from one system to another, but in general, the perturbations mentioned below should be considered

i) the N-body mutual perturbations; ii) the extended gravitational field of the planet, and satellites (when it is known); iii) the precession and the nutation of the central body; iv) the tidal effects between the planet and satellites; v) the post-Newtonian relativistic corrections.

Once the modeling is defined, the first step is to consider the equations for each body. If they are expressed in planetocentric coordinates, it is necessary to add the indirect perturbations from all the planets.

So we have

$$\frac{d^2 \mathbf{r}_i}{dt^2} = \frac{\mathbf{F}_i(\dots, \mathbf{r}_j, \dots, \mathbf{v}_j, \dots, \mathbf{p})}{m_i} \quad (2.2.1)$$

where,  $m_i$  is the mass of the satellite  $i$ ,  $\mathbf{r}_j$ ,  $\mathbf{v}_j$  are the position and velocity vectors of the same satellite, and  $\mathbf{p}$  is a set of physical parameters associated

with the selected model (masses, spherical harmonic coefficients  $C_{np}$ ,  $S_{np}$ , tidal parameters, etc.). Usually, the integration of  $3N$  ordinary second order differential equations of this system is easy to do. The initial conditions of the equation are usually taken from an earlier ephemeris. When unavailable, a simplified model is used for the first approach, with some constraints on inclinations and eccentricities.

If the observations are obtained, it is necessary to compare the predicted positions with the ones on the celestial sphere. The Cartesian coordinates resulting from the numerical integration must be transformed into the coordinates of the observations. Sometimes it can be a function, in addition to state vectors, which brings additional parameters  $\mathbf{p}'$ , when the variables change. Let us note  $g$  as a particular observation,  $\mathbf{p}'$  are close to the exact physical values. The difference between observing and calculating a position may be the first term of a Taylor expansion. In particular, when we limit at the first order, it comes

$$g(\mathbf{r}_i^o, \mathbf{v}_i^o, \mathbf{p}'^o) - g(\mathbf{r}_i^c, \mathbf{v}_i^c, \mathbf{p}'^c) \simeq \sum_{l=1}^{6N+p+p'} \left( \frac{\partial g}{\partial \mathbf{r}_i^c} \cdot \frac{\partial \mathbf{r}_i^c}{\partial c_l} + \frac{\partial g}{\partial \mathbf{v}_i^c} \cdot \frac{\partial \mathbf{v}_i^c}{\partial c_l} + \frac{\partial g}{\partial \mathbf{p}'^c} \cdot \frac{\partial \mathbf{p}'^c}{\partial c_l} \right) \Delta c_l \quad (2.2.2)$$

where  $o$  and  $c$  refer to the quantities of observations and calculation, respectively,  $c_l$  represents the adjusted physical quantities. It is clear that we have to consider as many linear equations as there are observations. The linear system obtained can be reversed by the least squares method, or one of its variants. In particular, the weight of each observation, the choice of adjusted physical parameters, and the way to adjust them (only once, or on every step) depends on the author of these ephemerides.

In the previous equation, the partial derivatives of the state vectors in function of the initial conditions and parameters are assumed to be known. There are several methods for using them. However, the most popular one is the integration of the variational equations (Peters.CF 1981 [10]). Starting from the equation (2.2.1), assuming that  $c_l$  is independent on time, we obtain after partial derivation

$$\frac{d^2}{dt^2} \left( \frac{\partial \mathbf{r}_i}{\partial c_l} \right) = \frac{1}{m_i} \sum_{j=1}^N \left[ \frac{\partial \mathbf{F}_i}{\partial \mathbf{r}_j} \cdot \frac{\partial \mathbf{r}_j}{\partial c_l} + \frac{\partial \mathbf{F}_i}{\partial \mathbf{v}_j} \cdot \frac{d}{dt} \left( \frac{\partial \mathbf{r}_j}{\partial c_l} \right) \right] + \frac{\partial \mathbf{F}_i}{\partial c_l} \quad (2.2.3)$$

where, the last term represents the explicit derivative of the force related to  $c_l$ . The numerical integration of variational equations reveals that it is more complicated than the ones from the equations of motion, and usually involving the integration of thousands ordinary differential equations together. In fact, the system (2.2.3) needs to be integrated simultaneously with the equation system (2.2.1).



Let us remind that the validity of the equation (2.2.2) implicitly assumes that the model is perfect and that the observations follow the Gaussian law.

### 2.2.2 Ephemeris from JPL and NOE

#### Online Ephemeris System of JPL

The Jet Propulsion Laboratory Horizons Online Ephemeris System (Giorgini, JD et al. 1996 [11]) provides access to key solar system data and flexible production of highly accurate ephemeris for solar system objects [2]. This includes 715,000+ asteroids, 3,420 comets, 178 natural satellites, all planets, the Sun, 99 spacecraft, and several dynamical points such as Earth-Sun L1 to L5 equilibriums, and system barycenters. The users may also define their own objects, then use the system to integrate the trajectory, or conduct parameter searches of the comet/asteroid database, searching on combinations up to 42 different parameters. Body rise, transit, and set may be identified to the nearest minute, along with eclipse circumstances for non-Earth natural satellites. Close-approaches by asteroids and comets to planetary bodies (and sixteen of the largest asteroids) can be rapidly identified, along with the encounter uncertainties and impact probabilities with the close-approach table output. Orbit uncertainties can be computed for asteroids and comets.

More than 100 different observational and physical aspects of quantities can be requested at intervals for both topocentric and geocentric situations in one of 9 coordinate systems and 4 time scales (TDB, TT, UT, Civil). Since 1900, predefined Earth station locations are available, along with several sites on other major bodies, in addition to being able to use spacecraft as “observer sites”. The users may search for or define topocentric site coordinates on any planet or natural satellite with a known rotational model if the desired site is not predefined. The output is suitable for observers, mission planners, and other researchers, although such determination is ultimately the user’s responsibility.

The JPL DE-431/LE-431 solar system solution is the basis of planetary barycentre motion data over the interval from 13201 B.C. to A.D. 17191; The site currently makes available only the sub-interval from 9999 BC to A.D. 9999. The Chebyshev polynomial representation of DE-431 permits rapid recovery of the barycenter’s original integrator state to the sub-meter level. All planet barycenter, Sun, Moon, Mercury, Venus and Earth are available over a 9999 B.C. to A.D. 9999 interval. Natural satellites and planet-centres are available over various shorter intervals, as warranted by their observational data arc, but generally hundreds of years. For Saturn, the satellites are known over a maximum interval of A.D. 1600 to A.D. 2500. JPL ephemeris in case of Saturn satellites has several informations in following:

- Types of output: Osculating orbital elements table

- Reference frame: J2000 (ICRF/J2000)
- Coordinate system: Ecliptic and mean equinox of frame Epoch (J2000.0)
- Output quantities:
  - JDTDB Epoch Julian Date, Barycentric Dynamical Time
  - EC Eccentricity
  - QR Periapsis distance
  - IN Inclination w.r.t. xy-plane (degrees)
  - OM Longitude of Ascending Node (degrees)
  - W Argument of Perifocus (degrees)
  - Tp Periapsis time (user specifies absolute or relative date)
  - N Mean motion (degrees/DU)
  - MA Mean anomaly (degrees)
  - TA True anomaly (degrees)
  - A Semi-major axis
  - AD Apoapsis distances
  - PER Orbital Period
  - Satellite Physical Properties of Titan:
    - Mean Radius (km) =  $2575.5 + -2.0$
    - Density ( $g/cm^3$ ) =  $1.880 + -0.004$
    - Mass ( $10^{22}$  g) = 13455.3
    - Geometric Albedo = 0.2
    - GM ( $km^3/s^2$ ) =  $8978.13 + -0.06$
    - 1 AU = 149597870.700 km
  - Satellite Orbital Data of Titan:
    - Semi-major axis, a (km) =  $1221.87 (10^3)$
    - Orbital period =  $15.945421d$
    - Eccentricity, e = 0.0288
    - Inclination, i (deg) = 0.28
    - Center radii :  $60268.0 \times 60268.0 \times 54364.0$  km  
Equator, meridian, pole
    - System GM:  $8.4596169226007571 \times 10^8 au^3/d^2$

### NOE program

NOE is a software built by Lainey et al. (Lainey.V et al. 2004a [3] and Lainey.V et al. 2004b [4]) and stated for Numerical Orbit and Ephemeris. At the beginning, it is an ephemeris for the Jupiter satellites, hereafter it describes the ephemeris of natural satellites in solar system, enable to use the sophisticated model. NOE not only has the post-newtonian terms, but also has the energy dissipation influence caused by tidal effect.

The time unit is in century referred to J2000.0 epoch.

NOE in case of Saturn satellites has several characteristics in following:

- Non-sphericity perturbation of Saturn (coefficients  $J_2, J_6$ , and  $J_6$  ).
- The mutual perturbations among the 8 major satellites.
- Non-sphericity perturbation of satellites ( $J_2, C_{22}$ , without Hyperion).
- General relativity (by PPN terms).
- Perturbations directly coming from the Sun and Jupiter, supposed punctual because of their large distance (ephemeris DE431)
- The mass of inner planets and the Moon, adding their mass to that of the Sun.
- The precession of rotation axis of Saturn is designed as

$$\begin{cases} \alpha = -0^\circ 035384885118 t + 40^\circ 581720073562 \\ \delta = -0^\circ 003738481472 t + 83^\circ 537621060881 \end{cases} \quad (2.2.4)$$

## 2.3 The ephemeris TASS

### 2.3.1 The theory

TASS (Vienne.A et al. 1995 [6]) was published in 1991 as "Theorie Analytique des Satellites de Saturne" (TASS), presenting positions, velocities and elements of the satellites Mimas, Enceladus, Tethys, Dione, Rhea, Titan, Hyperion and Iapetus. It was designed in form of series expansions of the potential perturbations, including 62 coefficients such as masses and oblateness, initial conditions.

In TASS, all the motions are referred to the center of Saturn and to the mean ecliptic and mean equinox for J2000.0 epoch, and the initial point is

on the direction of ascending node of the orbital plan and mean ecliptic for J2000.0. TASS uses the variables  $p, q, z, \zeta$  introduced by Duriez.L ( Duriez.L 1979 [12]) and Laskar.J (Laskar.J 1985 [13]). Those variables represent the discrepancies between the real motion and the uniform circular motion, for which the mean motion  $N$  can be observed (called mean mean motion).

The theory takes into account the main characteristics of the Saturnian satellites:

- Non-spherical perturbation of Saturn. Major influence of oblateness, including  $J_2, J_4$  and  $J_6$ , mainly in the four inner-satellites.
- The mutual perturbations among the satellites amplified by several resonances
  - Resonance 2:4 between Mimas and Tethys
  - Resonance 1:2 between Enceladus and Dione
  - Resonance 3:4 between Titan and Hyperion
  - Great inequality 1:5 between Titan and Jupiter.
- Perturbations coming directly from the Sun, mainly in the four outer-satellites.
- The mutual perturbations among the satellites, with a special treatment of the resonances and the great inequality 1:5 between Titan and Iapetus.
- Without precession of rotation axis rotation of Saturn.

So the dynamic problem is a planetary type problem for the mutual interactions of each satellite, and almost of lunar type, for the part from the Sun and the shape of Saturn. Furthermore, there are 3 resonances among 6 Saturnian satellites. The model was constructed in a completely analytic way with respect to the physical parameters (masses of the satellites, oblateness parameters of Saturn,  $J_2, J_4$  and  $J_6$ ), and all the constants in integration, to maintain an internal precision in a few kilometers throughout the calculations.

The result is called TASS (Théorie Analytique des Satellites de Saturne), with accuracy of a few kilometers for the Mimas, Enceladus, Tethys, Dione, Rhea and Titan, and about two hundred kilometers for Hyperion and Iapetus.

The realization of TASS has been made with the following operations:

1. Analytic separation between critical or long term terms (such as secular, resonant and solar terms) and short-term terms on the other hand. Each variable  $x$  is shared in  $x_0 + \Delta x$ , where  $x_0$  is the general solution of the critical system, and  $\Delta x$  is the explicit solution of the short-period system.
2. Analytic construction of critical system at order 2 of the masses and order 3 of  $J_2$  (with truncation eliminated terms which, evaluated numerically, no more than 1 km over 100 years).
3. Analytic integration of short period terms, constructed up to 2-order of mass and 3-order of  $J_2$  (with truncation eliminated in all the terms with an amplitude in 100 meters). The obtained solution of short-period is an explicit function of the critical system solution.
4. Numerical integration of the critical system, with a step of 4 days in 1200 years for Mimas, Enceladus, Tethys and Dione, a step of 100 days in 9400 years for Rhea, Titan, and Iapetus. Integration times are chosen much longer to easily identify the intrinsic frequencies of the critical system (commonly called 'proper frequency') by a frequency analysis. The initial conditions at J1980 are gotten from Dourneau's theory. And the motion of the Sun follows the JASON solution of Simon and Bretagnon ( Simon & Bretagnon 1984[14]).
5. Frequency analysis of the time series, from this numerical integration, based on Laskar method( Laskar.J 1993 [9]), supplemented by the adjustment (by the least squares method) of the terms obtained.
6. Identification of the frequencies in a form of an integer combination of the fundamental frequencies. It allows to present the results of the numerical integration in the form of finite series with periodic terms of long period.
7. The variation of the initial conditions of the numerical integration, around the nominal value. In the series (amplitude and argument), the terms are linear with respect to these initial conditions, the masses of Saturn and its satellites, and the oblateness coefficients of the planet.
8. Transfert of the long-term solution in the analytic expressions obtained for short-period terms.

### 2.3.2 Representation of TASS

The solution presented here is referred as TASS1.6. It does not contain Hyperion which has been developed separately (in TASS1.7). This satellite is not used in this work.

The Tables presented in [6] give the solution of the elliptic elements  $p$ ,  $\lambda$ ,  $z$  and  $\zeta$  of the satellites obtained after a fit over one century of observations.

Each solution is presented as a series of periodic terms (in sine for  $\lambda$ , in cosine for  $p$ , and complex exponential for  $z$  and  $\zeta$ ). In [6] only terms greater than 20 km are given (the complete series grows up to include terms greater than 1 km). The series are given with the long period terms in first place, followed by the short period terms (for example we have  $z_1 = z_{01} + \Delta z_1$  with  $z_{01}$  and  $\Delta z_1$  for long period and short period terms respectively). The time  $t$  is expressed in Julian years from J1980 ( $t = (\text{Julian date} - 2444240)/365.25$ ). In most cases, the argument of each term has been identified as an integer combination of fundamental arguments. The notations used for these fundamental arguments are:

- $\lambda_{oi}$   $i = 1, 8$  the long period part of  $\lambda_i$ . We have  $\lambda_{oi} = N_i \times t + \lambda_{oi}^{(0)} + \delta\lambda_i$ , the linear part is given in the title of the corresponding table.
- $\rho_1 = \lambda_{o1} - 2\lambda_{o3}$  (resonance Mimas-Tethys)
- $\rho_2 = \lambda_{o2} - 2\lambda_{o4}$  (resonance Enceladus-Dione)
- $\phi_1$ , so that  $\phi_1 - \rho_1$  is close to the pericenter of Mimas.
- $\Phi_1$ , so that  $\Phi_1 - \rho_1$  is close to the node of Mimas.
- $\omega_2$  is the libration argument of the resonance Enceladus-Dione. This argument takes the place of  $\phi_2$  corresponding to the proper pericenter of Enceladus whose frequency is zero.
- $\Phi_2$ , so that  $\Phi_2 - \rho_2$  is close to the node of Enceladus.
- $\phi_3$ , so that  $\phi_3 - \rho_1$  is close to the pericenter of Tethys.
- $\omega_1$  is the libration argument of the resonance Mimas-Tethys. This argument takes the place of  $\Phi_3$  corresponding to the proper node of Tethys which is linked to  $\Phi_1$  by the resonance.
- $\phi_4$ , so that  $\phi_4 - \rho_2$  is close to the pericenter of Dione.
- $\Phi_4$ , so that  $\Phi_4 - \rho_2$  is close to the node of Dione.
- $\phi_i$  and  $\Phi_i$   $i = 5, 6$  and  $8$  which are close to the pericenters and the nodes respectively of Rhea, Titan and Iapetus.
- $\lambda_9$ ,  $\varpi_9$  and  $\Omega_9$  are respectively the saturnicentric mean longitude, the longitudes of the pericenter and of the node of the Sun.
- $\mu$  is fundamental argument of JASON84 (Simon & Bretagnon 1984 [14]).

The argument  $\mu$  is mainly present in the Iapetus' solution. In the present series  $\mu$  indicates the indirect perturbations of the planets, mainly of Jupiter. The only arguments surely detected are the great inequality  $-2\lambda_J + 5\lambda_9$  (or  $19\mu$ ), the synodic inequality  $\lambda_J - \lambda_9$  (or  $880\mu$ ) and the inequality  $\lambda_J - 2\lambda_9$  (or  $287\mu$ ).

The partial derivatives of the solution with respect to the initial conditions and to physical parameters do not appear in the tables of [6] because they are too voluminous. But they are present in the complete series of TASS. If we note  $\sigma$  the amplitude, the phase or the frequency of any term in the tables, we have in fact:

$$\sigma = \sigma_o + \sum_{k=1}^{61} \left( \frac{\partial \sigma}{\partial x_k} \right)_o \delta x_k \quad (2.3.1)$$

where  $\sigma_o$  is the nominal value and where  $x_k$  is one of the following parameters:

- $\{m_i\}$   $i = 1, \dots, 6, 8$  the masses of the satellites
- $J_2, J_4$  and  $J_6$  the oblateness coefficients of Saturn
- 6 initial conditions per satellite
- $i_a$  and  $\Omega_a$  the inclination and the node of the equatorial plane of Saturn in the J2000 system
- $M_S$  is the mass of Saturn.

Then, note that the parameters are independent of each other: the dynamical consistency is the main characteristic of TASS.

## 2.4 Use of theses ephemerides

In research, it is convenient to download ephemerides from the on line service of IMCCE, or Horizons of JPL. Such ephemerides, based on recent observations, have a very good precision. Meanwhile, the analytical theories, like TASS, also well used in researching work. TASS shows the details of the system motion in the combination of the proper frequencies. No doubt, TASS is useful to study the influences between different satellites in the Saturn system.

We take use of TASS version 1.6 in our calculation, for the positions and velocities of the satellites Mimas, Enceladus, Tethys, Dione, Rhea, Titan and Iapetus referred to the center of Saturn in mean ecliptic and mean equinox for J2000.0 epoch (with the precision in 100km over the recent 100 years). Based on the analytic development of equations, we have seen that TASS

shows the details of the system motion in the combination of the proper frequencies. However, TASS also has their shortcoming that in precision, it is not as good as numerical ephemeris directly fitted to observations.

We suppose that it is possible to get a similar presentation as TASS with a numerical integration ephemeris: with a series of proper frequencies, as constant parameters to constitute the action-angle variables in the integrable dynamics systems. Based on that, the combinations of proper frequencies, should be considered to describe the perturbation relationship between the different satellites in the Saturn system.

At last, in the manuscript, three ephemeris are continuously compared. In order to reduce some sentences, we give them a short name. They are:

- **TASS-t** for the template of TASS. It corresponds to TASS concerning the precision, but the representation uses the proper frequencies. Its representation has been obtained with a frequency analysis of TASS version 1.6 over 10,000 years. See next chapter and the appendix.
- **TASS-s** for a shorter time span of TASS version 1.6, that is over 1,000 years only. More precisely, when the value of a parameter is said coming from TASS-s, it means that this value comes from computations using TASS over 1,000 years. TASS-s is mainly used in Chapter 6 in order to test our method.
- **JPL**. It is available over 1,000 years. To obtain its representation in the same form as TASS-t is the aim of our work.



## Chapter 3

# Frequencies and synthetic representation of motion

In the modern celestial mechanics, the dynamical systems should be defined as a quasi-integrable Hamilton system. Hence, most of the equations in celestial mechanics should be written in a Hamiltonian form. In a conservative system, the Hamiltonian is a constant, depending on the initial value of the coordinates and momenta of motion. Moreover, changing the coordinates and momenta of a Hamiltonian system will only change the form of the Hamiltonian, but will not alter the motion equations.

The work of Laskar.J in 1992 mentions that a dynamical system can be described by its frequencies (Laskar.J et al. 1992 [15]). The proper frequencies are the first derivatives of the action-angle variables of the system. In fact, we could not find exactly the real action-angle variables of the Saturnian system. However, it is possible to approach of the action-angle variables.

For these approaching variables, the motions are still on a torus, but the projection on each variable is no longer a circular motion. It means that in any set of action-angle variables, the angles are  $2\pi$ -periodic and the coordinates can be described in a multi Fourier series (similar as the one of the 2-body problem). We can get the proper frequencies by analyzing the approached variables. The frequency analysis is a method for studying the stability of the orbits, based on a refined numerical search for a quasi-periodic approximation of its solutions over a finite time interval (Laskar.J 1990 [16], 1993 [9]; Laskar.J et al. 1992 [15]).

The frequency analysis is implemented in C language (FA for short). It obtains the frequency components of the orbital elements by starting with a Fast Fourier Transform (FFT) and refining the search for the frequency by a quadrature. Then the elements could be represented as the combinations of the proper frequencies, in which all the combinations are following the D'Alembert rule. This software is made by Saillenfest.M (Saillenfest.M 2014

[17]). The description below comes mainly from this reference, with the main idea coming from the papers of Laskar.J.

### Reminder of notations

We remind the definition of variables  $p$ ,  $q$ ,  $z$  and  $\zeta$  :

$$\begin{aligned} a &= A(1+p)^{-2/3} \iff n = N(1+p) \\ \lambda &= Nt - \sqrt{-1}q \\ z &= e \exp \sqrt{-1}\varpi \\ \zeta &= \sin \frac{i}{2} \exp \sqrt{-1}\Omega \end{aligned} \tag{3.0.1}$$

where  $a$ ,  $e$ ,  $i$ ,  $\Omega$ ,  $\varpi$  and  $\lambda$  are the classical elliptic elements, The reference frame takes the Saturnicentric equatorial plane in which the origin corresponds to the node with the mean ecliptic J2000.

$n$  is the osculating mean motion and  $N$  is the mean mean motion, in such a way that  $q$  has no linear component in time ( $q$  has only the quasi-periodic parts).

## 3.1 Integrable system, quasi-periodics series and proper frequencies

Considering an integrable Hamilton system with  $m$  degree of freedom based on Hamiltonian  $H$ , if the system evolves within the hypothesis of the Arnold-Liouville theorem, there exists some coordinates called action-angle  $(J, \theta)$ , with which the description dynamics of the system is quite simple:

$$H(J, \theta) = H_0(J) \implies \begin{cases} J(t) = J_0 \\ \theta(t) = \omega(J)t + \theta_0 \end{cases} \quad \text{when } (J, \theta) \in \mathbb{R}^m \times \mathbb{T}^m \tag{3.1.1}$$

The dynamics of the system can be described by the variable  $J_j \exp i\theta_j(t)$ : the motion takes place on a  $m$  dimension torus, around  $J_j$ , with the constant angular velocities  $\omega_j$ . Unfortunately, we have no way to know the possible coordinate modification of those variables : it is the difficulty of analytical theories. However, the action-angle coordinates are intrinsic of the system, in other words, it means that: Even if a system is written with “bad” variables, it should still evolve with its proper frequencies  $\omega_j$ .

Let a function  $f(t)$  describing a mechanical system. For example,  $f(t)$  may stand for one of the variables in equation (3.0.1). The previous properties allow us to write  $f(t)$  as a Fourier series of  $\theta$  :

$$f(t) = \sum_{h \in \mathbb{Z}^m} a_h \exp ih \cdot \theta(t) \text{ with } a_h \in \mathbb{C} \quad (3.1.2)$$

By developing the scalar product  $h \cdot \theta(t)$ , we then obtain a series in form:

$$f(t) = \sum_{k \in \mathbb{N}} A_k \exp i\nu_k t \text{ with } A_k \in \mathbb{C} \quad (3.1.3)$$

where the  $\nu_j$  are integer combination of the proper frequencies  $\omega_j$ .

Suppose that we know the dynamics solution  $f(t)$  of the system, for example, coming from the numerical integration of equations. The frequency analysis, detailed in (3.1.3), allows us to determine the amplitude  $A_k$  and the frequencies  $\nu_k$  of the expansion of  $f(t)$ . To finish, we only have to identify the  $\nu_k$  as the integer combinations in order to have the proper frequencies. Note that if the system is degenerated, that is:

$$\det \frac{\partial \omega(J)}{\partial J} = \det \frac{\partial^2 H_0(J)}{\partial J^2} \neq 0 \quad (3.1.4)$$

then, the application  $J \rightarrow \omega(J)$  is a diffeomorphism, and the system is described equivalently by its proper frequencies or by its actions. The dynamics of the system is therefore fully characterized.

The series (3.1.2), numerically determined, are also continuous analytical functions describing the evolution of the system: they can be used for ephemeris or for other analytical studies, of the same system or some related systems.

In the case of a disturbed integrable Hamiltonian  $H(J, \theta) = H_0(J) + \varepsilon H_1(J, \theta)$ , the KAM theorem implies that, for a sufficiently small perturbation, the system has an invariant torus traversed with a constant velocity (Arnol'd.VI 2013 [18]). It stays integrable, and the decomposition in series (3.1.3) is still valid. On the other hand, if the perturbation is too large, the motion becomes chaotic and its Fourier series is only an approximation. Actually, the frequencies obtained numerically are no longer constant (the 'proper' frequencies does not exist anymore).

In the following, we assume that the system is integrable, or at least, close to an integrable system.

## 3.2 The D'Alembert rule

If the analytical computations are well performed we should obtained a form like (3.1.2).

We note  $\mathcal{R}$  the perturbing potential from the Keplerian motion, the Lagrange equations for our variables are:

$$\begin{aligned}
\frac{dp}{dt} &= -3\sqrt{-1} \frac{(1+p)^{4/3}}{NA^2} \frac{\partial \mathcal{R}}{\partial q} \\
\frac{dq}{dt} &= \sqrt{-1} Np + \sqrt{-1} \frac{(1+p)^{1/3}}{NA^2} \left[ 3(1+p) \frac{\partial \mathcal{R}}{\partial p} + \phi\psi \left( z \frac{\partial \mathcal{R}}{\partial z} + \bar{z} \frac{\partial \mathcal{R}}{\partial \bar{z}} \right) + \right. \\
&\quad \left. \frac{1}{2\phi} \left( \zeta \frac{\partial \mathcal{R}}{\partial \zeta} + \bar{\zeta} \frac{\partial \mathcal{R}}{\partial \bar{\zeta}} \right) \right] \\
\frac{dz}{dt} &= \sqrt{-1} \frac{(1+p)^{1/3}}{NA^2} \left[ 2\phi \frac{\partial \mathcal{R}}{\partial \bar{z}} - \phi\psi z \frac{\partial \mathcal{R}}{\partial q} + \frac{z}{2\phi} \left( \zeta \frac{\partial \mathcal{R}}{\partial \zeta} + \bar{\zeta} \frac{\partial \mathcal{R}}{\partial \bar{\zeta}} \right) \right] \\
\frac{d\zeta}{dt} &= \sqrt{-1} \frac{(1+p)^{1/3}}{2\phi NA^2} \left[ \frac{\partial \mathcal{R}}{\partial \bar{\zeta}} - \zeta \frac{\partial \mathcal{R}}{\partial q} + \zeta \left( -z \frac{\partial \mathcal{R}}{\partial z} + \bar{z} \frac{\partial \mathcal{R}}{\partial \bar{z}} \right) \right]
\end{aligned} \tag{3.2.1}$$

where  $\phi = \sqrt{1 - z\bar{z}}$  and  $\psi = 1/(1 + \phi)$ . Here we define  $i = \sqrt{-1}$ .

In order to develop and solve the equations (3.2.1), the function  $\mathcal{R}$  should be expressed in osculating elements  $p, q, z, \zeta$ . We expand them in trigonometric series. Duriez.L's method (Duriez.L 1977 [19]) allows us to describe such kind of series in form of simple polynomials with variables  $z$  and  $\zeta$  for all the bodies considered. In this formalism,  $\mathcal{R}$  is simply expressed as a sum of generic terms  $T$ , like:

$$T = c p_i^{g_i} p_j^{g_j} z_i^{n_i} z_j^{n_j} \zeta_i^{\nu_i} \zeta_j^{\nu_j} \bar{z}_i^{\bar{n}_i} \bar{z}_j^{\bar{n}_j} \bar{\zeta}_i^{\bar{\nu}_i} \bar{\zeta}_j^{\bar{\nu}_j} e^{\sqrt{-1}(k_i \lambda_i + k_j \lambda_j)} \tag{3.2.2}$$

where  $c$  is the numerical coefficient depending on the relative integers  $g_i, g_j, n_i, n_j, \bar{n}_i, \bar{n}_j, \nu_i, \nu_j, \bar{\nu}_i, \bar{\nu}_j, k_i$  and  $k_j$ , and computed for the values of the semi-major axis  $A_i$  and  $A_j$  of the satellites  $i$  and  $j$ ; in factor, it has the mass  $m_j$ .

### The D'Alembert rule in analytical developments

The integers  $k_i$  and  $k_j$  from (3.2.2) define an inequality and verify the property of D'Alembert; set:

$$\begin{aligned}
C_I &= k_i + k_j \\
C_M &= \bar{n}_i - n_i + \bar{\nu}_i - \nu_i + \bar{n}_j - n_j + \bar{\nu}_j - \nu_j
\end{aligned} \tag{3.2.3}$$

We have (Laskar.J 1985 [13]) :

$$C_I = C_M \tag{3.2.4}$$

This property is carried to the Lagrange equation in almost the same form. The generic term is also as (3.2.2), and we have:

$$C_I = C_M + \delta(e) \tag{3.2.5}$$

with:

$$\begin{aligned}\delta(e) &= 0 && \text{if } e \text{ means the equation relative to } p \text{ or } q \quad (3.2.6) \\ \delta(e) &= 1 && \text{if } e \text{ means the equation relative to } z \text{ or } \zeta\end{aligned}$$

For the  $J_2$ ,  $J_4$  or  $J_6$  terms, due to the oblateness of planet, the variables with subscript  $j$  vanish in (3.2.2) and (3.2.3);  $c$  depends on the semi-major axis of the satellite  $i$  and is proportional to  $J_2$ ,  $J_4$  or  $J_6$ .

The D'Alembert property comes from the invariance by rotation of the problem. Furthermore note that, because of the invariance by symmetry with respect to the reference plane,  $\bar{\nu}_i + \nu_i + \bar{\nu}_j + \nu_j$  is even.

As an example, the D'Alembert rule mentions that the inequality  $\lambda_2 - 2\lambda_4$  has in factor the eccentricity and the inclination in degree 1 or more. Similarly as in the other planetary systems, in the Saturnian one, the eccentricities and inclinations are small. The lower degree terms are the most important. For the inequality  $\lambda_2 - 2\lambda_4$  the terms of lowest degree only concern the arguments.

$$\lambda_2 - 2\lambda_4 + \varpi_2 \text{ of } z_2 \exp \sqrt{-1}(\lambda_2 - 2\lambda_4)$$

and

$$\lambda_2 - 2\lambda_4 + \varpi_4 \text{ of } z_4 \exp \sqrt{-1}(\lambda_2 - 2\lambda_4)$$

For Enceladus and Dione, it is the argument  $\lambda_2 - 2\lambda_4 + \varpi_2$  which is in resonance.

For Mimas-Tethys, it is the argument  $2\lambda_1 - 4\lambda_3 + \Omega_1 + \Omega_3$ , called resonance 2 : 4. For this inequality, the arguments (of the lower degree) are:

$$\begin{aligned}2\lambda_1 - 4\lambda_3 + 2\varpi_1 & , & z_1^2 \\ 2\lambda_1 - 4\lambda_3 + \varpi_1 + \varpi_3 & , & z_1 z_3 \\ 2\lambda_1 - 4\lambda_3 + 2\varpi_3 & , & z_3^2 \\ 2\lambda_1 - 4\lambda_3 + 2\Omega_1 & , & \zeta_1^2 \\ 2\lambda_1 - 4\lambda_3 + \Omega_1 + \Omega_3 & , & \zeta_1 \zeta_3 \\ 2\lambda_1 - 4\lambda_3 + 2\Omega_3 & , & \zeta_3^2\end{aligned}$$

For this pair of satellites, only the fifth is really inside the resonance.

Thus, by the property of D'Alembert, the inequality provides immediately the minimum degree of eccentricity and inclination. The interest of the D'Alembert rule is also to allow to neglect some inequalities: the terms for which  $p + p'$  are high are generally negligible. For example, the inequality  $15\lambda - 40\lambda'$  has terms with degree 25 in eccentricity and inclination.

Note that some frequencies come from the libration of the argument concerned by the resonance. It is no need to take it into account in this addition since the sum of those coefficients is zero (it is the case of the angles  $\omega_1$  and  $\omega_2$  from the resonance Mimas-Tethys and Enceladus-Dione.)

### The D'Alembert rule in synthetical representations

In fact we observe a similar form of the D'Alembert rule in the synthetical representation.

For the two body problem Saturn-satellite, the action-angle variables are explicit. We can define a system with canonical coordinates (which are looked like the modified Delaunay variables). The angles are simply  $(\lambda, \varpi, \Omega)$ , and the related actions are  $(a, e, i)$ . The angles vary linearly with time ( $\lambda$  with the frequency  $N$ ,  $\varpi$  and  $\Omega$  with a null frequency), while the actions are constant.

Now, let us slightly disturb the two-body problem, the system remains integrable: the action-angle variables still exist, but no longer defined in the same way. However, they approach the previous variables ( $a$ ,  $e$  and  $i$ , vary "slowly"). We note the new proper angles as  $(\lambda^*, \varpi^*, \Omega^*)$ .

If we suppose that the d'Alembert rule is transported to the solution in the action-angle variables, then it can be written with the proper angles  $(\lambda^*, \varpi^*, \Omega^*)$ .

### Some particularities in the arguments of TASS

In TASS, the analytic resolution of the equations (3.2.2) for each satellite is performed to find the solution of this form :

$$f(t) = f_0(t) + \varepsilon \Delta f(f_0, t) \quad (3.2.7)$$

where  $f(t)$  represents generically  $p$ ,  $q$ ,  $z$  or  $\zeta$ .  $f_0$  describes the secular evolution of the variables,  $\varepsilon \Delta f$  is the oscillatory motion with a small amplitude ( $\varepsilon$  is a small parameter). Then, the Lagrange equations are expanded in Taylor series around  $f_0(t)$ , and separated into the long-period terms and the short-period terms. The integration of the short-period Lagrange equations is made analytically term by term (at the first order of the masses,  $i$  and  $e$  are assumed constant): we get a solution  $\Delta f(f_0; t)$ . Independently, the secular part is obtained by frequency analyzing of numerical integration and leads to the solution  $f_0(t)$ .

Concretely, TASS supplies the solutions  $f_0(t)$  and  $\Delta f(t)$  in form of trigonometric series. However, the description is ambiguous:  $\Delta f(t)$  depends implicitly of  $f_0(t)$ . The complete solution  $f(t)$  should behave like a trigonometric series of type (3.1.2), but the amplitudes and the frequencies are not written explicitly. For example, here is the preliminary expansion of the variable  $z$  of Enceladus which is given in TASS:

$$z_2 = a_1 \exp i(-\lambda_{o2} + 2\lambda_{o4}) + a_2 \exp i(-\lambda_{o2}) + a_3 \exp i(-\lambda_{o2} + 2\lambda_{o4} + \omega_2) + \dots \quad (3.2.8)$$

The amplitudes  $a_k$  are explicitly given in TASS, but the components  $\lambda_o$  have their own description:

$$\begin{cases} \lambda_{o2} = \lambda_2^* + b_1 \exp i(\omega_2) + b_2 \exp i(-\lambda_2^* + 2\lambda_4^* - \omega_4) + \dots \\ \lambda_{o4} = \lambda_2^* + c_1 \exp i(\omega_2) + c_2 \exp i(-\lambda_2^* + 2\lambda_4^* - \omega_4) + \dots \end{cases} \quad (3.2.9)$$

with  $\omega_2$ ,  $\lambda_2^*$ ,  $\lambda_4^*$  and  $\varpi_4^*$  the proper angles as explained and defined in Chapter 1.

To solve this problem, we will perform a frequency analysis of the ephemeris TASS in order to make an explicit series as form (3.1.2). These can then be compared with other ephemerides (JPL or NOE). The example of such a series is given in the Appendix and named TASS-t. We mention that the representation of TASS with a long time span has been already done by Saillenfest.M [17] in 2014 for which we have extended the procedure.

### 3.3 FA: the frequency analysis

Our purpose is to reconstruct a numerically quasi-periodic function  $f(t)$ , from a series of points over the interval  $[0; T]$ . Therefore it is necessary to determine the different frequencies involved and the associated complex amplitudes (Laskar.J 1992 [15]).

Consider a quasi-periodic function, in general form:

$$f(t) = \sum_{k=1}^N A_k e_k(t) \quad \text{where} \quad A_k \in \mathbb{C} \quad \text{and} \quad e_k(t) \equiv \exp(i\nu_k t) \quad (3.3.1)$$

The Fourier series of  $f(t)$  in  $[0, T]$  define as:

$$\hat{f}(t) = \sum_{n=-\infty}^{+\infty} \langle f, v_n \rangle v_n(t) \quad \text{with} \quad v_n(t) = \exp(in\nu_0 t), \quad \text{where} \quad \nu_0 = \frac{2\pi}{T} \quad (3.3.2)$$

Every  $\hat{f}(t)$  is the projection of  $f(t)$  on vector space generated by the vectors  $v_{nn \in \mathbb{Z}}$  and provided with the scalar product :

$$\langle f, g \rangle = \frac{1}{T} \int_0^T f(t) \overline{g(t)} dx \quad (3.3.3)$$

For this quadrature, we use Hardy's method. We suppose that  $f(t)$  is tabulated with a step small enough in order to neglect the numerical errors and the aliasing. Note that if  $\{\nu_k\}_{k=1, \dots, N}$  are not integer multiples of  $\nu_0$ , then  $\hat{f}(t)$  will be a very bad approximation of  $f(t)$ , in which the frequencies are obtained with the precision of  $\nu_0$  only.

In fact, we can obtain a much better approximation of the frequencies by studying the variations of the "amplitude function" defined by:

Figure 3.1: Amplitude function in the case of a single sinusoidal term (Sailenfest.M 2014 [17])

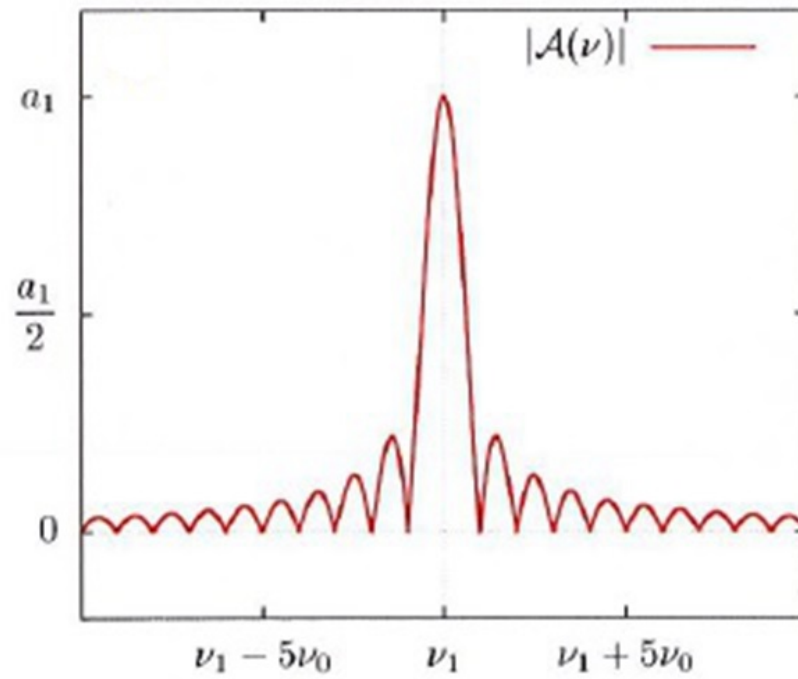




Table 3.1: The difference between the true longitude  $\nu_6^*$  and the mean longitude  $\lambda_6$  of Titan over 10,000 years

	Frequency (rad/year)	(rad/day)	Period (day)	Identification
1	143.915114	0.394018	15.946	$\lambda_6 - \varpi_6$
2	287.830228	0.788036	7.973	$2\lambda_6 - 2\varpi_6$
3	143.932982	0.394067	15.944	$\lambda_6 + \varpi_6$
4	143.506384	0.392899	15.992	$\lambda_6 + \varpi_6 - 2\lambda_S$
5	143.917039	0.394023	15.946	$\lambda_6 - \varpi_6 - \Omega_8$
6	143.913188	0.394012	15.947	$\lambda_6 - \varpi_6 + \Omega_8$
7	143.922077	0.394037	15.946	$\lambda_6 + \varpi_8 + 2\varpi_6 + 2\Omega_6$
8	431.745352	1.182054	5.315	$3\lambda_6 - 2\varpi_6 + \Omega_6$
9	143.924045	0.394043	15.946	$\lambda_6 - \varpi_6 - \Omega_6$
10	143.906183	0.393994	15.947	$\lambda_6 - \varpi_6 + \Omega_6$

$$\mathbb{A}(\nu) = \langle f, \exp(i\nu t) \rangle \quad (3.3.4)$$

If  $f(t)$  has only one term, we have :

$$|\mathbb{A}(\nu)| = |\langle A_1 \exp(i\nu_1 t), \exp(i\nu t) \rangle| = |A_1 \frac{\sin[(\nu_1 - \nu)T/2]}{(\nu_1 - \nu)T/2}| \quad (3.3.5)$$

The maximum of this function is reached when  $\nu$  is equal exactly to  $\nu_1$ , and we have  $\mathbb{A}(\nu_1) = A_1$  (Figure 3.1).

So to determine  $\nu_1$ , we have to find the maximum of the function  $|\mathbb{A}(\nu)|$ . In practice, we first perform a FFT (Fast Fourier Transform) in order to situate approximatively this maximum. Then we use an interpolation algorithm to find its precise value.

In a more realistic case where  $f(t)$  has several terms, a maximum is associated to each frequency  $\nu_k$ . But there is a distortion of the peaks associated to the other terms which have not the same height, and not exactly centered on the  $(\nu_k)$ . Fortunately, this effect is small for frequencies well separated. We add a weight function to the scalar product to correct it partially as shown in Figure (3.2).

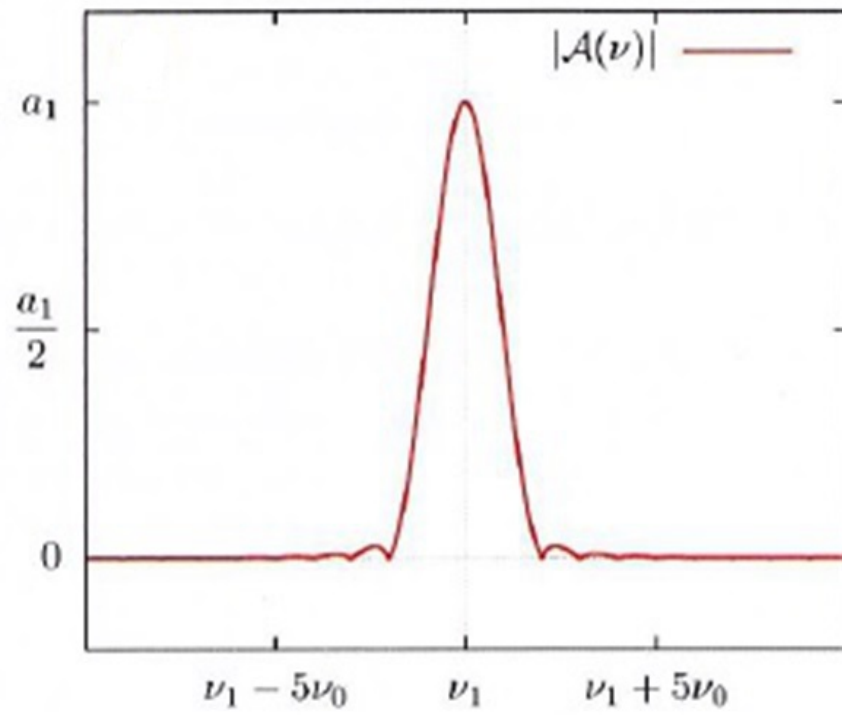
The scalar product is then defined by

$$\chi(t) = 1 - \cos(\nu_0 t) \quad (3.3.6)$$

$$\langle f, g \rangle = \frac{1}{T} \int_0^T f(t) \overline{g(t)} \chi(t) dx \quad (3.3.7)$$

For comparison with Table 1.1 of the introduction and as an example, in Table 3.1 we give the difference between the true longitude  $\nu_6$  and the

Figure 3.2: Amplitude function in case of a single sinusoidal term, with Hanning windows, (Saillenfest.M 2014 [17])



mean longitude  $\lambda_6$  of Titan over 10,000 years. We remove the major mean motion influence from the Sun, but keep the combination term, by using the mean longitude in our calculation instead of the true anomaly. For easier comparison between both results, we present the frequencies both in rad/year and rad/day.

We have made the frequency analysis of the elements of Titan given by TASS (over 10,000 years). They are given as a reference for the following Appendix. This representation is named TASS-t (template of TASS). It corresponds to TASS concerning the precision, but the representation uses the proper frequencies.



## Chapter 4

# Context and difficulties of the realization

Before we start our calculations to obtain the representation of the mean longitude of Titan in JPL ephemeris, it is necessary to make a complete comparison with TASS ephemeris. It is the very beginning and important base of our work. We have two main questions: what difference does exist between both ephemerides, and where do these differences appear? We should compare their orbital elements, positions, even though velocities. If they have some differences, most of time, it is impossible to know what cause them come from. However, we could get a preliminary understanding of our future work.

On our purpose of making a comparison between TASS and JPL, it is necessary to put both ephemerides into the same celestial frame reference. In this chapter, without special mention, all orbital elements are in the saturnicentric ring plane at J2000.0 epoch, fixed in J2000 ecliptic and equinox system by (we recall the values given in Chapter 1):

$$\begin{aligned}\Omega_a &= 169.5291^\circ \\ i_a &= 28.0512^\circ\end{aligned}$$

Among the elements of the Saturnian satellites, we take the mean longitude of Titan as an example. Not only it has a short period argument, like the mean longitude of the Sun, its double, and its triple harmonics, but also it includes some long-period arguments.

First, we make the comparison between two ephemerides in positions, then in elements  $\lambda_6$ ,  $z_6$  and  $\zeta_6$ . We give more attention to the mean longitude of Titan. We have to determine its mean mean motion  $N_6$  and the phase  $\lambda_0$  (constant term in  $\lambda_6$ ). It is easy to get the mean mean motion and  $\lambda_0$  together by a frequency analysis or to calculate them by the least squares method as a reference. The 1,000 years time span used is long enough in comparison with the period of Titan (16 days).

For more details, we also can compare two  $r$  (by FA and LSM), which are the residuals of  $r = \lambda_6 - Nt - \lambda_0$ . Each  $r$  has only periodic terms  $\sum_{i=1}^n A_i \sin(\omega_i t + \phi_i)$ . Our final aim is to determine them. In a numerical ephemeris, the determination of  $\lambda_0$  is degraded by some long period terms (up to 3000 years) in comparison to the 1,000 years time span. We will describe the problem and give the solution.

## 4.1 Comparison in positions and elements between TASS and JPL ephemerides

In this section, we make the comparison between two ephemerides of Titan in their osculating Keplerian elements and their positions in 1,000 years interval. Additionally, we focus on the time span over 200 years around  $J2000.0$  epoch, during which both ephemerides have their best precision. For JPL, including the observations on Earth base and space, it shows its best precision in several decades around  $J2000.0$  epoch. In TASS, most of the system parameters comes from the observations before 1980s. Then its best precision is in several decades around the 1980.0 epoch.

### 4.1.1 Comparison in positions

First, we compare the positions of both ephemerides in the three axis  $x, y, z$  in Cartesian coordinates. We take the Saturn ring plane as reference plane with the  $J2000.0$  epoch. We make the comparison of the instantaneous distance  $l$  (from Saturn to the satellite) between both ephemerides, which is equal to  $l = \sqrt{x(t)^2 + y(t)^2 + z(t)^2}$ . Here, some necessary explanations are given for the following figures:

1. The comparison is done over 1,000 years that is the time span from 1600-2600.
2. The horizontal axis is the time given in years. The origin signed as 0, means  $J2000.0$  epoch. For example,  $-20$  on this axis means 1980.
3. The vertical axis is the difference in  $x, y, z$  and  $l$  between both ephemerides given in kilometers.

Figure 4.1 shows the difference in x-axis between JPL and TASS ephemerides in 1,000 years. Figure 4.2 is a partial enlargement of the Figure 4.1. The difference between both ephemerides in x-axis over 1,000 years is about 3,000km, and about 500km in 200 years. In both figures, we can find that between 1980-2000, JPL and TASS ephemerides have their minimal differences.

Figure 4.1: Difference of the positions in x-axis between JPL and TASS ephemerides of Titan during 1,000 years, 1600-2600

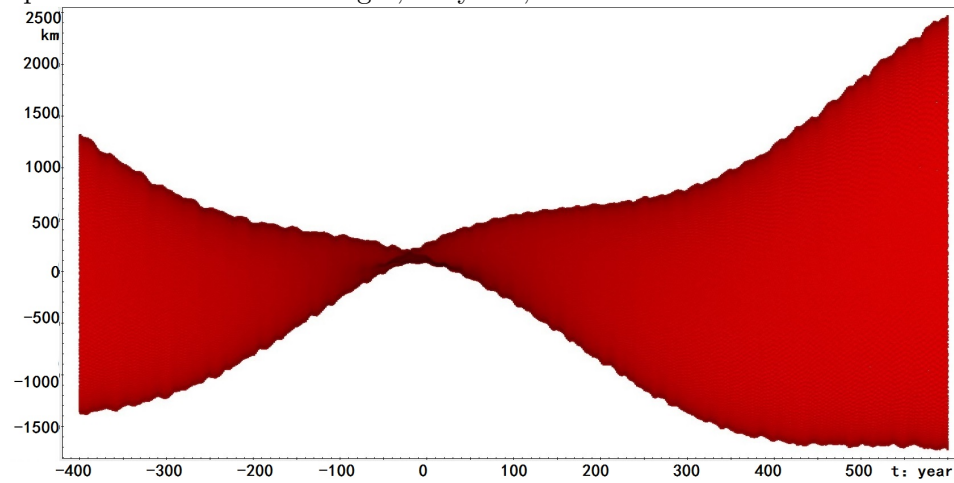


Figure 4.2: Partial enlargement of the Figure 4.1 over 200 years, 1900-2100

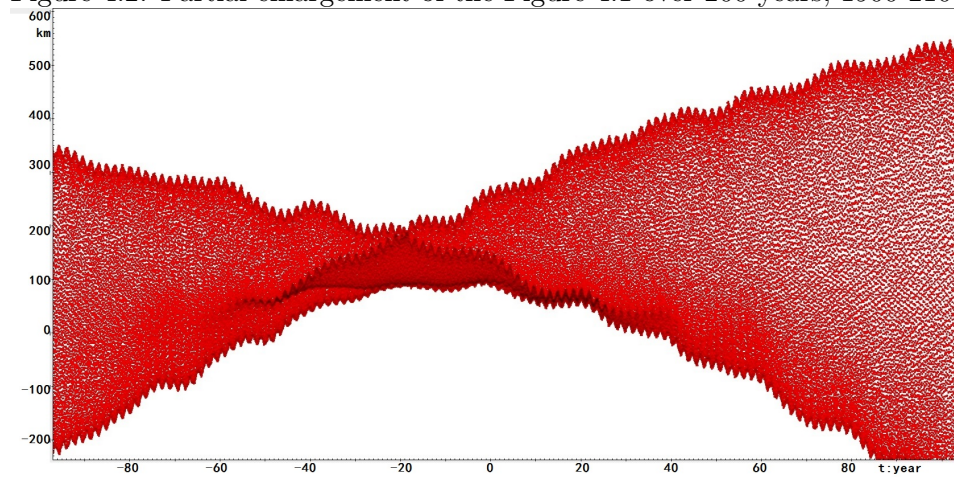


Figure 4.3: Difference of the positions in y-axis between JPL and TASS ephemerides of Titan during 1,000 years, 1600-2600.

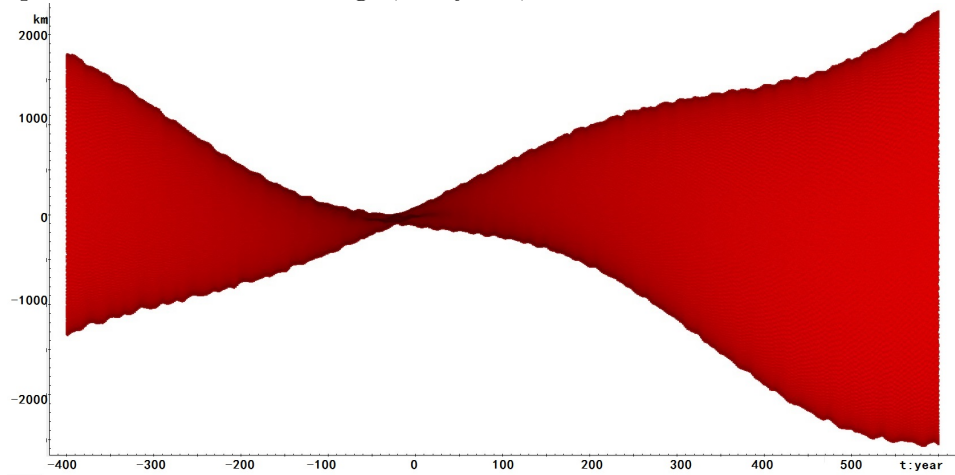
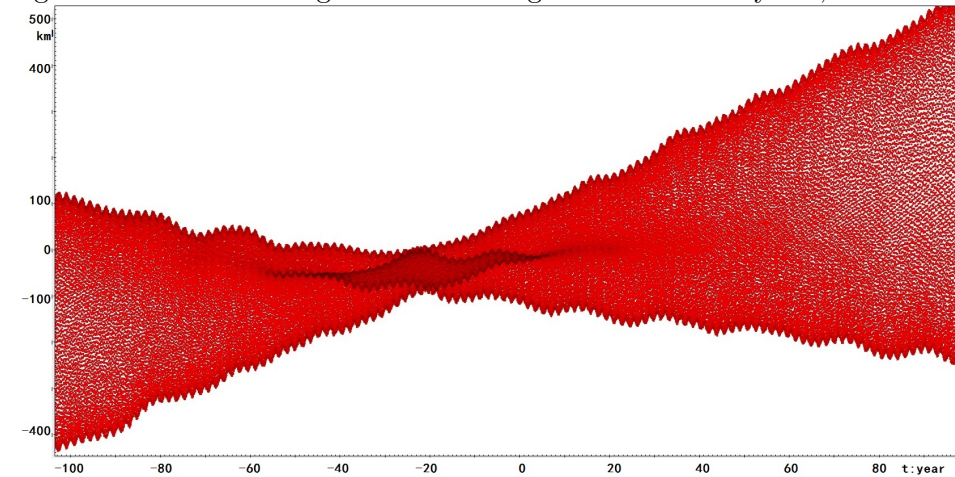


Figure 4.4: Partial enlargement of the Figure 4.3 over 200 years, 1900-2100





Figures (4.3) and (4.4) express the difference between JPL and TASS for the positions in y-axis of Cartesian coordinates in 1,000 years. Figure (4.4) is a partial enlargement of the Figure (4.3). In these figures, we show the same characters which have been found in both figures above, that is between 1980-2000, JPL and TASS ephemerides have their minimal differences.

Figure 4.5: Difference of the positions in z-axis between JPL and TASS ephemerides of Titan over 1,000 years, 1600-2600.

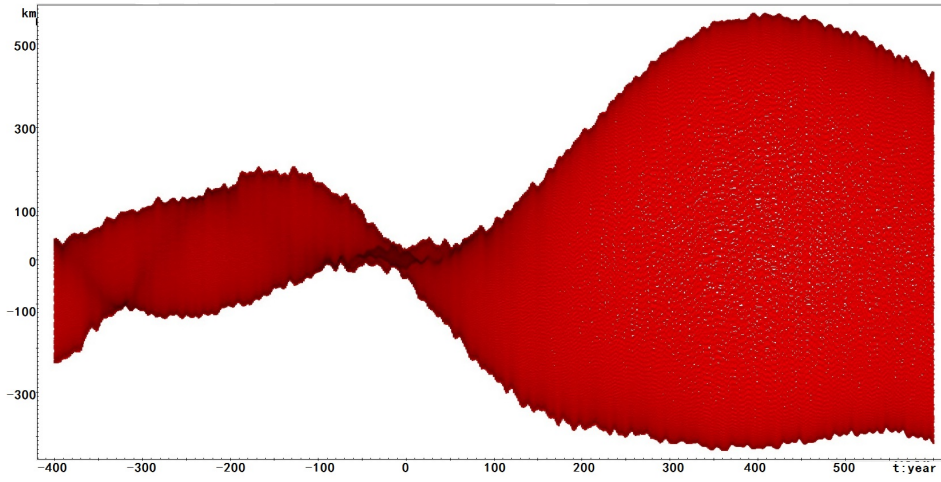


Figure (4.5) shows the difference between JPL and TASS in 1,000 years, for the positions in z-axis of Cartesian coordinates. By contrast with the situations in x-axis and y-axis, the difference of z-axis increases slowly before 2000 (about 100-150 km), but varies quite rapidly after 2010.

We show in the Figure (4.6) the difference of the instantaneous distance  $l$  (from Saturn to the satellite) in 1,000 years, from 1600 to 2600. When we enlarge the Figure (4.6) partially in the Figure (4.7), it is shown that from 1950 to 2010, while we have various sets of observations, both ephemerides keep the minimal differences into 100 km in distance.

It is clear that the positions of Titan in both ephemerides have some differences. In recent 200 years (1900-2100), their differences keep stable and increase rarely. We suppose that the same tendency should be found in the comparison of the orbital elements.

#### 4.1.2 Comparison in elements

In this section, we make the comparison of the orbital elements  $\lambda_6$ ,  $z_6$  and  $\zeta_6$  between JPL and TASS. The differences are given in kilometers by multiplying by the nominal value of the semi major axis of Titan. Additionally, some necessary explanations are given for the following figures:

- The comparisons is made over 1,000 years that is the time span of

Figure 4.6: Difference in instantaneous distance  $l$  between JPL and TASS of Titan during 1,000 years, 1600-2600

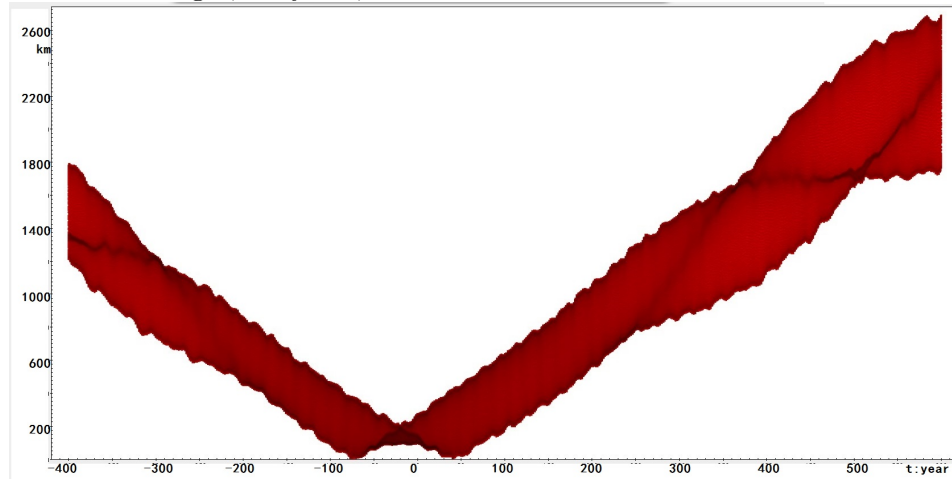
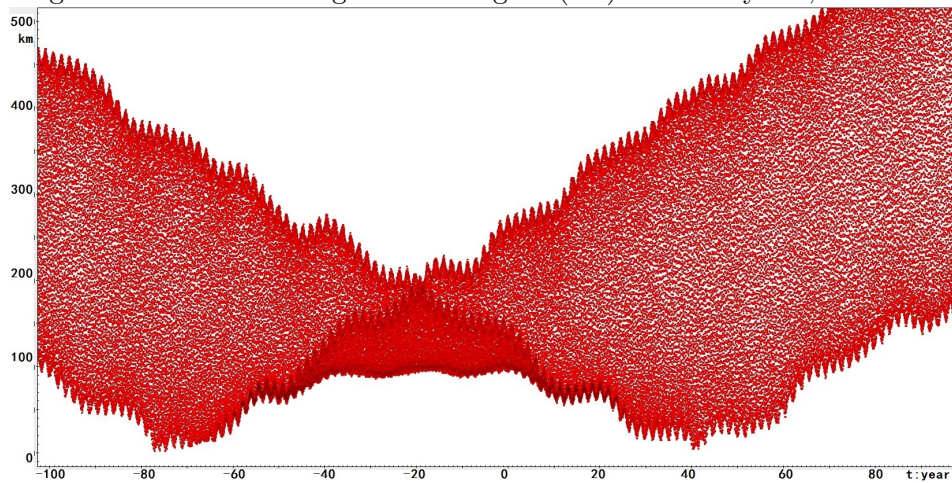


Figure 4.7: Partial enlargement of Figure (4.6) over 200 years, 1900-2100



JPL, from 1600-2600.

- The horizontal-axis is the time, with unit in years. The coordinate origin signed as 0, means J2000.0 epoch. for example,  $-20$  in this axis means 1980.
- The vertical-axis is the difference between both ephemerides, with unit in kilometers.

Figure (4.8) shows the difference between JPL and TASS for  $\lambda_6$  over 1,000 years. Figure (4.9) is a partial enlargement of Figure (4.8) around J2000.0 epoch.

The mean longitude  $\lambda_6$  in both ephemerides depends on the observations from both ground base and space. The scientists record the observations, giving the positions in the Saturn system, for only 200 years.

In the figures, there is a big difference larger than 3000 km over 1,000 years. If we consider only a circular uniform motion, it is not a real difference between the ephemerides. Our results of the corresponding mean mean motion are expressed in Table 4.1. When we remove in the mean longitude of the ephemerides the mean mean motions and the phases, they do not show a large difference. A small difference in the mean mean motions, accumulating again and again after every period, causes a huge disparity between both mean longitudes over 1,000 years.

In fact, the difference of the mean longitude between both ephemerides, is the discrepancy of both remaining parts, where we have removed  $N \times t$  and the phase  $\lambda_0$  from the mean longitude. It is the difference of the non-linear part of the mean longitude, which is smaller than in Figure (4.8). In the following section, we will focus on the mean mean motion  $N$  and the phase  $\lambda_0$ . It is important to make a choice of  $N$  and  $\lambda_0$  for TASS and JPL with difference time spans.

Figure (4.10) shows the difference between JPL and TASS of  $z$  in 1,000 years.  $z$  is equal to  $e \exp \sqrt{-1} \varpi$ . The red curve is its real part  $e \cos \varpi$ , and the blue curve is its imaginary part  $e \sin \varpi$ . The difference between both ephemerides is about 200 km during 1,000 years.

Figure (4.11) shows the difference between JPL and TASS in 1,000 years, for  $\zeta$ , which is identified as  $\zeta = \sin \frac{i}{2} \exp \sqrt{-1} \Omega$ . The red curve is its real part  $\sin \frac{i}{2} \cos \Omega$  and the blue curve is its imaginary part,  $\sin \frac{i}{2} \sin \Omega$ . Figure (4.12) is a partial enlargement of Figure (4.11) from 1900 to 2100.

It is clear in the partial enlargement of the figure that the difference in  $\zeta$  is about 60 kilometers over the recent 200 years. It is not a big difference and it confirms the fact that both ephemerides are close during the period where we have observations.

Figure 4.8: Difference between JPL and TASS of the osculating element  $\lambda$  of Titan over 1,000 years.

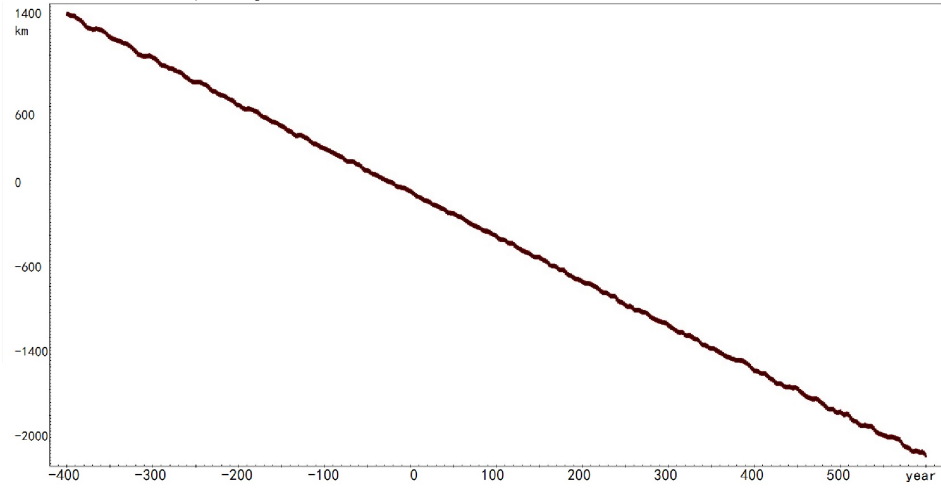


Figure 4.9: Partial enlargement of Figure (4.8) over 160 years, 1940-2100

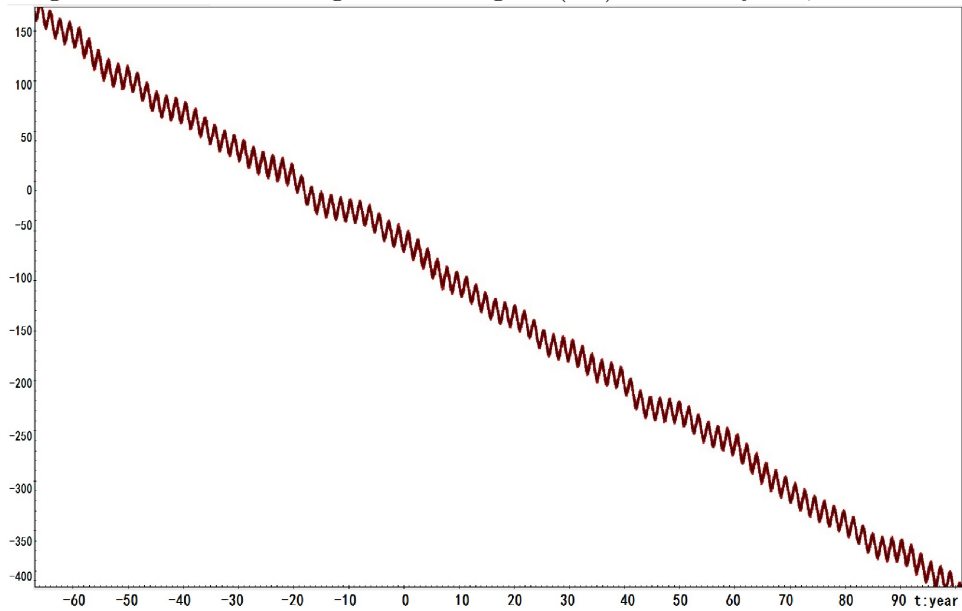


Figure 4.10: Difference between JPL and TASS ephemerides of Titan over 1,000 years, for the osculating element  $z$ , 1600-2600

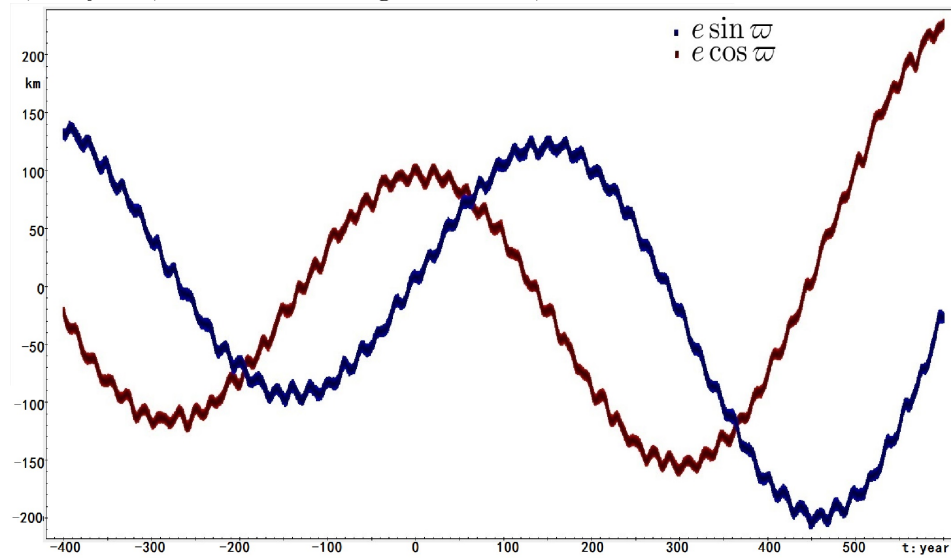


Figure 4.11: Difference between JPL and TASS ephemerides of Titan over 1,000 years, 1600-2600, in osculating element  $\zeta$

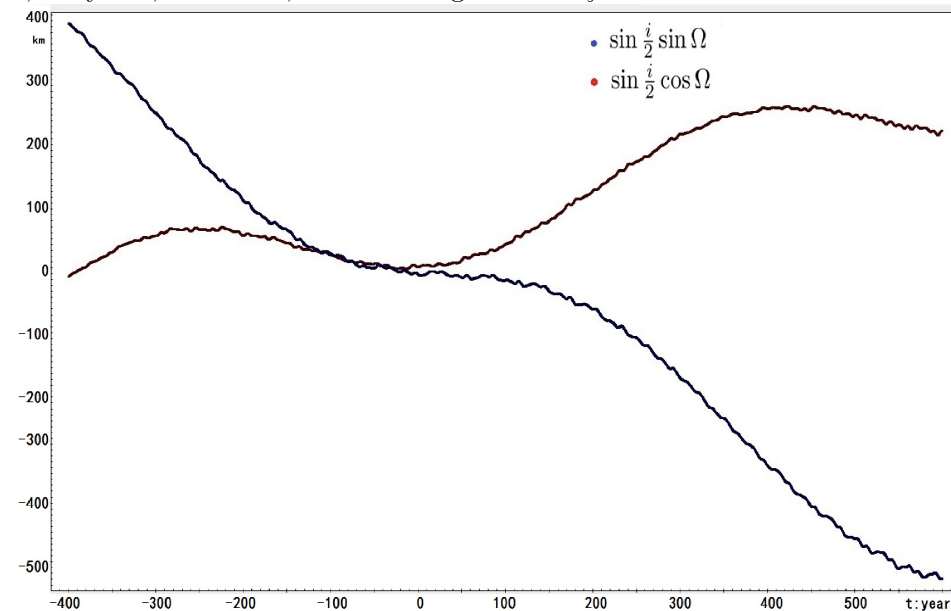
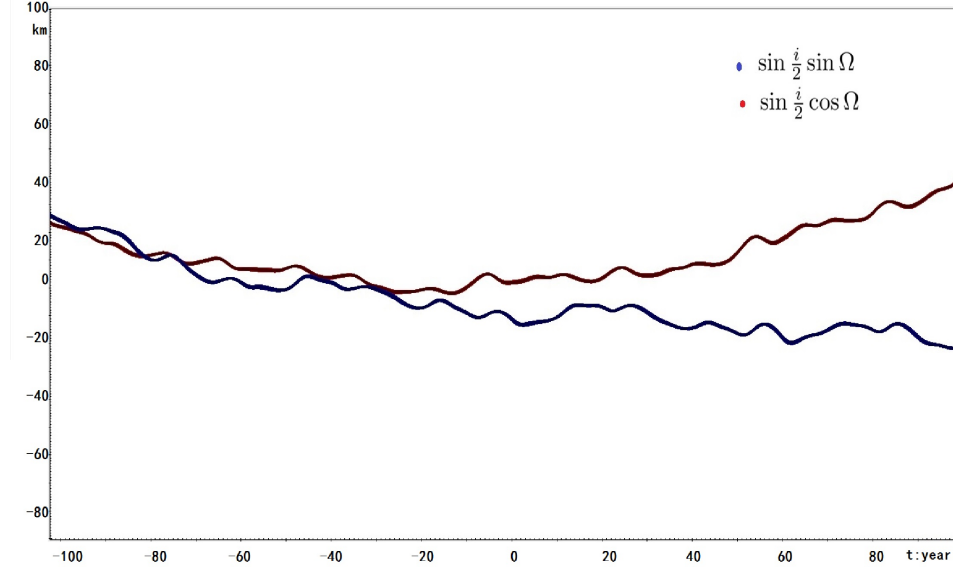


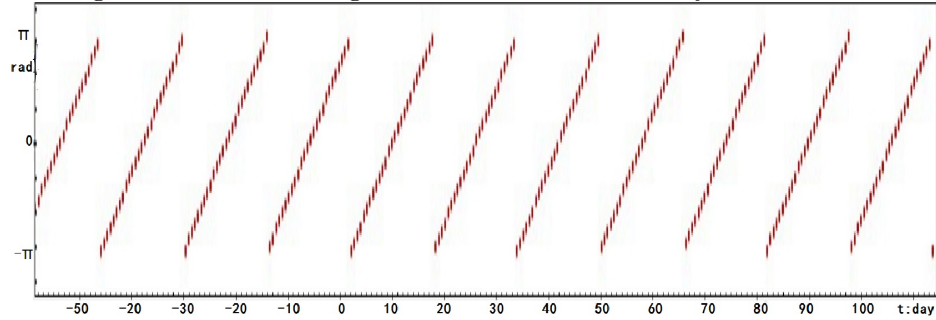
Figure 4.12: Same as Figure (4.11) with enlargement over 200 years, 1900-2100



## 4.2 The main slope in mean longitude : $N$ and $\lambda_0$

The mean longitude of Titan  $\lambda_6$  is a quasi periodic variable with a cycle of about 16 days into  $[-\pi, \pi)$  (and  $[0, 2\pi)$  in JPL). The time interval in Figure (4.13) is about 200 days. Here, we take 0.6 day for the time step.

Figure 4.13: Mean longitude  $\lambda$  of Titan in 200 days with TASS.



We need to add  $2\pi$  to  $\lambda_6$  at the end of every loop to make  $\lambda_6$  linear with time. Then we can get the mean mean motion of  $\lambda_6$  as a slope (Figure 4.14).

We calculate the mean mean motion with 1,000 years  $\lambda_6$  in TASS, which is called  $N_{T1}$  for short. Similarly,  $N_{T10}$  is the mean mean motion of 10,000 years  $\lambda_6$  in TASS, and  $N_{J1}$  signifies the mean mean motion with 1,000 years  $\lambda_6$  in JPL.

In our calculations, we deal with the same data by two different methods. The first one is the least squares method for which we suppose that  $\lambda_6$  is linear in time: the mean mean motion  $N$  is the slope of the equation  $\lambda_6 \approx N \times t + \lambda_0$ , and  $\lambda_0$  is a constant term that called the phase in the frequency analysis. The other way is to consider  $(\cos \lambda_6, \sin \lambda_6)$  in the frequency space.  $N$  and  $\lambda_0$  are the frequency and the phase of the biggest component in the spectrum.

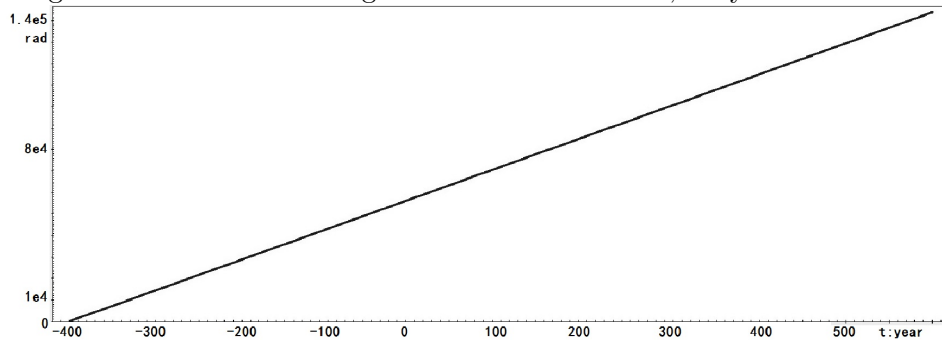
We show the results in Table 4.1. Here, we have the results from both methods, in 1,000 and 10,000 years for TASS and in 1,000 years for JPL. We take the following subscripts to separate values, J for JPL, T for TASS, 1 for 1,000 years and 10 for 10,000 years. Then  $N_{T10}$  means the mean mean motion of TASS over 10,000 years. In the same way, we take FA for Frequency Analysis, and LSM for Least Squares Method. Note that the line from FA over 1,000 years is noted ‘‘TASS-s’’ but we will see in Sect.4.4 that we have to adopt  $\lambda_{T10}$  for TASS-s (and then for JPL).

Table 4.1: The frequency of the mean mean motion  $N$  and phase  $\lambda_0$  of TASS and JPL for different intervals.

	Span (year)	ID	Frequency (rad/year)	ID	$\lambda_0$ (rad)	Method
TASS-t	10,000	$N_{T10}$	143.924047849167	$\lambda_{T10}$	5.71887846	FA
TASS			143.924047828061		5.71891639	LSM
TASS-s	1,000	$N_{T1}$	143.924047835237	$\lambda_{T1}$	5.71754788	FA
TASS			143.924047832049		5.71748146	LSM
JPL	1,000	$N_{J1}$	143.924045534754	$\lambda_{J1}$	5.71749214	FA
			143.924045017377		5.71742743	LSM

The difference  $2.110542 \times 10^{-8}$  rad/year between  $N_{T10}$  (FA) and  $N_{T10}$  (LSM) is not very obvious to evaluate. Hence, it is better to take the difference in kilometers. Then, over 1,000 years, the difference in position is about 25 km (and 250 km for 10,000 years). It is not a big difference. We can

Figure 4.14: The mean longitude of Titan  $\lambda$  over 1,000 year with TASS.



consider that for the mean mean motion of 10,000 years TASS ephemeris, both methods FA and LSM give the same results. We also consider that the two  $N_{T1}$  obtained by both FA and LSM are the same (and idem for  $N_{J1}$ ). From now on we take  $N_{T10} = 143.924047849167$  rad/year as the mean mean motion  $N$  of TASS ephemeris for Titan.

We have to note that, from the principle of FA and LSM, even though the difference in their results are very small (now, in  $N$  and  $\lambda_0$ ), LSM can perturb the constant  $\lambda_0$ , if there exist some long period components in  $\lambda_6$ . So on all the situations we prefer to take the results of FA.

Now we discuss the difference between  $N_{T10}$  and  $N_{T1}$ (LSM), that is more meaningful for us. The difference is about  $1.7118 \times 10^{-5}$  rad over 1,000 years, which means 21km in position, which is even smaller than the difference caused by the different methods and even far beyond the accuracy that we need. Hence, we account that both methods find the same value of the mean mean motion in our calculations, no matter the interval or ephemeris.

In the following work, when we talk about the mean mean motion of Titan in TASS, we will use the value of  $N_{T10} = 143.924047849167$  rad/year from the frequency analysis. We will use  $N_{J1} = 143.924045534754$  rad/year from the frequency analysis as the parameter of mean mean motion of Titan in JPL.

### 4.3 Comparison in $r$ between TASS and JPL

#### 4.3.1 The periodic part $r = \lambda - Nt - \lambda_0$

Now, the mean longitude  $\lambda$  of Titan can be described as a sum of three parts. The linear part  $Nt$ , the constant  $\lambda_0$ , and the smaller part which can be described as a sum of periodic terms. The argument of each one is a combination of the proper frequencies :

$$\lambda = Nt + \lambda_0 + \sum_{i=1}^m A_i \sin(\omega_i t + \phi_i) \quad (4.3.1)$$

$i$  is the number of the term.

$\lambda_0$  is the constant in  $\lambda$ .

$N \times t + \lambda_0$  is the affine part of  $\lambda$ .

$A_i \sin(\omega_i t + \phi_i)$  is one of the components of mean longitude.

$A_i$  is the amplitude of the term.

$\phi_i$  is the phase of the term.

$\omega_i$  is the frequency of the term

Removing the major linear part of the mean longitude ( $N \times t$  and  $\lambda_0$ ), we can get a combination only depending on the proper frequencies, which is cyclical in time, with invariable slight amplitudes. We define  $r$  as:



$$r = \lambda - Nt - \lambda_0 = \sum_{i=1}^n A_i \sin(\omega_i t + \phi_i) \quad (4.3.2)$$

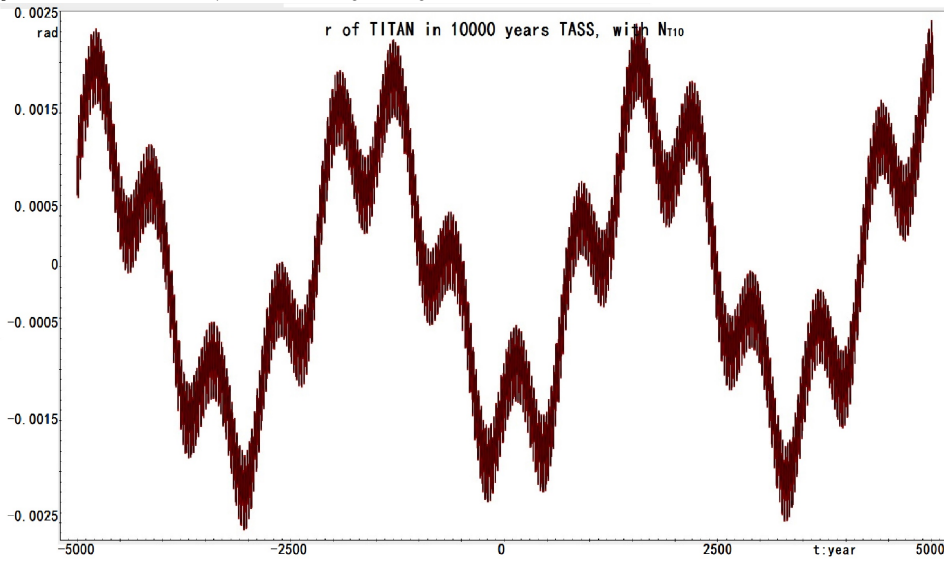
where

$$\omega_i = \sum_{j=1}^m k_{i,j} \omega_j^* \quad (4.3.3)$$

The frequencies  $\omega_j^*$  are the proper frequencies as described in Chapter 3.

An analytical ephemeris like TASS has a complete representation of proper frequencies and other parameters with the Saturn system. It is convenient to get the combination of  $r$  in TASS with a frequency analysis. In Figure (4.15), we multiply by the semi-major axis of Titan, so the unit of  $r$  here is the kilometer.

Figure 4.15: The periodic part  $r$  of the mean longitude of Titan over 10,000 years with TASS, with  $N_{T10} \lambda_{T10}$



In TASS, to describe the combination of  $r$  with Equation (4.3.2) is very simple by a frequency analysis. Using the mean longitude of Titan in 10,000 years, the step of calculation is taken as 0.6 day. Based on the report of Saillentest (Saillentest 2014 [17]), the choice of the step is very important. It influences the sampling point number, and improves the frequency resolution, but reduces the precision of the amplitude determination. In total, there are 610,000 points of  $r$  during 10,000 years. The frequency analysis transfers all these data into the frequency space. Next, comparing the components to the proper frequencies of TASS, it is possible to find the good combinations based on the d'Alembert rule. Finally, we get the analytical

representation of mean longitude of Titan with TASS ephemeris like Table 10.2 in Appendix.

Table 10.2, TASS-t, is a template of the amplitude and phase of the 9 major components in  $r$  of Titan with a frequency analysis of TASS. Those components include not only the long-periodic terms, like  $\Omega_8$ , which has a period larger than 3,000 years, but also short periodic terms, like  $\lambda_5 - \lambda_6$  with a very small period of 6.03 days. Moreover, we can distinguish the perturbations from the Saturn system like  $\Omega_8, -\Omega_6, 2\varpi_6$ , and  $\lambda_5 - \lambda_6$ , or from the outer Saturn system, like the three harmonic terms of the mean longitude of the Sun  $\lambda_s, 2\lambda_s$  and  $3\lambda_s$ .

There is a component with the frequency 0.0068679973 rad/year, named  $\Lambda_6^*$ . It is difficult to identify it in the range  $\varpi_6^* - \varpi_8^*$ ,  $-\Omega_6^* + \Omega_8^*$ , and  $2\lambda_J^* - 5\lambda_S^*$ . Their periods are similar, and we have no way to make the identification of this frequency. In TASS, this term is considered as the perturbation from the 2:5 resonance between Jupiter and Saturn.

For the JPL ephemeris we do not know anything about the proper frequencies, even if they exist or not. With a time span of 1,000 years, it is uncertain that we could distinguish these proper frequencies in most components.

As Laskar (Laskar.J et al. 1992 [15]) said, “If the system is integrable, without managing to find exactly the action-angle variables  $W^*$ , but variable  $W$  near  $W^*$ , the motion are still on torus but the projection on each  $W_j$  is not a circular motion.” In another words, the proper frequencies of JPL can be found by a frequency analysis of the osculating orbital elements.

That means, for JPL, we can use FA to get the proper frequencies. However, the combination of the mean longitude of Titan is more complicated. FA program can not distinguish the long period terms, instead, it mixes all the long time span components together. We need another way, for example, the least squares method, to identify the combinations of JPL.

Before we discuss about the proper frequency of JPL, we will represent our results with TASS over 1,000 years, during 1600-2600, which is the same interval as JPL. We take TASS ephemeris over 1,000 years as a test to improve our method, which is also useful for JPL. That will be done in Chapter 6 and will lead to TASS-s.

### 4.3.2 The comparison

Figure (4.16) shows the difference between  $r$  in JPL and in TASS with their own  $\lambda_0$  ( $\lambda_{T1}$  for TASS,  $\lambda_{J1}$  for JPL) over 1,000 years. In this figure, the difference is reduced and evolves from 70 km to  $-70$  km over 1,000 years, and tends toward 0 near J2000.0. When we change their own  $\lambda_0$  of 1,000 years by  $\lambda_{T10}$ , the Figure (4.17) shows the same tendency as in Figure (4.16).

When we take those two differences above together in Figure (4.18), they present similar changes, and the discrepancy between maximum and

minimum values is about  $\pm 70$  km over 1,000 years, which is close to the difference of the mean longitude between TASS and JPL at J2000.0 epoch. The perturbation parts of the mean longitude in TASS and JPL are similar, but their difference seem quasi-periodic. It means that, in TASS and JPL, the value of  $r$  depends on the  $\lambda_0$  used. The problem is now to choose the suitable  $\lambda_0$  both for TASS-s and JPL.

Figure 4.16: The difference between  $r$  of TASS and JPL ephemerides with their own  $\lambda_0$  (with  $\lambda_{T1}$  and  $\lambda_{J1}$  respectively)

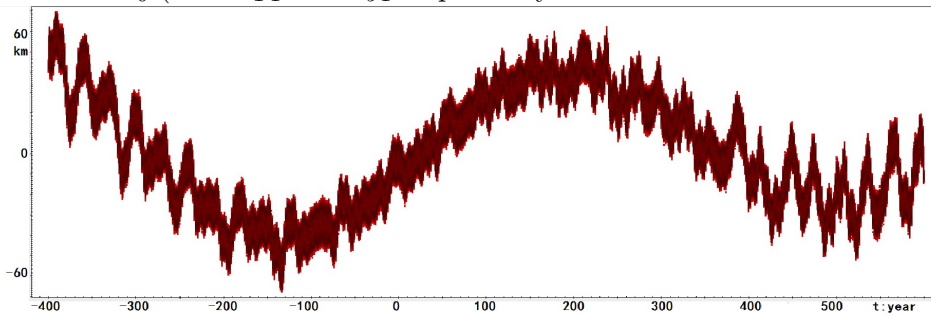


Figure 4.17: The difference between  $r$  of TASS and JPL ephemerides (with  $\lambda_{T10}$  and  $\lambda_{J1}$  respectively)

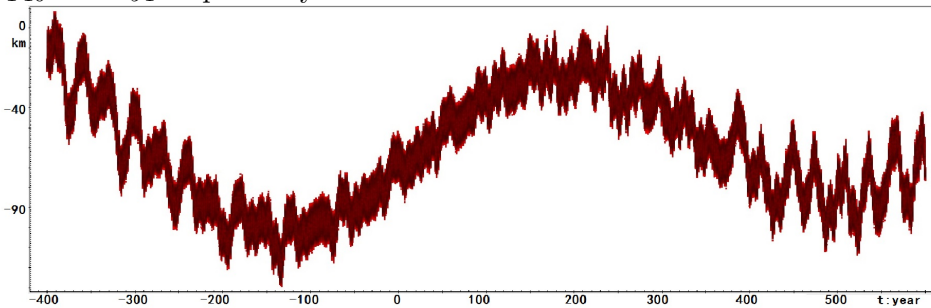
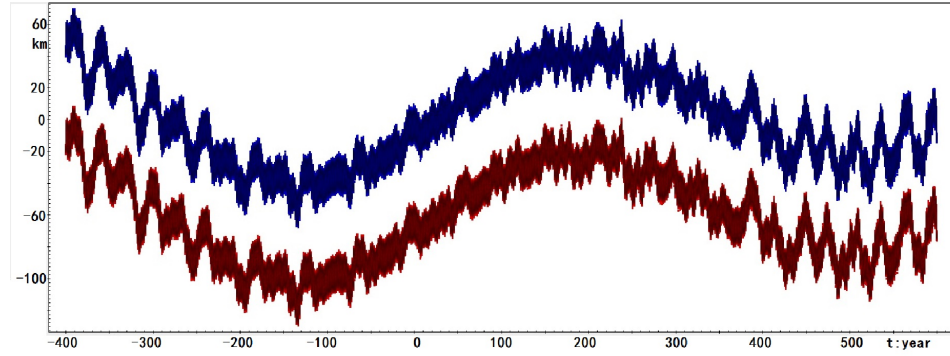


Figure 4.18: The difference between  $r$  of TASS and JPL ephemerides with  $\lambda_{T10}$ ,  $\lambda_{T1}$  and  $\lambda_{J1}$



## 4.4 Correlation of $\lambda_0$ with the time span

### 4.4.1 $\lambda_0$ of TASS

The situation of  $\lambda_0$  is more complicated. The results obtained not only for different durations, but also for the same interval by two methods, are different. Let us take  $\lambda_{T10}$  in two methods as an example. Figure (4.19) is the graphics of two  $r$ , of the mean longitude of Titan in TASS with the same mean mean motion  $N_{T10}$ , but different  $\lambda_0$ , in 10,000 years. The x axis is the time in years. The y axis is the amplitude of  $r$  in kilometers. In the figure, the two curves basically coincide. Comparing with the amplitude of  $r$ , the differences are hard to find, but we can get their difference in Table 4.1.

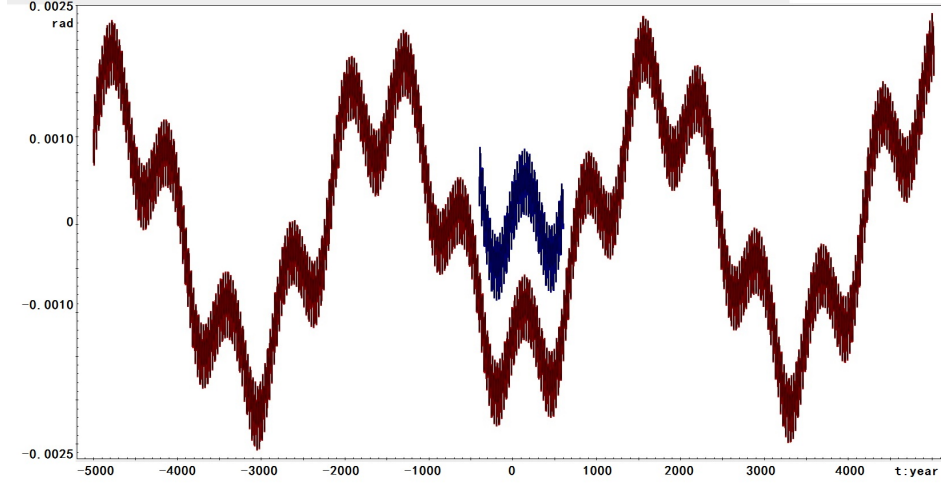
$\Delta\lambda_0$  can not be ignored, so we have to decide which value of  $\lambda_0$  to take. Here, we need to think about the principle of both methods. The frequency analysis distinguishes all the components of the frequencies, that eliminates the influences coming from the long-period terms, also in the least squares method they are usually considered as constants into  $\lambda_0$ . Then, we choose the value of  $\lambda_{T10}$  from FA and not from LSM over 10,000 years mean longitude in TASS in our following calculations.

Subsequently, it is necessary to make a choice between  $\lambda_{T10}$  and  $\lambda_{T1}$ . Figure (4.19) is an image of two different situations with TASS ephemeris.

-The  $r$  in red, is the result coming from  $\lambda_{T10}$ , which we get from TASS-t.

-The  $r$  in blue, is the result coming with  $\lambda_{T1}$ , which we get from 1,000 years ephemeris. To be clearer, we show only  $r$  blue over 1,000 years. The offset is  $-39$  km.

The conclusion is very clear:  $\lambda_{T10}$  is the best choice which we shall use in all other calculations for TASS-s.  $\lambda_{T1}$  makes the range of  $r$  symmetrical about  $r = 0$ . However comparing with 10,000 years result,  $\lambda_{T1}$  bring the

Figure 4.19:  $r$  of Titan in TASS with  $\lambda_{T1}$  and  $\lambda_{T10}$ 

deviation to  $r$ .

There is no doubt that,  $\lambda_{T10}$ , which we get from TASS-t is the most reasonable value, that we should use in all the calculation with TASS, no matter the span of ephemeris.

#### 4.4.2 $\lambda_0$ of JPL

The  $\lambda_0$  of JPL behaves as we have discussed in the case of TASS. Both results approximate the value of the mean longitude of Titan in J2000.0 epoch, which corresponds to the characteristics of the ephemeris. However, these values of  $\lambda_{J1}$  are not the ones expected.

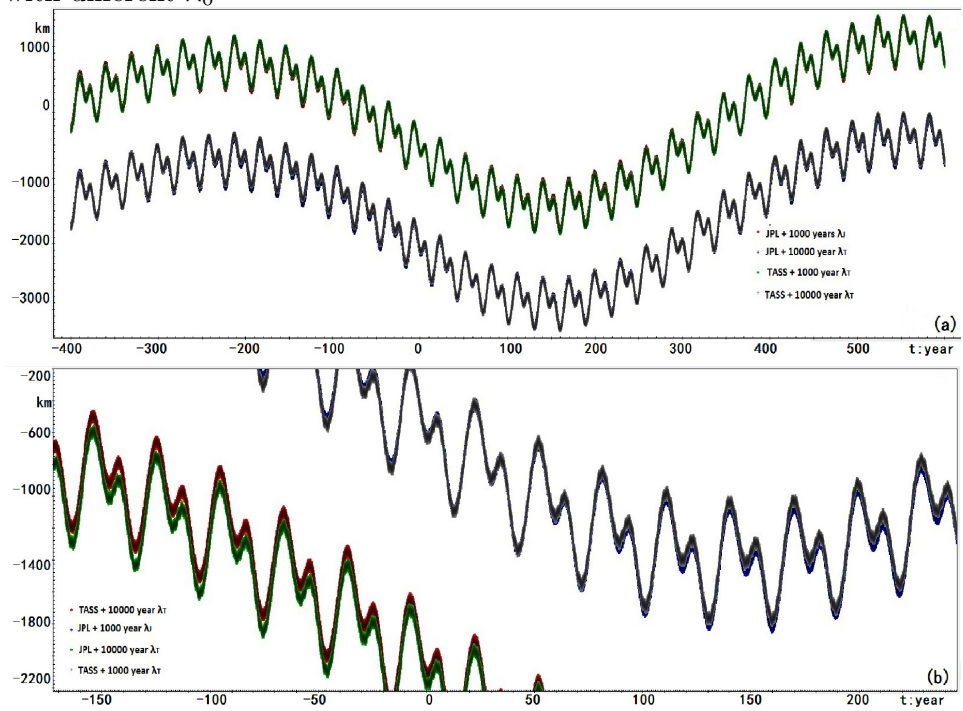
In this section, we have a problem in the JPL ephemeris, that it has only 1,000 years data. That means, it is no way to get a suitable  $\lambda_0$  of JPL over 10,000 years. We have showed in Figure (4.8) the difference between mean longitude of Titan of TASS and JPL in 1,000 years.

In Table 4.1, we know the values of the mean longitude of Titan of TASS and JPL. We can find that the difference between  $\lambda_0$  in 1,000 years TASS and JPL is  $\Delta\lambda = \lambda_{T1} - \lambda_{J1} = 5.574 \times 10^{-5}$  rad, which mean a difference about 68.11 km in position. It is smaller than the difference between  $\lambda_{T10}$  and  $\lambda_{J1}$ , which is  $1.386319 \times 10^{-3}$  rad, and 1693.90 km in position. TASS and JPL correspond to the same physical system especially for the position and velocity of satellites.

Then we have a strong presumption that  $\lambda_{T10}$  should be a better choice than others. Moreover the values of  $\lambda_{T1}$  and  $\lambda_{J1}$  are so close that the value of  $\lambda_{J10}$  if it does exist, should be closer to  $\lambda_{T10}$  than to  $\lambda_{J1}$ .

Figure (4.20) shows  $r$  of TASS and JPL in 1,000 years. The different

Figure 4.20: The comparison between two  $r$  in TASS and JPL ephemerides with different  $\lambda_0$



curves correspond to the different  $\lambda_0$  to obtain  $r$ . We distinguish different situations in different colors:

- The red curve is  $r$  of TASS with  $\lambda_{T10}$ ;
- The green curve is  $r$  of JPL with  $\lambda_{T10}$ ;
- The blue curve is  $r$  of JPL with  $\lambda_{J1}$ ;
- The grey curve is  $r$  of TASS with  $\lambda_{T1}$ .

The colors in Figure (4.20a) are difficult to distinguish, so we make an enlargement in the Figure (4.20b) over 200 years around J2000.0.

With  $\lambda_{J1}$ ,  $r$  fluctuates around 0, however  $\lambda_{T10}$  brings a big deviation away from 0. It is the same as TASS, when we take  $\lambda_{T10}$ , and  $\lambda_{T1}$ .

It exists a very interesting situation which should support our assumption. The two  $r$  for JPL with  $\lambda_{T10}$  and  $\lambda_{J1}$ , demonstrate a similar distribution in values like the two  $r$  for TASS with  $\lambda_{T10}$  and  $\lambda_{T1}$ , especially in Figure (4.20b) (200 years). On the top of the figure, two  $r$  (grey for TASS and blue JPL), almost coincided. On the bottom of the figure, two  $r$  (red for TASS and green from JPL) with  $\lambda_{T10}$ , even from the beginning of them, are a little bit larger than the one above, but also keep their global resemblance.

In summary, we prefer the  $\lambda_{T10}$  from TASS-t as the value of constant  $\lambda_0$  than the one  $\lambda_{J1}$  from JPL itself,  $\lambda_{T10}$  is the most approached value, that we can get, from the real  $\lambda_0$  from 10,000 years JPL.

## 4.5 Conclusion

In this section, we compare the two kinds of ephemerides of Titan in their osculating Keplerian elements and their positions in 1,000 years interval. Additional, we focus on the time span over 200 years around J2000.0 epoch, during which the ephemeris has the best precision. It is clear that in recently 200 years (1900-2100) those differences keep stable.

For the difference in their osculating Keplerian elements, the situations are different. In  $\zeta$ , the difference is smaller than 1,000km over 1,000 years, which during 1,900-2,100, it is about 60km. The difference in  $z$  is more stable that it seems quasi-period changed with amplitude no more than 400km over 1,000 years. However, the difference between two  $\lambda$  over 1,000 years is more than 3,000km. In fact, it is not a real difference in  $\lambda$ , but a superposition error coming from the difference of the mean mean motion over many cycles. When we remove the influence from the mean mean motion and the constant term  $\lambda_0$ , the difference is about  $\pm 70$ km over 1,000 years.

The different intervals of ephemerides make nothing wrong with mean mean motion in recent precision. However, it influences the values of  $\lambda_0$ . Then, we can not use  $\lambda_{T1}$  or  $\lambda_{J1}$  directly. For TASS, the best choice is

$\lambda_{T10}$ . Although it seems to bring some deviation to  $r$ , it is in accordance with 10,000 years mean longitude. Based on a discussion of the similarities between two ephemerides, it is better to use  $\lambda_{T10}$  in the calculations of  $r$  in 1,000 years JPL ephemeris also.  $\lambda_{T10}$  is closer to the real  $\lambda_0$  of JPL with longer span.

Therefore, in our following work of getting the combination of  $r$  in JPL ephemeris, we will use  $\lambda_{T10}$  as  $\lambda_0$  in J2000.0 epoch of Titan, which is obtained from TASS-t.

Last but important in this chapter, in the calculation of the mean mean motion  $N$  and the constant term  $\lambda_0$ , the results show us that the least squares method and the frequency analysis are almost equivalent.



## Chapter 5

# Extension of the frequency analysis by the least squares method

Based on the descriptions in chapters aforesaid, we have a basic understanding of the structure of the numerical integration ephemeris and the theory analysis ephemeris. Moreover, we compare the difference between JPL and TASS in ephemerides of Titan. We suppose that it is possible to find in JPL a similar representation of the mean longitude of Titan.

In the representation of the mean longitude in TASS-t, Table 10.2 in Appendix, the biggest component  $\Omega_8^*$  attracts our attention because it is a particular term with a long period, over 3263.24 years and a large amplitude, about 1903.38 kilometers.  $\Omega_8^*$  is the major part of the longitude of the ascending node of Iapetus. The interval of JPL ephemeris, which is only 1000 years, is far away from a complete cycle of  $\Omega_8^*$ . In other words, if we can find a similar term in JPL ephemeris like  $\Omega_8^*$  in TASS, it should be a good evidence to our purpose to find the proper frequency and the representation of the osculating elements with this ephemeris.

Unfortunately we can not use the frequency analysis to obtain directly the amplitude and phase of the term associated to  $\Omega_8^*$ . Further worse we know nothing about the proper frequency of JPL ephemeris. However we have two different descriptions of the same Saturn system, and from our comparison between two ephemeris made in Chapter 4, we consider that it may exist a relation between two ephemeris. So we can use the proper frequency of TASS-t for the JPL ephemeris as an experiment. By that, it should expose not only some resemblance from JPL to TASS, but also the possible existence of proper frequencies and combinations of osculating elements in JPL.

## 5.1 The least squares method, term by term

First of all, we remove the major part of the mean longitude, i.e. the mean mean motion changing over time  $N \times t$  and the constant part  $\lambda_0$ . The residual part is identified as  $r$  in the previous chapter. If we want to find the first term in  $r$ , we remove all the other 8 terms with the proper frequencies, amplitudes, and phases, listed in the representation TASS-t in Table 10.2 :

$$A_1 \sin(\omega_1 t + \phi_1) = r - \sum_{i=2}^n A_i \sin(\omega_i t + \phi_i) \quad (5.1.1)$$

with

$$A_1 \sin(\omega_1 t + \phi_1) = A_1 [\sin(\omega_1 t) \cos \phi_1 + \cos(\omega_1 t) \sin \phi_1] \quad (5.1.2)$$

Let us write :

$$r - \sum_{i=2}^n A_i \sin(\omega_i t + \phi_i) = Y_{1,t} \quad (5.1.3)$$

Then we separate the biggest component of  $r$  (with  $\Omega_8^*$ ) and subscript as  $Y_{1,t}$  in equation (5.1.3). It is a series with a step of 0.6 days over 1000 years. Then we take the value of  $\Omega_8^*$  from TASS-t as the proper frequency, which is noted  $\omega_1$  in Equation (5.1.2).

Then we take the unknown variables of the equations as :

$$\begin{cases} a_1 = A_1 \cos(\phi_1) \\ a_2 = A_1 \sin(\phi_1) \end{cases} \quad (5.1.4)$$

The known variables  $X_{1,1}, X_{1,2}$  also change with time with a step of 0.6 days :

$$\begin{cases} \sin(\omega_1 t) = X_{t,1} \\ \cos(\omega_1 t) = X_{t,2} \end{cases} \quad (5.1.5)$$

During the 1,000 years, with the step of 0.6 days, we have a huge equations group, which includes  $m = 608,750$  equations, with only two unknown variables. Then, it is easy to make some simple transfers and to use a least squares method to calculate the amplitude  $A_1$  and phase  $\phi_1$ .

$$\begin{aligned} a_1 X_{1,1} + a_2 X_{1,2} &= Y_{1,t_1} \\ a_1 X_{2,1} + a_2 X_{2,2} &= Y_{1,t_2} \\ &\dots \\ a_1 X_{m,1} + a_2 X_{m,2} &= Y_{1,t_m} \end{aligned} \quad (5.1.6)$$

$$\begin{pmatrix} X_{1,1} & X_{1,2} \\ \vdots & \vdots \\ X_{m,1} & X_{m,2} \end{pmatrix} \begin{pmatrix} a_1 \\ a_2 \end{pmatrix} = \begin{pmatrix} Y_{1,t_1} \\ \vdots \\ Y_{1,t_m} \end{pmatrix} \quad (5.1.7)$$

Let us left multiply the transpose of matrix  $(X_{i,1}, X_{i,2})^T$  on both side of equation (5.1.7), we can get the equations of  $(a_1, a_2)$  :

$$\begin{pmatrix} X_{1,1} & \cdots & X_{m,1} \\ X_{1,2} & \cdots & X_{m,2} \end{pmatrix} \begin{pmatrix} X_{1,1} & X_{1,2} \\ \vdots & \vdots \\ X_{m,1} & X_{m,2} \end{pmatrix} \begin{pmatrix} a_1 \\ a_2 \end{pmatrix} = \begin{pmatrix} X_{1,1} & \cdots & X_{m,1} \\ X_{1,2} & \cdots & X_{m,2} \end{pmatrix} \begin{pmatrix} Y_{1,t_1} \\ \vdots \\ Y_{1,t_m} \end{pmatrix}$$

$$\begin{pmatrix} \sum_{i=1}^m X_{i,1}^2 & \sum_{i=1}^m X_{i,1}X_{i,2} \\ \sum_{i=1}^m X_{i,1}X_{i,2} & \sum_{i=1}^m X_{i,2}^2 \end{pmatrix} \begin{pmatrix} a_1 \\ a_2 \end{pmatrix} = \begin{pmatrix} \sum_{i=1}^m X_{i,1}Y_{1,t_i} \\ \sum_{i=1}^m X_{i,2}Y_{1,t_i} \end{pmatrix} \quad (5.1.8)$$

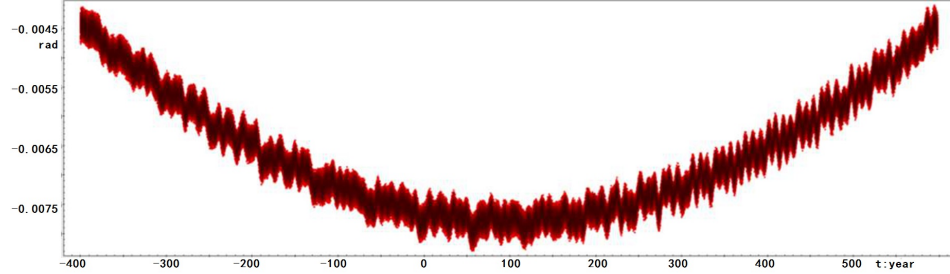
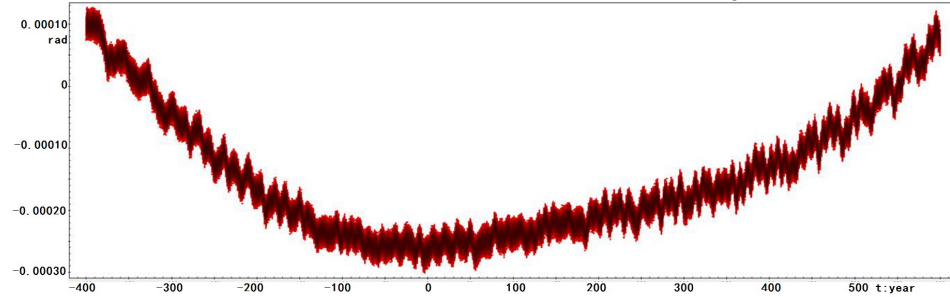
Based on the solution of Equation (5.1.8),  $(A_1 \cos(\phi_1), A_1 \cos(\phi_1))$ , it is easy to get the amplitude  $A_1$  and phase  $\phi_1$  of the biggest component of  $r$  in the mean longitude of Titan.

It is the well-known procedure of the least squares method. But we prefer to use (5.1.8) instead of the two matrix in (5.1.7) to avoid including too many equations in the same time. Table 5.1 shows our results of amplitude and phase as an experience. We plot the curve of the residuals (5.1.3)  $Y_{1,t}$ , in Figure (5.2), and the curve of the similar residuals involved with TASS in Figure (5.1).

Table 5.1: Amplitude and phase of the component involved of  $\Omega_8$  in the mean longitude of Titan for TASS and for JPL

	Frequency(rad/year)	Period(year)
	0.001925441172	3264.24
	TASS	JPL
Amplitude (rad)	0.0007787385	0.00018501463
Phase(rad)	-1.3751233	-1.4551164

Figure (5.1) and Figure (5.2), exhibit complex frequency characteristics which can be approximated as a long-period change involving small short-period changes. To compare them, the envelope curve of TASS, Figure (5.1), is smoother and more regular than the one of JPL. Both curves show pulses, which are caused by the other faint short period terms that we did not list in Table 10.2. For Figure (5.2) even if the envelope of the curve is not as good as the one of TASS, it expresses the possibility of a similar existence of

Figure 5.1:  $Y_{1,t}$  of  $r$  removed other major components in TASS, involved  $\Omega_8^*$ Figure 5.2:  $Y_{1,t}$  of  $r$  in JPL ephemeris removed other major components with amplitude, phase and proper frequency of TASS,  $\Omega_8^*$ 

$\Omega_8^*$ , like in TASS. That means that the irregularity in Figure (5.2) is due to an unsuitable proper frequency with a false amplitude and phase. Moreover but not so important, we also see the truncation error caused by the unlisted faint amplitude terms of the combination.

We can proof the existence of  $\Omega_8^*$  by a term by term least squares method, but it is impossible to distinguish the value of every component in our calculations. Hence, the method used in this section, is not useful in practice. We prefer a least squares method including several terms.

## 5.2 Reference plane and transformation error

It is possible to find the major frequency component by analyzing the other osculating elements of JPL ephemeris, but we are not sure that it is the correct value. For example, we can get the proper frequency  $\Omega_8^*$  by making an analysis of the osculating element  $\zeta = \sin \frac{\zeta}{2} e^{i\Omega}$  of Iapetus. We will show the results in Chapter 6, TASS-s and the results for JPL ephemeris in Chapter 7.

Here we face a small problem coming from the reference plane. The JPL ephemeris takes the ecliptic plane as the reference plane. In our research

we prefer to take the ring plane of Saturn as the reference plane because the orbit of most Saturnian satellites are close to this plan. It is necessary to change the reference plane of JPL ephemeris from the ecliptic plane to the ring plane of Saturn. In this step, we need to think about the error of transformation.

As TASS gives the orbital elements in the ring plane as well as the positions and velocities in the ecliptic plane, we can inspect the transformation error of our software. The software takes the positions and the velocities of TASS ephemeris in the ecliptic plan, then it transforms them into the ring plane of Saturn in form of osculating elements  $(a, \lambda, z, \zeta)$ . By comparing the difference between the elements obtained by the transformation program, and the original output of TASS ephemeris, we show the magnitude of the error in our software.

Figures (5.3), (5.4) and (5.5) give the residuals of the reference plane transformation in the three orbital elements  $(\lambda, z, \zeta)$ . We only show the situation of the real part of  $z$  and  $\zeta$  in Figures (5.4) and (5.5). The errors from the transformation software are smaller than 120 meters over 1000 years. We do not know exactly the source of the error. The comparison should be exact as it is only a geometrical transformation, but the difference of 120 meters over 1000 years is small enough to be accepted. It does not bring other additional error to our results in the following calculations.

Figure 5.3: Residuals from the reference plane transformation for the mean longitude  $\lambda$  of Titan with TASS over 1000 years (unit of x-axis is year, unit of y-axis is kilometer)

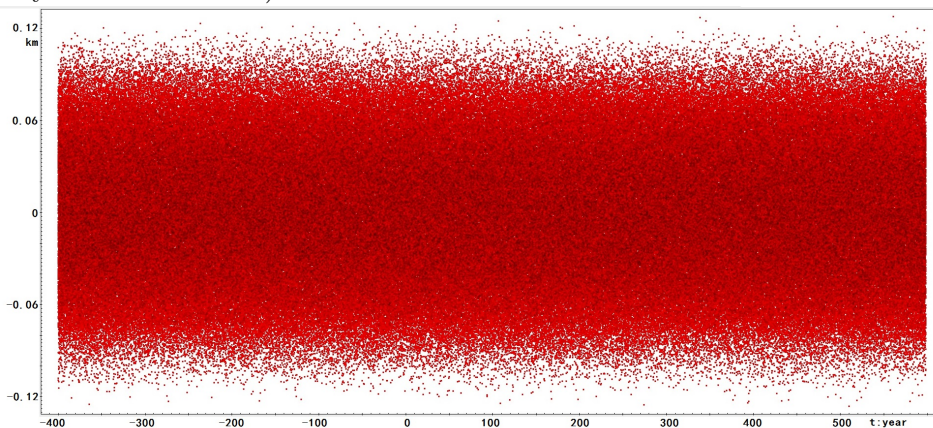


Figure 5.4: Residuals from the reference plane transformation for the element  $z$  of Titan with TASS over 1000 years (unit of x-axis is year, unit of y-axis is kilometer)

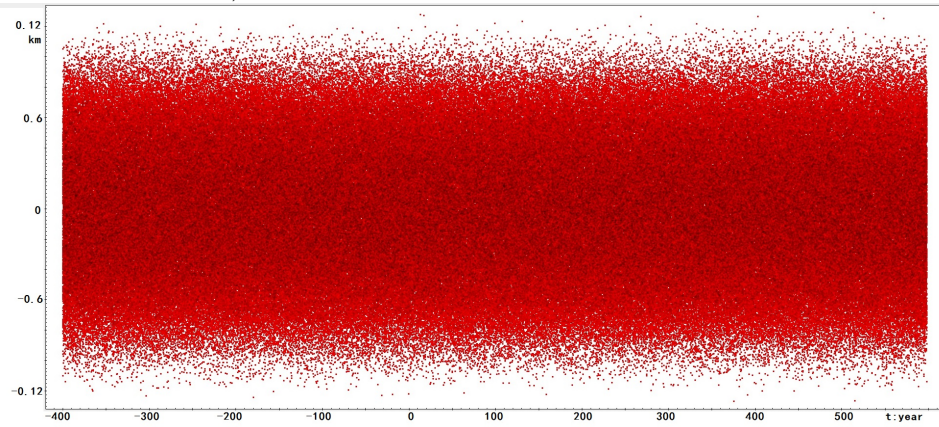
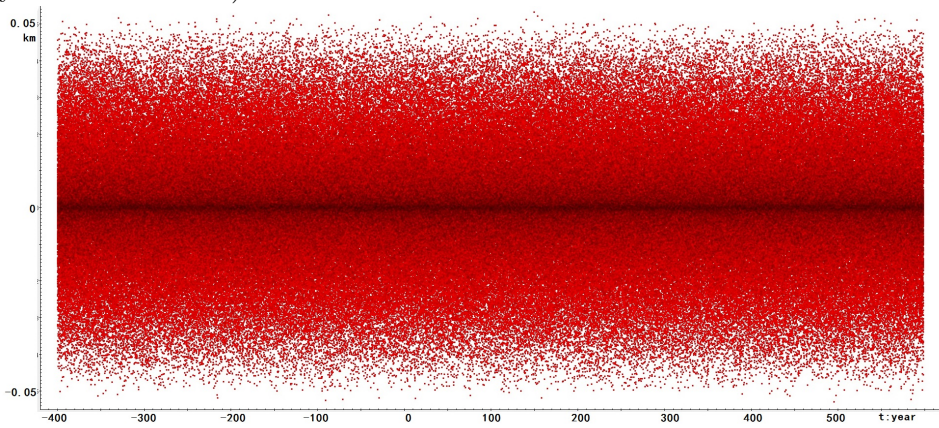


Figure 5.5: Residuals from the reference plane transformation for the element  $\zeta$  of Titan with TASS over 1000 years (unit of x-axis is year, unit of y-axis is kilometer)



### 5.3 The least squares method for several terms

During our calculations in Chapter 4 about the mean motion of Titan with both JPL and TASS, we have found that it is impossible to get the specific combinations by the frequency analysis of the mean longitude in 1000 years. We adopt the least squares method in our research of the representation of  $r$ .

In  $r$ , there are some short period terms, for example, the three terms involved in the mean longitude of the Sun, identified as  $\lambda_s$ ,  $2\lambda_s$ , and  $3\lambda_s$ . In fact, the mean longitude of the Sun which we used in TASS is the mean longitude of Saturn. These three terms have a period of several decades, that should be detected easily by the frequency analysis in the region close to the given value, and be removed with their amplitude and phase.

For the least squares method to get the combination of the other terms, we use:

$$Y(t) = \lambda - Nt - \sum_{i=1}^3 A_i \sin(k_i \omega_s t + \phi_i) \quad (5.3.1)$$

In  $Y(t)$ , we have removed the three components involved in the mean longitude of the Sun.

Unlike Sect. 5.1, we prefer to use the least squares method for several terms. So:

$$Y(t) = \sum_{i=1}^{n_t} A_i \sin(\omega_i t + \phi_i) \quad (5.3.2)$$

With a step of 0.6 day during 1000 years, we have 608700 equations for the mean longitude of Titan. We define  $[X]$  as the  $[m \times n]$  matrix of equations, and  $[A] = (a_1, a_2, \dots, a_n)$  as the one dimensional unknown matrix.  $m = 608700$ , is the number of equations.  $n$  is equal to the number of parameters, which is two times  $n_t$  the number of terms. For every step  $t_i$ , the frequency of phase and amplitude of the components does not change, the difference between every equation depends on the time and  $Y(t)$ . In other words, the amplitude and the phase of every component are the parameters of equations, from the least squares method, the equation is transformed to the first order multiple equations.

$$\begin{cases} \sin(\omega_1 t_i) = X_{i,1} \\ \cos(\omega_1 t_i) = X_{i,2} \\ \sin(\omega_2 t_i) = X_{i,3} \\ \dots \end{cases} \quad (5.3.3)$$

$$\begin{cases} a_1 = A_1 \sin \phi_1 \\ a_2 = A_1 \cos \phi_1 \\ a_3 = A_2 \sin \phi_2 \\ \dots \end{cases} \quad (5.3.4)$$

So the equation is written as :

$$\begin{cases} a_1 X_{1,1} + a_2 X_{1,2} + \dots + a_{n-1} X_{1,n-1} + a_n X_{1,n} = Y_{t_1} \\ a_1 X_{2,1} + a_2 X_{2,2} + \dots + a_{n-1} X_{2,n-1} + a_n X_{2,n} = Y_{t_2} \\ \dots \\ a_1 X_{m,1} + a_2 X_{m,2} + \dots + a_{n-1} X_{m,n-1} + a_n X_{m,n} = Y_{t_m} \end{cases} \quad (5.3.5)$$

$$\begin{pmatrix} X_{1,1} & X_{1,2} & \dots & X_{1,n-1} & X_{1,n} \\ \vdots & \vdots & & \vdots & \vdots \\ X_{m,1} & X_{m,2} & \dots & X_{m,n-1} & X_{m,n} \end{pmatrix} \begin{pmatrix} a_1 \\ \vdots \\ a_n \end{pmatrix} = \begin{pmatrix} Y_{t_1} \\ \vdots \\ Y_{t_m} \end{pmatrix}$$

In both sides of the equation, let us left multiply the transpose matrix  $[X]^T$  to simplify the equations. After this operation, the number of equations is simplified from 607800 to  $n$ , most of time  $n$  is equal to 10 or 12.

$$\begin{pmatrix} X_{1,1} & \dots & X_{m,1} \\ \vdots & & \vdots \\ X_{1,n} & \dots & X_{m,n} \end{pmatrix} \begin{pmatrix} X_{1,1} & \dots & X_{1,n} \\ \vdots & & \vdots \\ X_{m,1} & \dots & X_{m,n} \end{pmatrix} \begin{pmatrix} a_1 \\ \vdots \\ a_n \end{pmatrix} = \begin{pmatrix} X_{1,1} & \dots & X_{m,1} \\ \vdots & & \vdots \\ X_{1,n} & \dots & X_{m,n} \end{pmatrix} \begin{pmatrix} Y_{t_1} \\ \vdots \\ Y_{t_m} \end{pmatrix}$$

Finally, the equations are simplified like Equation (5.3.6):

$$(\mathcal{X}) \times (\mathcal{A}) = (\mathcal{Y}) \quad (5.3.6)$$

Here,

$$\mathcal{X} = \begin{pmatrix} \sum_{i=1}^m X_{i,1}^2 & \sum_{i=1}^m X_{i,1} X_{i,2} \dots & \sum_{i=1}^m X_{i,1} X_{i,n-1} & \sum_{i=1}^m X_{i,1} X_{i,n} \\ \vdots & \vdots & \vdots & \vdots \\ \sum_{i=1}^m X_{i,n} X_{i,1} & \sum_{i=1}^m X_{i,n} X_{i,2} \dots & \sum_{i=1}^m X_{i,n} X_{i,n-1} & \sum_{i=1}^m X_{i,n}^2 \end{pmatrix}$$

$$(\mathcal{A}) = \begin{pmatrix} a_1 \\ \vdots \\ a_n \end{pmatrix}$$



$$\mathcal{Y} = \begin{pmatrix} \sum_{i=1}^m X_{i,1} Y_{t_i} \\ \vdots \\ \sum_{i=1}^m X_{i,m} Y_{t_i} \end{pmatrix}$$

(5.3.6) allows to find the representation of the mean longitude of Titan for the JPL ephemeris. In the next chapter, we will take TASS ephemeris as an example to calculate TASS-s, the solution in 1000 years interval, and compare with TASS-t, the representation of TASS in 10,000 years. With this way, we can discuss the precision of the least squares method solutions.



## Chapter 6

# Test of the method with TASS over 1,000 years

Table 10.2 in the Appendix gives the presentation named TASS-t of the mean longitude of Titan with TASS over 10,000 years, which is easy to get by a frequency analysis. With a limited interval of the numerical integration ephemeris, for example with JPL in 1,000 years, the frequency analysis is difficult. Hence, we discuss the least squares method in the previous chapter to get a similar presentation with the numerical integration ephemeris.

After having designed a suitable method, we want to valid it by using TASS ephemeris itself limited in 1,000 years, as the period of JPL ephemeris. By constructing TASS-s in such way, we almost face the same difficulties that we will find with the numerical integration ephemeris. Furthermore, we will be able to estimate the accuracy of the method by comparing the parameters of TASS-s with the known values from TASS-t.

### 6.1 Proper frequencies

From our discussions in Chapter 4 we know that even if the proper frequencies have their consistency in the whole system, it does not mean that we could get the correct values of them during a limited interval. Therefore, in this chapter, we will use only the 1,000 years ephemeris with TASS to see if our method can find out the right value of the proper frequencies by the least squares method and the frequency analysis: it is very important to appraise our results of JPL of the next chapter.

As we focus on the mean longitude of Titan, we only discuss the proper frequencies involved in its representation, such as the mean mean motion of Rhea, the major part of the ascending node of Iapetus and Titan itself, the biggest frequency component of the pericenter of Iapetus and Titan, and an influence coming from the 2:5 resonance between Jupiter and Saturn.

In total, all the proper frequencies used in our representation are:

$\lambda_5^* (N_5)$	proper frequency of the mean longitude of Rhea.
$\lambda_6^* (N_6)$	proper frequency of the mean longitude of Titan.
$\varpi_6^*$	proper frequency of the pericenter of Titan.
$\varpi_8^*$	proper frequency of the pericenter of Iapetus.
$\Omega_6^*$	proper frequency of the ascending node of Titan.
$\Omega_8^*$	proper frequency of the ascending node of Iapetus.

The other values  $\Lambda_6^*$  and  $\lambda_s^* (N_s)$  used are directly taken from the system value of TASS-t.

We use the frequency analysis of the corresponding element of the satellite. The major component in this analysis is the value of their proper frequency. For example, we make an analysis of  $z_6$  in order to get the frequency of  $\varpi_6^*$ . Here, we only focus on the frequency instead of the phase and amplitude. These quantities depend on the initial time, unit of distance, and other system parameters.

#### Mean mean motion of Rhea: $\lambda_5^*$

Tables 6.1 and 6.2 give the representations of the mean longitude of Rhea, with different intervals of ephemerides. More exactly it is  $\exp \sqrt{-1} \lambda_5$  to avoid the discontinuity and to obtain  $\lambda_5^*$ . Table 6.1 is obtained with 10,000 years ephemeris of Rhea in TASS, and Table 6.2 the frequency analysis result within 1,000 years ephemeris, from 1,600-2,600. We take the series  $(\cos \lambda_5, \sin \lambda_5)$  as the input form, with a step of 0.6 day.

We begin our calculations with the proper frequency of the mean longitude of Rhea in TASS that we have experimented to get the mean mean motion of Titan by a frequency analysis. With the results both over 1,000 years and over 10,000 years intervals. The situation is similar as in the mean longitude of Titan : the difference between the value of frequency is tiny and that of the phase in J2000.0 epoch is much bigger.

The difference in frequency is  $\Delta f = -9.2949 \times 10^{-08}$  rad/y. It means a  $-49$  km difference in position after 1,000 years. It is tiny enough to use the value of the mean longitude of Rhea which we get from 1,000 years ephemeris as the proper frequency of the whole system.

Table 6.1: Representation for ephemeris in TASS during 10,000 years : The mean longitude of Rhea  $e^{\sqrt{-1}\lambda_5}$ 

	Frequency (rad/year)	Amplitude (rad)	Phase (rad)	Period (year)
1	508.009319749448	0.9999999053	0.21389514	0.0124
2	1016.018639498876	0.4999998105	-2.71380237	0.0062
3	1524.027959248450	0.3333330492	0.64168542	0.0041
4	1792.851776747876	0.2499996211	-0.85558056	0.0035
5	1284.842456997944	0.1999995264	2.07211695	0.0049
6	776.833137249084	0.1666660983	-1.28337085	0.0081
	...	...	...	...

Table 6.2: Representation for ephemeris in TASS during 1,000 years : The mean longitude of Rhea  $e^{\sqrt{-1}\lambda_5}$ 

	Frequency (rad/year)	Amplitude (rad)	Phase (rad)	Period (year)
1	508.009319842398	0.9999999694	0.21335581	0.0124
2	1016.018639684877	0.4999999388	-2.71488104	0.0062
3	1524.027959527070	0.3333332416	0.64006744	0.0041
4	1792.851776372940	0.2499998777	2.28806055	0.0035
5	1284.842456534343	0.1999998471	-1.06688829	0.0049
6	776.833136690737	0.1666664832	1.86134867	0.0081
	...	...	...	...

**Longitude of the pericenter of Titan:  $\varpi_6^*$** 

In TASS, the pericenter of Titan is connected with 2 of the elements, which are the real and imaginary parts of  $z = e \exp \sqrt{-1}\varpi$ . Here,  $e$  is the eccentricity, and  $\varpi$  is the pericenter of Titan. The period of  $\varpi_6^*$  is about 703 years. In 1,000 years interval, it only ends its cycle once. We doubt that the limited ephemeris will bring error in the frequency.

TASS-t in Table 10.3 gives the representation of  $e \exp \sqrt{-1}\varpi$  of Titan. The major part is the proper frequency of the longitude of pericenter of Titan. Table 6.3 shows our results for the frequency analysis with 1,000 years ephemeris, also in TASS. We have only detected 4 components. The most important things are:

- We can not get a correct value of the proper frequency of the longitude of the pericenter. Our result with 1,000 years ephemeris shows a difference as  $2.245698253 \times 10^{-6}$  rad/year, which is about 0, 17 years in period, about 79.03 km in position after 1,000 years (it is obtained by multiplying the difference of proper frequency over 1,000 years by the eccentricity and the semi-major axis). Actually, it is not the

real measure of the influence of our result in the representation of the mean longitude of Titan. From the representation in Table 10.2, the amplitude of the component with  $\varpi_6^*$  is about 34 km.

- To compare the four components in Table 6.3 with the first four components in Table 10.3, we can find that the frequency analysis works better for the short period terms than for the long period terms. The second term, which is identified as  $-\varpi_6^*$  in Table 10.3 is polluted by the other terms which are difficult to distinguish with 1,000 year interval. That means that even we have a completed result from the frequency analysis, without the example of TASS, we can not confirm the correctness of that. That is why TASS is so basic and meaningful for our research.

Table 6.3: Representation for TASS during 1,000 years :  $e \cdot e^{\sqrt{-1}\varpi}$  of Titan

	Frequency (rad/year)	Amplitude (rad)	Phase (rad)	Period (year)
1	0.008931618591	0.0289345001	2.86813920	703.48
2	-0.009039756171	0.0001890730	0.44764913	-695.06
3	0.417745454028	0.0000744538	-0.73030039	15.04
4	143.924047788794	0.0000668787	-0.56564858	0.04

We will take the proper frequency of  $\varpi_6^*$  of TASS, 0.008931618591 rad/y from Table 6.3, in our following calculations.

#### Longitude of the ascending node of Titan: $\Omega_6^*$

The situation of the ascending node of Titan is more complicated because it exists a constant term. Thus we also have to face to the determination of the constant : one from the 10,000 years representation, the other from the least squares method with 1,000 years ephemeris. In TASS, this variable is presented in the argument of  $\zeta = \sin \frac{i}{2} \exp \sqrt{-1}\Omega$ .

We take the representation TASS-t from Table 10.4. In this representation, it exists a constant term with an amplitude of about 0.005602 radian, and a major period term with a long period equal to 703.5 years. From the previous study on the longitude of pericenter which has a similar period, the limited interval of ephemeris should bring error to the proper frequency. As in the problem of the phase caused by different intervals in ephemeris of the mean longitude of Titan and Rhea, we need to pay attention to the constant term existing in the longitude of the ascending node.

With a constant term, it is impossible to get the proper frequency directly by the frequency analysis over 1,000 years. It is convenient to use the least squares method to obtain the constant with different ephemeris

Table 6.4: Constant in the longitude of the ascending node of Titan obtained by the frequency analysis and the least squares method, with different ephemeris intervals in the ring plane of Saturn.

	Constant term (rad)	Interval of ephemeris (year)	method
1	-0.005583725984	10,000	FA
2	-0.005448610014	10,000	LSM
3	-0.005793205614	1,000	LSM

intervals. In Table 6.4 the first line is the value obtained from TASS-t (Table 10.4). Here we have to mention that in Table 10.4 the constant term is in form of an amplitude and a phase. Whereas in Table 6.4, it presents as the value of the constant itself (the result of the amplitude multiply by the cosine phase). The second line shows the one obtained within 10,000 years by the least squares method. It is close to the value of the frequency analysis, but there is still a difference of about 165.1 km. The third line is the value obtained within 1,000 years ephemeris by the least squares method. We know nothing about the influence caused by the different constant terms. It is clear that for the constant term within 10,000 years, the result obtained by the frequency analysis is better than the one from the LSM. Hence, the two obtained constant values, the one of TASS-t by FA and the other with 1,000 years TASS by LSM are both tested in our calculations.

Table 6.5: The first term in the representation of  $\zeta_6$  by FA over 1,000 years, with the value of the constant term obtained by FA over 10,000 years and by the least squares method over 1,000 years.

Frequency (rad/year)	Amplitude (rad)	Phase (rad)	Period (year)	Interval
-0.008208620055	0.0029613939	-0.34167406	-765.44	1,000
-0.008773851378	0.0028360646	-0.28523224	-716.13	10,000

In Table 6.5, there is not doubt that the result using the constant term of TASS-t is different from the one using the constant term obtained by the least squares method with 1,000 years. There is a 11 years difference in the period with the proper frequency of TASS. It is more than 3127.31 km difference in position over 1,000 years (it is obtained by multiplying the difference of proper frequency over 1,000 years to  $\sin \frac{i}{2}$  and semi-major axis).

In this case, in the second component in the representation of the mean longitude of Titan, the accuracy of  $\Omega_6^*$  is very important. It is difficult to determine which frequency is good for our following calculations. We prefer to keep the value from the limited interval as an alternative that we can make an experiment with it.

We will take the proper frequency of  $\Omega_6^*$  of TASS as  $-0.008773851378$  rad/y in our following calculations, that is obtained by FA over 1,000 years but with the constant term from TASS-t.

**Longitude of the pericenter of Iapetus:  $\varpi_8^*$**

The process to deal with the frequency of the pericenter of Iapetus is similar as what we had done to obtain the pericenter of Titan. We make an analysis of the element  $z_8 = e_8 \exp \sqrt{-1}\varpi_8$ . Here,  $e_8$  is the eccentricity of Iapetus, and  $\varpi_8$  is the longitude of pericenter. The period of  $\varpi_8^*$  is about 3182 years. In 1,000 years interval, it can not finish its cycle even once. When we compare the frequency of the pericenter of Iapetus in TASS-t (Table 10.5) to the result with FA over 1,000 years (Table 6.6), the difference is big.

We can not get a correct frequency of the pericenter. Our result within 1,000 years gives a difference of about 305.3 years in period, that means a disparity about 0.173 rad in longitude of pericenter over 1,000 years, which means 17,614 km in position. The limited interval brings a huge mistake in proper frequency which is too far away from acceptable.

Table 6.6: The first term in the representation of  $z_6$  by FA over 1,000 years for  $z = e \exp \sqrt{-1}\varpi$  of Iapetus.

Frequency (rad/year)	Amplitude (rad)	Phase (rad)	Period (year)
0.001801807851	0.0290471199	-2.79754165	3487.16

The frequency obtained from the limited interval should not be used in rewriting the representation of Titan. The same problem will happen in JPL.

We will take the proper frequency of  $\varpi_8^*$  of TASS-t as  $-0.001974690826$  rad/y in our following calculations obtained by FA over 10,000 years.

**Longitude of the ascending node of Iapetus:  $\Omega_8^*$**

For the proper frequency of the ascending node of Iapetus, the experiment with Titan shows a solution. We use TASS-t (Table 10.6). In Table 6.7 we analyze  $\sin \frac{i_8}{2} \exp \sqrt{-1}\Omega_8$  over 1,000 years. In TASS-t, it exists a constant term with an amplitude equal to 0.132016534139 radian, and a major period term with a frequency of  $-0.001925543543$  rad/y, which means that the long period is equal to 3,263.06 years. Based on the case of Titan, the limited interval of ephemeris brings an error in the amplitude of the constant term and has an influence on the frequency of the node.

Consequently we choose the same method as the one used for Titan: we directly remove the constant value from the template of the representation to get the frequency of the node within 1,000 years. The result is showed



in Table 6.8. Comparing with the ones in Table 6.7, there is no doubt that an accurate constant leads to a good result for the frequency. The same situation appears in JPL ephemeris. In a limited time span, we can not get a correct value of the constant in the longitude of the ascending node of Iapetus which influences the determination of the proper frequency (with long-period). The difference between the values of Table 6.8 and the ones of TASS-t leads to a difference in position of about 5,230 km after 1,000 years.

Table 6.7: First term in the representation for TASS during 1,000 years :  $\sin \frac{i}{2} e^{\sqrt{-1}\Omega}$  of Iapetus, with constant obtained within 1,000 years by the least squares method.

Frequency (rad/year)	Amplitude (rad)	Phase (rad)	Period (year)
-0.001639133278	0.0775794294	-1.53930364	-3833.24

Table 6.8: Representation for TASS during 1,000 years : for the first term of  $\sin \frac{i}{2} e^{\sqrt{-1}\Omega}$  of Iapetus, with constants obtained TASS-t.

Frequency (rad/year)	Amplitude (rad)	Phase (rad)	Period (year)
-0.001946457996	0.0672825419	-1.27245240	-3228.01

$\Omega_8^*$  being the biggest component in the representation of the mean longitude of Titan, its accuracy of is very important. It is difficult to determine which frequency is good for our following calculations. We prefer to keep the value of the limited interval as an alternative that we will experiment with it.

We will take the proper frequency of  $\Omega_8^*$  of TASS-t as  $-0.001946457996$  rad/y in our following calculations.

### The other proper frequencies involved

Now, we have obtained the major proper frequencies needed to rewrite the mean longitude of Titan, over 1,000 years with TASS. But it is not enough, we have to mention two special frequencies, which are considered constant : the mean longitude of the Sun, and the 2:5 resonance between Jupiter and Saturn.

The mean longitude of the Sun, is used to describe the motion of the Sun around the center of mass of the Saturnian System. Actually, it equals the motion of Saturn around the Sun. In TASS, the mean longitude of the Sun is a parameter. Its proper frequency is 0.213382895534 rad/y (For JPL ephemeris, it is not difficult to get this proper frequency). In our calculations, we take that value directly.

The frequency named  $\Lambda$  is more complicated. In fact, there exist several possible combinations for this term. In TASS, the authors use  $-2\lambda_J + 5\lambda_S$ , an indirect perturbation of Jupiter. In this chapter we follow the definition of TASS.

### Proper frequencies involved: system values and obtained values

Now, we have all the involved values of the proper frequencies for rewriting the representation of the mean longitude of Titan. Table 6.9 shows the proper frequencies in TASS-t and the homologous values got from limited 1,000 years TASS ephemeris. Some of them are not the ones obtained from the limited interval ephemeris, but are the selected values after our comparison of the results. We mark them with \* in Table 6.9. They are used to compute TASS-s. In the following section, we will use these two groups of frequencies to examine the precision of the least squares method, and the error coming from the inaccurate proper frequency of the selected group.

Table 6.9: The proper frequencies from TASS and those adapted for the computation of TASS-s, TASS within 1,000 years (the selected values were marked with \*).

	TASS-t system value (rad/year)	1,000 years TASS system value & obtained value (rad/year)	ID
1	143.924047849167	143.924047832049	$\lambda_6^*$
2	508.009320172829	508.009319842398	$\lambda_5^*$
3	0.008933864296	0.008931618591	$\varpi_6^*$
4	0.001974690826	0.001974690826	* $\varpi_8^*$
5	-0.008931239595	-0.008773851378	$\Omega_6^*$
6	-0.001925543593	-0.001946457996	$\Omega_8^*$
7	0.213382895534		* $\lambda_s^*$
8	0.006867993783		* $\Lambda_6^*$

## 6.2 Determination of the short period and semi-long period terms

In TASS-t, we find some short period and semi-long period terms. Especially for the mean longitude of Titan, it exists three terms involving of the mean longitude of the Sun which are extracted from Table (10.2) and presented in Table 6.10. It is more convenient to remove these short period and semi-long period terms before we consider all the terms in the least squares method. Because such terms turn hundreds or thousands of times in 1,000 years, there

amplitudes and phases are easier to find. We make a small modification in the software in order to find the amplitude and phase of a peak which is close to a given frequency.

They are given in Table 6.11. Comparing with Table 6.10, there are some differences in frequency, amplitude and phase, but the disparities are not big. Figure (6.1) shows the original curve of  $r$  (blue), and the one removing the three short period and semi-long period terms (red), which eliminates all high frequencies. It is the good method to obtain the short period and semi-long period terms by a frequency analysis.

Table 6.10: The three terms involved in the mean longitude of the Sun in the mean longitude of Titan in 10,000 years TASS, determined by FA

Id	Frequency (rad/year)	Amplitude (rad)	Phase (rad)
$\lambda_s$	0.213299120062	0.0001839936	2.41533633
$2\lambda_s$	0.426598240156	0.0002064532	-1.15851073
$3\lambda_s$	0.639897360242	0.0000291064	-1.91809699

Table 6.11: The three terms involved of the mean longitude of the Sun in the mean longitude of Titan over 1000 years TASS, determined by FA.

Id	Frequency (rad/year)	Amplitude (rad)	Phase (rad)	Period (year)
$\lambda_s$	0.213382895534	0.0001829765	2.41992955	29.45
$2\lambda_s$	0.426696677075	0.0002067852	-1.15803311	14.73
$3\lambda_s$	0.639898005931	0.0000291063	-1.91815485	9.82

### 6.3 Determination of the long period terms

Now, we focus on the long period terms in the mean longitude of Titan, and rewrite them by the least squares method. In this step, we make the calculations in the two groups of the proper frequencies. The first column of Table 6.9 includes all the system frequencies, for which the result is compared with TASS-t, and only illustrates the precision of the least squares method. The second column of Table 6.9, includes all the proper frequencies from limited interval ephemeris. The results will show the precision of the further representation with the limited interval ephemeris (Chapter 7 for JPL).

The long period term  $2\Omega_8$  with a tiny amplitude (12 km) and slow changing is too correlated with  $\Omega_8^*$  because of the limit of the interval. Therefore, we will take 5 terms in total into the calculations. They are  $\lambda_5^* - \lambda_6^*$ ,  $\varpi_6^*$ ,  $\Omega_6^*$ ,  $\Omega_8^*$ , and  $\Lambda$ .

Table 6.12 shows our results of TASS with system proper frequencies of TASS-t with two methods: the frequency analysis and the least squares method. For each component in the table:

- The first column of the table shows the ID which is the combination of the frequency component.
- For each ID, we give 2 lines of values.
  - The first line comes from TASS-t. These values are considered as theoretical values, including the frequency, the amplitude in rad, in kilometer, and the phase of each component. These values are the

Figure 6.1: Influence of the 3 short-period terms involving the mean longitude of the Sun.

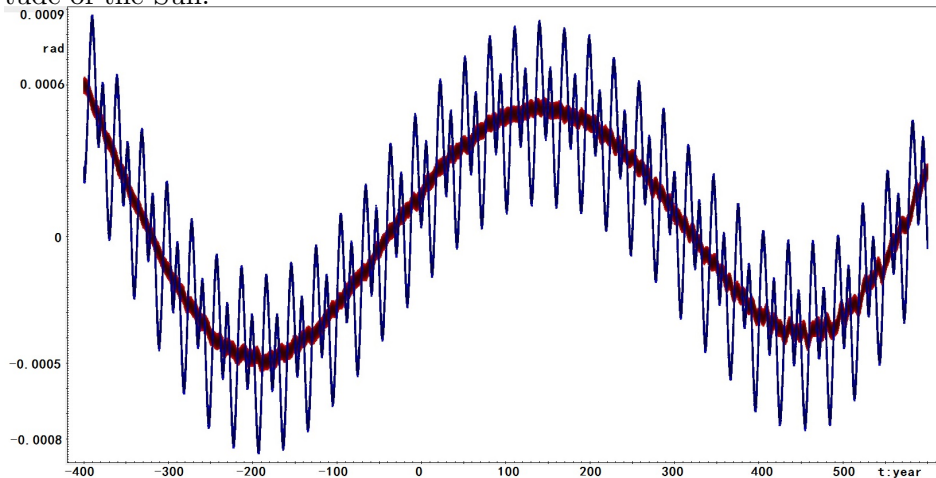


Table 6.12: Representation TASS-t compared with the representation with the same system proper frequency by the least squares method.

ID	Frequency	Amplitude		Phase
	rad/year	rad	km	rad
$-\Omega_8^*$	0.001925544359	0.0014891848	1819.590232	-1.76176914
	0.001925543543	0.0014868264	1816.708569	-1.74449801
$-\Omega_6^*$	0.008931239596	0.0006277976	767.087054	0.34279510
	0.008931239596	0.0006286233	768.095939	0.34292180
$\Lambda_6^*$	0.006867993783	0.0000320522	39.163622	2.55841019
	0.006867993783	0.0000309323	37.795294	2.60240660
$2\varpi_6^*$	0.017867728608	0.0000278284	34.002687	2.44323143
	0.017867728598	0.0000279911	34.201540	2.44186907
$\lambda_5^* - \lambda_6^*$	364.085272881417	0.0000120882	15.740789	0.77823556
	364.085272883577	0.0000120881	14.770126	0.77944087
$\lambda_s^*$	0.213299200062	0.0001839936	224.816260	2.41533633
$2\lambda_s^*$	0.4265982410156	0.0002064532	252.258971	-1.15851073
$3\lambda_s^*$	0.639897360242	0.0000291064	35.564237	-1.91809699

same as that in Appendix.

- The second line shows the results of the least squares method with proper frequencies of TASS system. The frequency of each component is very close to the first one but is not exactly the same. In fact, it is the theoretical value which is obtained by the system proper frequency, based on the representation of the system. The following values are the amplitude in radians, the amplitude in kilometers, and the phase of each component.

- The three short-period terms come from the representation of the 10,000 years ephemeris.

From the results in Table 6.12, there is no doubt that the least squares method can get a good solution of the representation with the system proper frequencies. The biggest difference between the amplitudes is smaller than 5 km. It means that the solution of the least squares method is credible.

Table 6.13 shows our solution by the least squares method with the obtained proper frequencies. This table corresponds to TASS-s. For each component, we show their ID at very beginning. In the first column, there are their frequencies obtained with the limited interval, and the solution of amplitude and phase of each component by the least squares method. The three short-period terms including the mean longitude of the Sun, are obtained by the frequency analysis of the 1,000 years ephemeris.

Table 6.13: TASS-s : representation of  $\lambda_6$  for TASS over 1,000 years with the obtained proper frequencies by the least squares method.

ID	Frequency	Amplitude		Phase
	rad/year	rad	km	rad
$-\Omega_8^*$	0.001946457996	0.0014851266	1814.631612	-1.73740199
$-\Omega_6^*$	0.008773851378	0.0006884030	841.138985	0.34890892
$\Lambda_6^*$	0.006867993783	0.0000885665	108.216796	-3.05325855
$\lambda_5^* - \lambda_6^*$	364.085272883577	0.0000120881	14.770084	0.77944420
$2\varpi_6^*$	0.017867728598	0.0000265389	32.427052	2.41822124
$\lambda_s^*$	0.213382895534	0.0001829765	223.573472	2.41992955
$2\lambda_s^*$	0.426696677075	0.0002067852	252.664598	-1.15803311
$3\lambda_s^*$	0.639898005931	0.0000291063	35.564093	-1.91815485

We give in Table (6.14) the statistics of the residuals of the two solutions in the limited interval.

Table 6.14: Statistics of the residuals of the two solutions obtained in the limited interval.

	System values	Obtained values (TASS-s)
MEAN (m)	0.77937	-58.60758
Standard Deviation (km)	16.15811	16.17248

From the table 6.12, we see that, with the same frequency components, the difference in amplitude between the frequency analysis and the least squares method are very small. Most of the disparities are about several kilometers. Figure (6.2) shows the residuals of the mean longitude of Titan removing all the components obtained by the least squares method, the mean mean motion with its phase, and the three short-period terms. The solution of the least squares method has a good precision. The mean of the residuals is no more that 1 meter, and the deviation of the residuals is about 16 km. It means that the major error of the least squares method is the truncation error. With the frequency analysis we can ignore the slight difference in the amplitude terms which can not be ignored in the least squares method.

Figure (6.3) shows the residuals of the mean longitude of Titan removing the representation TASS-s. With inaccurate proper frequency, the result from  $-\Omega_6^*$  has a deviation of about 70 km. It influences the near component  $\Lambda_6^*$  to absorb it (68 km difference in amplitude). The mean of the residuals is about  $-58$  meters, and the deviation of the residuals is about 16 km. The curve in Figure (6.3) keeps almost smooth and symmetrical.

We do not focus on the difference of the phase. The disparities from phase are so small that they can be ignored.

Figure 6.2: The residuals of the least squares method with the system proper frequencies of TASS.

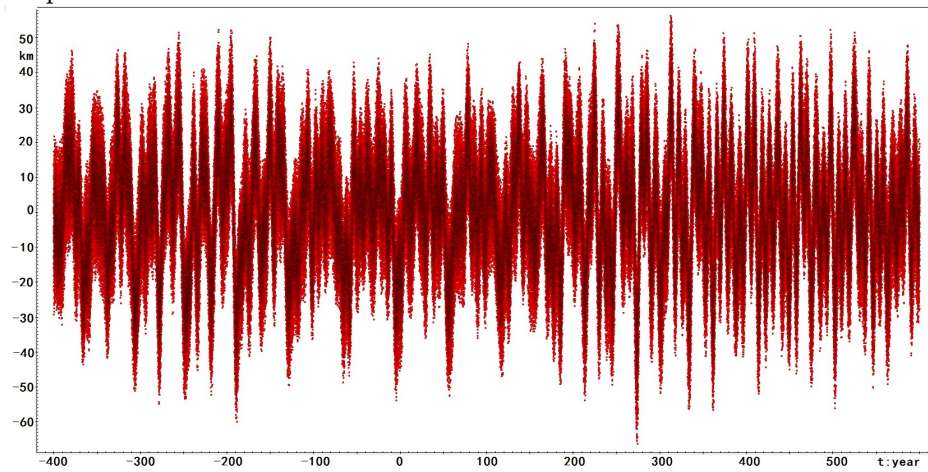
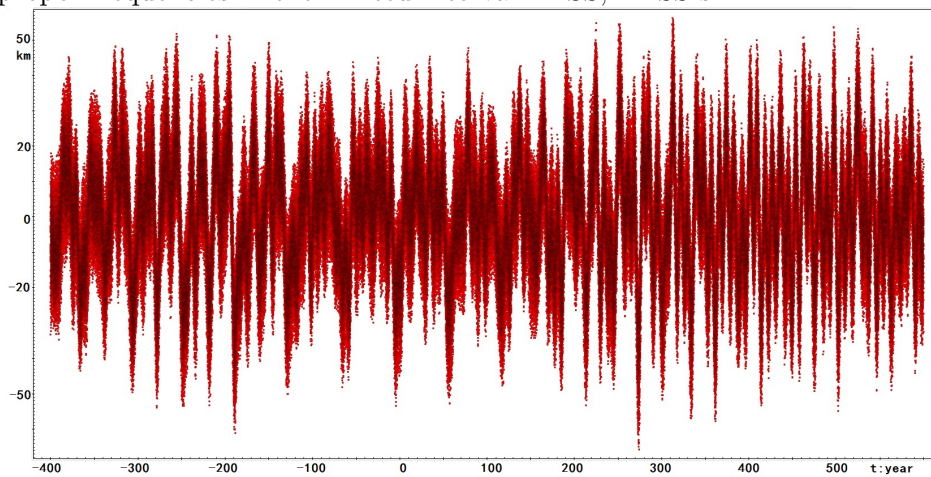


Figure 6.3: The residuals of the least squares method with the obtained proper frequencies in the limited interval TASS, TASS-s.



## 6.4 Conclusion

We make a conclusion of our experiment with TASS, which is meaningful for our following work.

The limited interval ephemeris has an influence on the proper frequency, which depend on the periods. The long-period terms such  $-\Omega_6^*$ ,  $-\Omega_8^*$ ,  $-\varpi_8^*$  and  $-\varpi_6^*$ , are more affected, while the short-period terms like  $\lambda_s$ ,  $\lambda_6$ , and  $\lambda_5$  are almost unaffected. The magnitude of the influence ranges from tens of kilometers to hundreds of kilometers.

After that, we have also obtained the amplitudes and the phases of the short-period terms before the calculations by the least squares method, which proves the accuracy of our experiment.

Finally, we find the representation of the mean longitude of Titan named TASS-s with the least squares method with a limited truncation error of 10 kilometers. That means that we can use the same method to get the representation of the mean longitude of Titan with JPL.

Last, the inaccurate proper frequency  $-\Omega_6^*$  causes a deviation of about 70 km. It has the same influence of about 68 km on the amplitude of  $\Lambda$  which is near by  $-\Omega_6^*$ .



# Chapter 7

## Results for the mean longitude of Titan

Table 10.2 gives TASS-t i.e. TASS analyzed over 10,000 years. In this chapter we present a similar table for the numerical integration ephemeris JPL for which the time span is 1,000 years only. We will use the method described in Chapter 5, with the help of the test done in Chapter 6 (TASS-s).

### 7.1 Proper frequencies in the JPL ephemeris

After changing the reference plane with these angles

$$\begin{aligned}\Omega_a &= 169.5291^\circ \\ i_a &= 28.0512^\circ\end{aligned}$$

and analyzing the major part of the osculating elements of JPL ephemeris, we get a list of proper frequencies. Here, we only list those in use in the representation of the mean longitude of Titan in the JPL ephemeris. They are :

$\lambda_5^*$ ( $N_5$ )	the proper frequency of mean longitude of Rhea.
$\lambda_6^*$ ( $N_6$ )	the proper frequency of mean longitude of Titan.
$\varpi_6^*$	the proper frequency of pericenter of Titan.
$\varpi_8^*$	the proper frequency of pericenter of Iapetus.
$\Omega_6^*$	the proper frequency of ascending node of Titan.
$\Omega_8^*$	the proper frequency of ascending node of Iapetus.
$\lambda_s^*$ ( $N_s$ )	the proper frequency of mean longitude of the Sun.
$\Lambda_6^*$	$\varpi_6^* - \varpi_8^*$ , $-\Omega_6^* + \Omega_8^*$ , or $2\lambda_J^* - 5\lambda_S^*$

Then we need to get the mean longitude of Jupiter and Saturn beforehand and also the mean mean motion of the Sun.

All the ephemeris and parameters in our calculations are published by the JPL website.

**Mean mean motion of Rhea :  $\lambda_5^*$** 

Table 7.1 presents the mean mean motion of Rhea calculated with 1,000 years ephemeris of its mean longitude, first from JPL from 1,600-2,600, and second from TASS. Here we take the series of  $(\cos \lambda_5, \sin \lambda_5)$  as the input form.

The difference in frequency is  $\Delta f = f_T - f_J = -0.000010643385$  rad/year, which corresponds to 5609.78 km after 1,000 years. It is a big difference. Taking into account the period of Rhea, which is 0.012368 years, a small difference into the mean mean motion causes after multiple cycles a huge quantity. It can also disturb the recognition of the long periods. However, in the previous chapter we got from TASS-t (10,000 years) and TASS-s (1,000 years) the mean mean motions of Rhea and Titan. The corresponding differences have been found much smaller. So we can be confident in the present value of JPL (1,000 years) and we suppose that the difference comes from the system value of JPL. In that case, we take the value of JPL in the use of our calculations.

We take the proper frequency for the mean mean motion of Rhea  $\lambda_5^*$  of JPL equal to 508.009309199013 rad/y in our following calculations.

Table 7.1: Mean mean motion of Rhea and phase in both TASS and JPL during 1,000 years.

Id	Frequency (rad/year)	Phase (rad)	Period (year)
JPL	508.009309199013	0.213208266476	0.012368
TASS	508.009319842398	0.213355809712	0.012368

**Longitude of the pericenter of Titan:  $\varpi_6^*$** 

We discuss the situation of the longitude of the pericenter of Titan, or more exactly the corresponding proper frequency  $\varpi_6^*$ . In JPL, this variable is presented separately from the eccentricity. We use the same form as in TASS, which is  $z = e \exp \sqrt{-1}\varpi$ . Here,  $e$  is the eccentricity for which we can get its instantaneous value from the JPL ephemeris. So when we make an analysis of  $(e \cos \varpi, e \sin \varpi)$  of JPL we can compare directly to TASS-t.

Table 7.2 is the representation of  $e \exp \sqrt{-1}\varpi$  for the JPL ephemeris in 1,000 years by a frequency analysis. Table 7.3 gives the proper frequency of the pericenter  $\varpi_6^*$  of Titan in TASS and in JPL in 1,000 years. The period of  $\varpi_6$  is about 703 years for TASS, but about 704 years for JPL. We only find 4 components in 1,000 years Titan ephemeris. Let us mention:

- We can not get a correct value of the proper frequency of the longitude of the pericenter. Our result with 1,000 years ephemeris shows a dif-

ference as 0.000008770709 rad/y in frequency, which is about 308.64 kilometers in position after 1,000 years, and 0,69 years for the periods.

- The four components presented in Table 7.2 and Table 6.3 are similar, not only in frequency but also in amplitude and phase. The second term, identified as  $-\varpi_6^*$  in Table 10.3, is found polluted by the other terms which are difficult to distinguish with 1,000 years interval.

Table 7.2: Representation for the JPL ephemeris during 1,000 years :  $e \exp \sqrt{-1}\varpi$  of Titan.

	Frequency (rad/year)	Amplitude (rad)	Phase (rad)	Period (year)
1	0.008922847882	0.0288561951	2.86729807	704.17
2	-0.009074407804	0.0001888799	0.45870297	-692.41
3	0.417762498182	0.0000747162	-0.73753434	15.04
4	143.924045533325	0.0000670170	-0.56569307	0.044

Table 7.3:  $\varpi_6^*$  of Titan for TASS and for JPL during 1,000 years in the ring plane of Saturn.

Id	Frequency (rad/year)	Phase (rad)	Period (year)
JPL	0.008922847882	2.86729807	704.17
TASS	0.008931618591	2.86813920	703.48

In fact, this disparity in distance is not a real difference of  $\varpi_6^*$ . The interesting quantity is the difference between the amplitudes and between the phases in the representation of  $z_6$ . The comparison in  $z$  between the two ephemerides made in Chapter 4 shows that the value obtained from 1,000 years ephemeris is satisfactory and can be used in our following calculations.

Hence, we adopt the proper frequency of  $\varpi_6^*$  of JPL equal to  $8.922847882 \times 10^{-3}$  rad/y from Table 7.2.

### Longitude of the ascending node of Titan : $\Omega_6^*$

The situation of the ascending node of Titan is more complicated because of its constant term. In TASS, this variable is presented as the orbital element  $\zeta = \sin \frac{i}{2} \exp \sqrt{-1}\Omega$ . In JPL, this variable is given separately : the longitude of the ascending node and the inclination  $i$ . We transfer each value into the same form as  $\zeta$  to get a better reference with TASS.

Because of the constant term in Table 7.4, it is impossible to get the frequency by a frequency analysis : the main term has a period larger than 700 years which can not be separated from the constant term. As we have

done for TASS-s in the previous chapter, it is reasonable to use the value from TASS-t directly. Table 7.4 shows the value of the constant term obtained from JPL, and also for TASS in different time spans. The value of JPL is close to the one of TASS-s (1,000 years) which reminds the situation in the previous chapter : in the recent 1,000 years, the ephemerides TASS and JPL are approximatively close.

The frequency in Table 7.5 uses the constant term obtained by the least squares method with 1,000 years with TASS and JPL. As what we find with TASS-s, it is not an appropriate value. However, the frequency calculated with the 10,000 years TASS constant also shows a great difference with TASS-t and with TASS-s.

It exists a difference of 327.28 km over 1,000 years between the use of the two major frequencies of  $\Omega_6^*$  with their own constant term over 1,000 years (Table 7.5). In Table 7.6 we see the value of  $\Omega_6^*$  over 1,000 years with the constant from TASS-t. It leads to a difference a little bit larger than 522.05 km. We conclude that  $\Omega_6^*$  of JPL is not convenient here. It is closer to  $-0.008773851378$  rad/y but is not equal. Also, in this quantity the value of TASS can not be a reference. We can not use the value of  $\Omega_6^*$  from TASS.

Table 7.4: Constant in the longitude of the ascending node of Titan obtained by the frequency analysis and the least squares method, with different ephemerides intervals, in TASS and in JPL.

	Constant term (rad)	Interval of ephemerides (year)	method
JPL	-0.005721473948	1,000	LSM
TASS	-0.005583725984	10,000	FA
TASS	-0.005793205614	1,000	LSM

Table 7.5: The main term in  $\zeta_6$ ,  $\Omega_6^*$ , during 1,000 years with the constant obtained over 1,000 years ephemeris by the least squares method.

	Frequency (rad/year)	Amplitude (rad)	Phase (rad)	Period (year)
TASS	-0.008208620055	0.0029613939	-0.34167406	-765.44
JPL	-0.008104781730	0.0029293235	-0.33893737	-775.24

Therefore, the value of the proper frequency of the longitude of the ascending node in JPL, in the limited time span of ephemeris, can not be better. The value of TASS can only support the magnitude of the error of our work on JPL. We have to use  $-0.008773851378$  rad/y in our following calculations (line TASS of Table 7.6).

**Longitude of the pericenter of Iapetus :  $\varpi_8^*$** 

The result obtained from JPL ephemeris in Table 7.7 is meaningful, as we use two different methods to describe the same Saturnian System. We know that the proper frequency of JPL system should be close to the value of the TASS system. Between them, the difference in position over 1,000 years is 1557.54 kilometers, and the difference in period is 28.78959 years. So, even though the proper frequency of the pericenter of Iapetus in TASS is not so close to the real one in the JPL system (hundreds of kilometers difference over 1,000 years), it is still more accurate than the one obtained directly from the 1,000 years JPL ephemeris.

So, we take the value 0.001974690829 rad/y of TASS-t (Table 10.6) as the proper frequency of the pericenter of Iapetus for JPL.

**Longitude of ascending node of Iapetus :  $\Omega_8^*$** 

The main part of the longitude of the ascending node of Iapetus in the JPL ephemeris is pleasantly surprising. So we use the same process as for the constant term for Titan.

In Table 7.8 we give the two frequencies over 1,000 years for TASS and JPL obtained by the least squares method with the constant over 1,000 years also. The difference is small. It leads to a difference of 30.83 km over 1,000

Table 7.6: Representation of  $\zeta = \sin \frac{i}{2} \exp \sqrt{-1}\Omega$  of Titan, with the constant from TASS-t, over 1,000 years.

	Frequency (rad/year)	Amplitude (rad)	Phase (rad)	Period (year)
JPL	-0.008693210603	0.0028108581	2.68207640	-722.77
TASS	-0.008773851378	0.0028360646	-0.28523224	-716.13

Table 7.7: Representation of  $z = e \exp \sqrt{-1}\varpi$  of Iapetus over 1,000 years.

	Frequency (rad/year)	Amplitude (rad)	Phase (rad)	Period (year)
TASS	0.001801807851	0.0290471199	-2.79754165	3487.156139
JPL	0.001816807217	0.0289910263	-2.79535991	3458.366549

Table 7.8: Main term in the representation of  $\zeta = \sin \frac{i}{2} \exp \sqrt{-1}\Omega$  of Iapetus, obtained by the least squares method with the constant over 1,000 years.

	Frequency (rad/year)	Amplitude (rad)	Phase (rad)	Period (year)
JPL	-0.001639193498	0.0776049608	-1.53971151	-3833.10
TASS	-0.001639133278	0.0775794294	-1.53930364	-3833.24

Table 7.9: Main term in the representation of  $\zeta = \sin \frac{i}{2} \exp \sqrt{-1}\Omega$  of Iapetus, obtained by the least squares method with the constant from TASS-t.

	Frequency (rad/year)	Amplitude (rad)	Phase (rad)	Period (year)
JPL	-0.001957029522	0.0672082216	1.67368482	-3210.572572
TASS	-0.001946457996	0.0672825419	-1.27245240	-3228.009708

years and no more than 0.14 year for the period. The proper frequency of the longitude of ascending node of Iapetus is almost the same. We also see the values obtained with TASS and JPL over 1,000 years but with the constant term from TASS-t (Table 7.9). The error caused by an inaccurate value of the constant term makes a difference as 2682.69 kilometers over 1,000 years. We prefer the value of  $-0.001925543543$  rad/y of TASS-t (Table 10.4) as the proper frequency of ascending node of Iapetus of JPL.

#### Mean mean motion of the Sun : $\lambda_s^*$

The mean longitude of the Sun is one of the arguments which we do not need to calculate. As it corresponds to the circular motion of Saturn around the Sun, it equals the mean longitude of Saturn that we download from JPL web site for the Saturn ephemeris over 1,000 years. Then we make a frequency analysis of the mean longitude of Saturn. The major component of the representation is the mean mean motion of the Sun. Table 7.10 shows the mean mean motion, the phase and the period of the mean longitude of the Sun for JPL.

Table 7.10: Mean mean motion of the Sun.			
	Frequency (rad/year)	Phase (rad)	Period (year)
JPL	0.213342329926	0.87292588	29.45

#### Resonance 2:5 between Jupiter and Saturn: $\Lambda_6$

$\Lambda_6^*$  is not clearly identified. In TASS, it is considered as the influence coming from the 2:5 resonance between Jupiter and Saturn. Moreover in some previous researches, this term should be explained as several combinations with similar values :  $\varpi_6^* - \varpi_8^*$ ,  $-\Omega_6^* + \Omega_8^*$ , or  $2\lambda_J^* - 5\lambda_S^*$ . In Table 7.11, we give these possible combinations of  $\Lambda_6^*$  and the corresponding values in frequency. We do not know which combination is the real one in the ephemeris of JPL. In our work, we can only test all these values in our calculations and make the comparisons between the mean and standard deviations of the corresponding residuals. The results are in Table 7.12. From the mean and the standard

deviations, we conclude that the distributions of the residuals are almost the same, except the last line. This last is mentioned as (TASS,PHASE) in Table 7.12. A detailed explanation is given in section “Determination of long period terms” Sect. 7.3.

The choice of  $\Lambda_6^*$  makes no difference in our results. Hence we prefer to use the same value as TASS.

Table 7.11: The possible combinations of  $\Lambda_6^*$ .

	ID	Frequency (rad/year)
JPL	$2\lambda_J^* - 5\lambda_S^*$	0.007294999177
	$-\Omega_6^* + \Omega_8^*$	0.006736181081
	$\varpi_6^* - \varpi_8^*$	0.006572353561
TASS	$2\lambda_J^* - 5\lambda_S^*$	0.006874219340

Table 7.12: The mean and the standard deviation of the residuals for different uses of the value of  $\Lambda_6$ .

$\Lambda_6$	Frequency (rad/year)	Mean (m)	Standard Deviation (km)
$-2\lambda_J + 5\lambda_S$	0.007294999177	377.36	30.21872
$-\Omega_6 + \Omega_8$	0.006736181081	339.33	29.71464
$\varpi_6 - \varpi_8$	0.006572353661	331.03	29.61418
$-2\lambda_J + 5\lambda_S$ (TASS)	0.006874219340	257.42	28.70089
$-2\lambda_J + 5\lambda_S$ (TASS,PHASE)	0.006874219340	-312.62	25.56549

### The proper frequencies in use

Now, we have all the involved values of the proper frequencies in order to obtain the representation of the mean longitude of Titan. Table 7.13 shows the proper frequencies that we adopt to determine the representation of the JPL ephemeris. Some of them are not the ones from the limited interval ephemeris, but the selected values after our comparison with TASS. In the following section, we will use this group of frequencies to get the amplitudes and the phases in the representation of the mean longitude of Titan with JPL ephemeris, what is our ultimate purpose.

Table 7.13: The adopted value of the proper frequencies for the JPL ephemeris(see text for more details).

ID	Frequency (rad/year)
$\lambda_6^*$	143.924045534754
$\lambda_5^*$	508.009309199013
$\lambda_s^*$	0.213342329926
$\varpi_6^*$	0.008922847882
$\varpi_8^*$	0.001974690829
$\Omega_6^*$	-0.008693210604
$\Omega_8^*$	-0.001925543593
$\Lambda_6^*$	0.006867993783

## 7.2 Determination of the short period and semi-long period terms

As what we did with TASS in the previous chapter it is possible to find the short-period terms involving the mean longitude of the Sun by a frequency analysis. We take the mean longitude, its double and its triple frequencies as a target to find the neighborhoods of the peak in the frequency area. The frequencies are then modified by the FA software.

Table 7.14 shows all the target frequencies of the possible short-period terms in the mean longitude of Titan for JPL. Table 7.15 shows the short-period terms obtained by a frequency analysis of the mean longitude of Titan, including the amplitude and phase of every terms. When we compare the frequencies in both tables, we note some small differences. Considering the influence of the tiny amplitude of the long-period terms which remain in the mean longitude, we consider that the components in Table 7.15 are the same as the ones listed in Table 7.14. Hence, we remove these three terms to simplify our calculations with the least squares method.

Figure 7.1 shows two curves. The red one which is called  $r$ , is the mean longitude of Titan for the JPL ephemeris in which we have removed the mean mean motion part and the phase. The blue curve is the follow-up results when taking out the short-period components which involve the mean longitude of the Sun. The units of  $r$  in Figure 7.1 are radians.

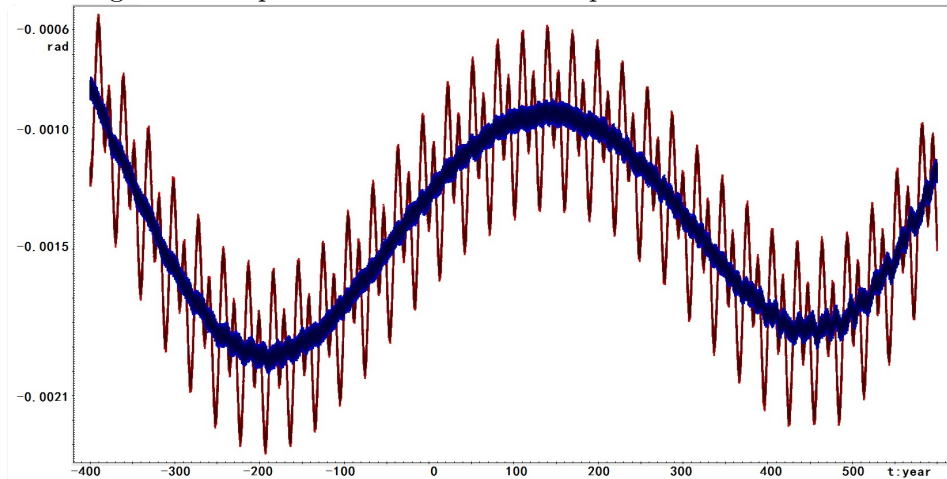


Table 7.14: Mean longitude of the Sun for JPL and the values of its double and triple times frequencies.

ID	Frequency (rad/year)	Phase (rad)
$\lambda_s$	0.21334233	0.8729258824
$2\lambda_s$	0.42668466	**
$3\lambda_s$	0.64002699	**

Table 7.15: The three terms involving the mean longitude of the Sun in the mean longitude of Titan determined by FA for the JPL ephemeris over 1000 years.

Frequency (rad/year)	Amplitude	Phase	Id
0.213381048936	0.0001830009	2.42011717	$\lambda_s$
0.426697846565	0.0002067870	-1.15815737	$2\lambda_s$
0.639897726868	0.0000291066	-1.91813725	$3\lambda_s$

Figure 7.1: Periodic part of the mean longitude  $r$  and its residuals after removing the short-period terms in the JPL ephemeris.

### 7.3 Determination of the long period terms

Now, we have prepared everything to focus on the long period terms of the mean longitude of Titan in 1,000 years JPL ephemeris (frequencies are fixed in Table 7.13), and we calculate its representation by the least squares method.

In the same way as in the previous chapter for TASS, among the 6 long period terms, the last one,  $2\Omega_8^*$  with a tiny amplitude and slow changing, is too correlated with  $\Omega_8^*$  because of the size of the interval. Hence we consider only these 5 terms :  $\lambda_5^* - \lambda_6^*$ ,  $\varpi_6^*$ ,  $\Omega_6^*$ ,  $\Omega_8^*$ , and  $\Lambda$ .

In this step, we will make the calculations twice. The difference between both computations is only the adopted value of  $\lambda_0$  which has puzzled us very much in Chapter 4. The first time, we use the value from TASS-t (Table 7.16). The second time we use the value from the 1,000 years JPL ephemeris itself (Table 7.17). Then, we get a proof that the choice of  $\lambda_0$  from TASS-t (10,000 years) is necessary and important.

The representation of the 1,000 years JPL ephemeris is given in Table 7.16, mentioned JPL in the first line. For an easy comparison, the line TASS-t is extract from Table 10.2. For every component, we show its identification in the first column along with its frequency. After that, we see the amplitude, both in radian and kilometer, then their phase in radians. At last, it is the name of the ephemeris.

From the comparison between TASS-t and from the experiment of the least squares method in TASS-s ephemeris, we can get the conclusion :

- The difference of the amplitude of the term  $\Omega_8^*$  is about 60 kilometer, which corresponds to the system disparity of both ephemerides.
- Because of the error in the proper frequency of  $\Omega_6^*$ , and our experience of the comparison between TASS from different intervals, the error in the obtained amplitude by the least squares method is more than 100 kilometers. As in TASS-s, it makes an influence in the amplitude of the frequency close to the component  $\Lambda_6$ .
- The other results from JPL are very similar to TASS-t.

Figure 7.2 gives the image of the residuals. They correspond to the mean longitude of Titan in JPL when all the components of the line “JPL” are removed. So, they are the residuals between the real ephemeris and our representation. We can find that the curve scatter much more in the period away from J2000.0. We can not explain what causes such kind behavior. The mean of these residuals is about -312.62 meters, and the standard deviation is about 25.56549 kilometers. The biggest difference is no more than 100 kilometers over 1,000 years.

Table 7.16: Comparisons of the representation of the mean longitude of Titan between TASS-t and JPL.

ID	Frequency (rad/year)	Amplitude (rad)	(km)	Phase (rad)	
$\Omega_8^*$	0.001925544359	0.0014891848	1819.59023	-1.761791	TASS-t
	0.001925543543	0.0015385090	1879.85800	-1.733645	JPL
$\Omega_6^*$	0.008931239596	0.0006277976	767.08705	0.342795	TASS-t
	0.008693210603	0.0007328212	895.41222	0.359277	JPL
$\Lambda_6$	0.006867993783	0.0000320522	39.16362	2.558410	TASS-t
	0.006874219340	0.0001339679	163.69132	-2.904047	JPL
$\lambda_5^* - \lambda_6^*$	364.085272881417	0.0000128825	15.740789	0.778237	TASS-t
	364.085261349846	0.0000111378	13.608919	0.779450	JPL
$2\varpi_6^*$	0.017867728608	0.0000278284	34.00269	2.455682	TASS-t
	0.017845695764	0.0000249581	30.49560	2.386224	JPL
$\lambda_s^*$	0.213299200620	0.0001839936	224.81626	2.415336	TASS-t
	0.213381048936	0.0001830009	223.60326	2.420117	JPL
$2\lambda_s^*$	0.426598240156	0.0002064532	252.25897	-1.183717	TASS-t
	0.426697846565	0.0002067870	252.66679	-1.158157	JPL
$3\lambda_s^*$	0.639897360242	0.0000291064	35.56424	-1.195372	TASS-t
	0.639897726868	0.0000291066	35.56449	-1.918137	JPL

Figure 7.2: Residuals of our representation of the mean longitude of Titan of JPL.

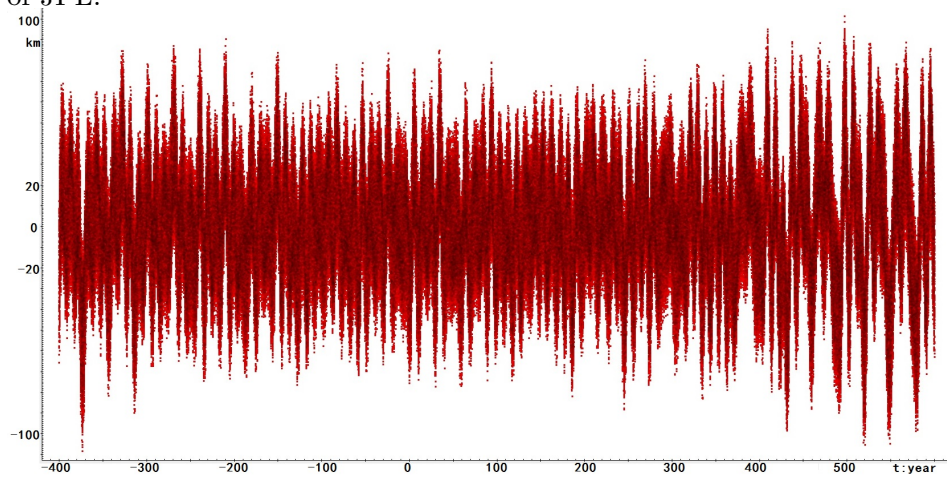
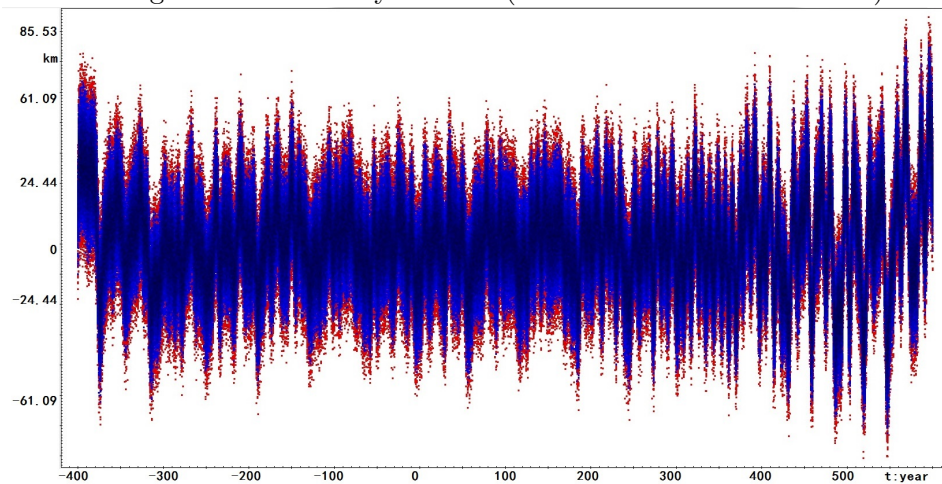


Figure 7.3: Residuals of our representation of the mean longitude of Titan of JPL using 5 terms and only 4 terms (see the text for more details).



Moreover, we also give in Figure (7.3) an image of the consistency of our solutions. We have made several experiments of the influence of the terms of the solutions. We take different numbers of terms : 1 term for the first time, 2 terms for the second time, and so on, into our least squares method equations. We compare the solutions of every test to make sure that we get the best solution. In Figure (7.3), the red curve corresponds to the residuals when we take 4 terms only and the blue one corresponds to the residuals with 5 terms. From the distribution of the residuals, we find that the solution with 5 terms is better than with 4 terms, and both solutions are consistent and stable. Here, note that the residuals in Figure (7.3) are not calculated with the final choice of the proper frequencies in our solution, but with the obtained proper frequencies in our initial experiment. That is why the blue curve in Figure (7.3) is not the same and not as good as Figure (7.3).

#### The choice of phase $\lambda_0$

In Chapter 4 the choice of the phase in the mean longitude of Titan,  $\lambda_0$  has puzzled us very much. Here, we give the solution when using the phase from the 1,000 years JPL ephemeris itself to proof our choice. It is given in Table 7.17 in the line *JP*. For comparison, in the same table, we give also the solution of the least squares method with the phase from TASS (our adopted JPL solution). It is clear that a bad choice for the phase gives a large error in the 3 major components  $\Omega_8^*$ ,  $\Omega_6^*$ , and  $\Lambda_6$ . Moreover it also affects the amplitude of  $2\varpi_6^*$ . The conclusion of our discussion on the phase in Chapter 4 is that the mean of the residuals is 257,42 meters and the standard deviation is 28.7 kilometers. If we did not have TASS-t as a reference in order to think about the difference in  $\lambda_0$  from different time spans, it would have being impossible to detect those mistakes only by the statistical indicators of residuals.

Table 7.17: Comparison of the solutions of the mean longitude of Titan from JPL with different values of  $\lambda_0$ .

ID	Frequency rad/year	Amplitude rad	km	Phase rad	
$\Omega_8^*$	0.001925543543	0.0015385090	1879.85800	-1.733645	
	0.001925543543	0.0030131523	3681.68050	-1.748134	<i>JP</i>
$\Omega_6^*$	0.008693210603	0.0007328212	895.41222	0.359277	
	0.008693210603	0.0005049251	616.95292	0.192544	<i>JP</i>
$\Lambda_6$	0.006874219340	0.0001339679	163.69132	-2.904047	
	0.006874219340	0.0003742662	457.30461	1.100993	<i>JP</i>
$\lambda_5^* - \lambda_6^*$	364.085261349846	0.0000111378	13.60892	0.779450	
	364.085261349846	0.0000111377	13.60881	0.779436	<i>JP</i>
$2\varpi_6^*$	0.017845695764	0.0000249581	30.49560	2.386224	
	0.017845695764	0.0000159298	19.46410	1.986390	<i>JP</i>

## 7.4 Conclusion

We get the representation of the JPL ephemeris. Our final solution is gathered in Table 7.18. It means that we can obtain the value of the mean longitude of Titan for the JPL ephemeris at any time by our formula:

$$\lambda_6 = N \times t + \lambda_0 + \sum_{i=1}^n A_i \sin(\omega_i t + \phi_i) \quad (7.4.1)$$

In the representation of JPL, it exists a 60 km difference between the amplitude of the major components  $\Omega_8^*$ . We consider that it corresponds to the system difference. The limited interval of the ephemeris makes some influence on the proper frequencies, which brings the error into the long period terms like  $\Omega_6^*$ . Moreover, that influences the near component  $\Lambda_6^*$ . The error is absorbed in the amplitude of this components. The total difference between the original ephemeris of Titan in JPL and our corresponding representation is no more than 100 kilometers over 1,000 years. The standard deviation is about 26 kilometers.

Table 7.18: The mean longitude of Titan from JPL ephemeris, in the ring plane with  $i_a, \Omega_a$  from Chapter 1 :  $\lambda_6 = N \times t + \lambda_0 + \sum_{i=1}^n A_i \sin(\omega_i t + \phi_i)$

	Frequency (rad/year)	Amplitude (rad)	Phase (rad)	ID
	143.924045534754			$N$
			5.718878	$\lambda_0$
1	0.001925543543	0.0015385090	-1.733645	$\Omega_8^*$
2	0.008693210603	0.0007328212	0.359277	$\Omega_6^*$
3	0.426697846565	0.0002067870	-1.158157	$2\lambda_s^*$
4	0.213381048936	0.0001830009	2.420117	$\lambda_s^*$
5	0.006874219340	0.0001339679	-2.904047	$\Lambda_6$
6	0.639897726868	0.0000291066	-1.918137	$3\lambda_s^*$
7	0.017845695764	0.0000249581	2.386224	$2\varpi_6^*$
8	364.085261349846	0.0000111378	0.779450	$\lambda_5^* - \lambda_6^*$





## Chapter 8

# Digitization and reduction of old astronomical plates of natural satellites

In this chapter, I will introduce the works about digitization and reduction of old observations with my Chinese colleagues during my thesis. All this work has been published on Monthly Notices of the Royal Astronomical Society Volume 457, Issue 3, 11 April 2016, Pages 2900–2907 as: Digitization and Reduction of Old Astronomical Plates of Natural Satellites

The major work of me in this article is to solve the non-linear error in the scan direction, that I will explain detailed in the section Scanner.

### 8.1 Background

The astrophotographic plates are widely using in astronomy observation in the last century. In that moment, most of the astromechanics measurements are by hand. Scientists mark the target on the plates and make a record of their positions. In recently, benefited by the developing of technique, we could digitize such kind of old plate and remeasure them with a high accuracy modern catalogue. This work is our primary experiment of old astronomical plates digitization with an advanced commercial scanner EPSON 10,000XL that we selected a set of 27 plates of Jupiter, Saturn and Uranus, which were taken during 1987 to 1990. 125 satellite positions were obtained from the remeasurement and reduction of these plates with the UCAC4 catalogue (Zacharias et al. 2013 [20]).

Table 8.1: Detailed informations of plates, with number of plates (N)

Planet	Obs-Time	N	Exposure time s	Site code
Saturn	1987.03.10	2	600-1200	334
	1987.05.20-22	8	60-600	286
	1988.05.12	6	240	286
Jupiter	1987.10.12-14	3	120-240	286
Uranus	1990.05.01-04	8	1200-1800	286

Table 8.2: Specifications of the telescopes at YAO and TTO

	Telescope A	Telescope B
Site code	YAO 286	TTO 334
Diameter of primary mirror (cm)	100	32
Focal length (mm)	13300	3580
Size of plates ( $cm \times cm$ )	$16 \times 16$	$16 \times 16$
Field of view ( $degree \times degree$ )	$0.75 \times 0.75$	$2.5 \times 2.5$
Scale (arcsec $mm^{-1}$ )	15.5	57.6

## 8.2 Plates

All 27 plates of the satellites of Jupiter(3), Saturn(16) and Uranus(8) selected here were taken on five successive missions during the period 1987 to 1990, in which those observations had been published in our previous work (Wu.J & Zhang.Y 1988 [21], Qiao.RC et al. 1995 [22]). The astrophotographic plates are Kodak 103ao with a size  $16cm \times 16cm$ .

Table 8.1 shows the information of the plate, including their observed time, number, exposure time and site code. Table 8.2 shows the parameters and other details about the two telescopes used. They are called as Telescope A, situated in Yunnan Astronomical Observatory and Telescope B, equipped in Tsingtao Observatory.

## 8.3 Digitization

In the work of Vicente (Vicente et al, 2007 [23]) in 2007, the commercial scanner has been used in astronomical forthputting. There are two advantages for plates digitization that it not only protect those precious plates away from damage in the transform, but also improve the possibility to remeasure the old observations.

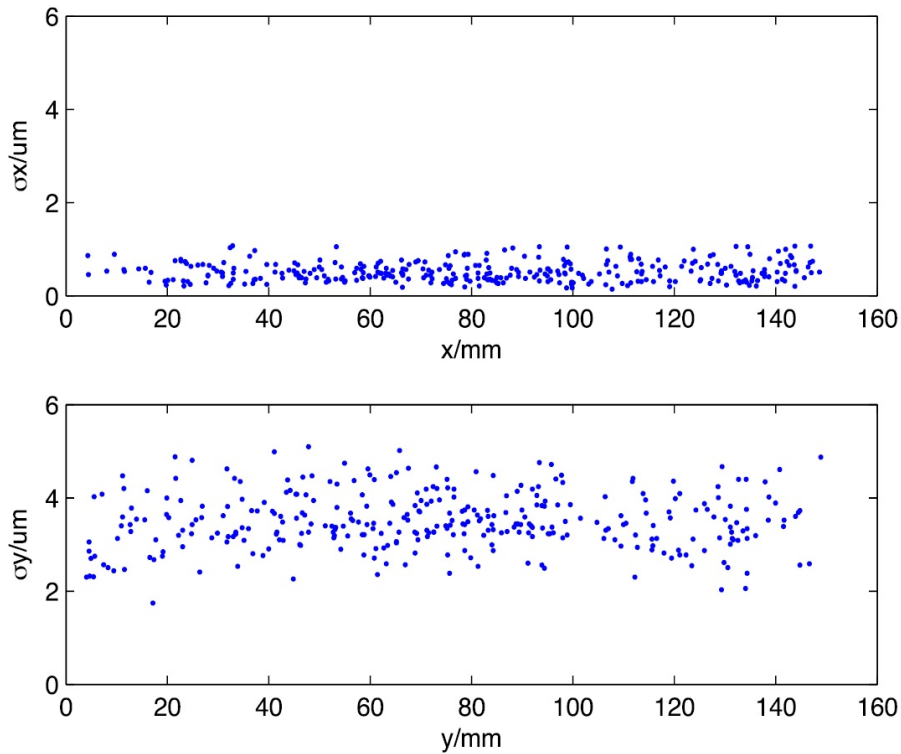
### 8.3.1 Scanner

We take the advanced commercial scanner EPSON 10000 XL in our work, which is equipped with a linear CCD camera with an optical resolution of up

to 2400 dpi, and the maximum scanning dimensions are  $31.0\text{cm} \times 43.7\text{cm}$ . In order to evaluate the accuracy and stability of the scanner for astronomical purposes, we take a plate of Uranian satellites as an example to scan repeatedly 10 times. Each time, we make a record of measurement results and obtain the standard deviation of the residuals of measured coordinates  $X$  and  $Y$  for all stars on the plate.

Figure (8.1) shows the standard deviations of residuals in  $X$  and  $Y$ , expressed in  $\mu\text{m}$ . Here,  $X$ - and  $Y$ -axis correspond to the scanning and linear CCD directions. The values of the mean standard deviations are  $0.58 \mu\text{m}$  in the linear CCD direction ( $X$ ) and  $3.71 \mu\text{m}$  in the scanning direction ( $Y$ ).

Figure 8.1: The standard deviations of residuals in  $X$  and  $Y$ , expressed in  $\mu\text{m}$ , for each star on the plate, versus the corresponding star coordinates, expressed in mm. The measured coordinates  $X$  and  $Y$  correspond to the linear CCD and the scanning direction, respectively

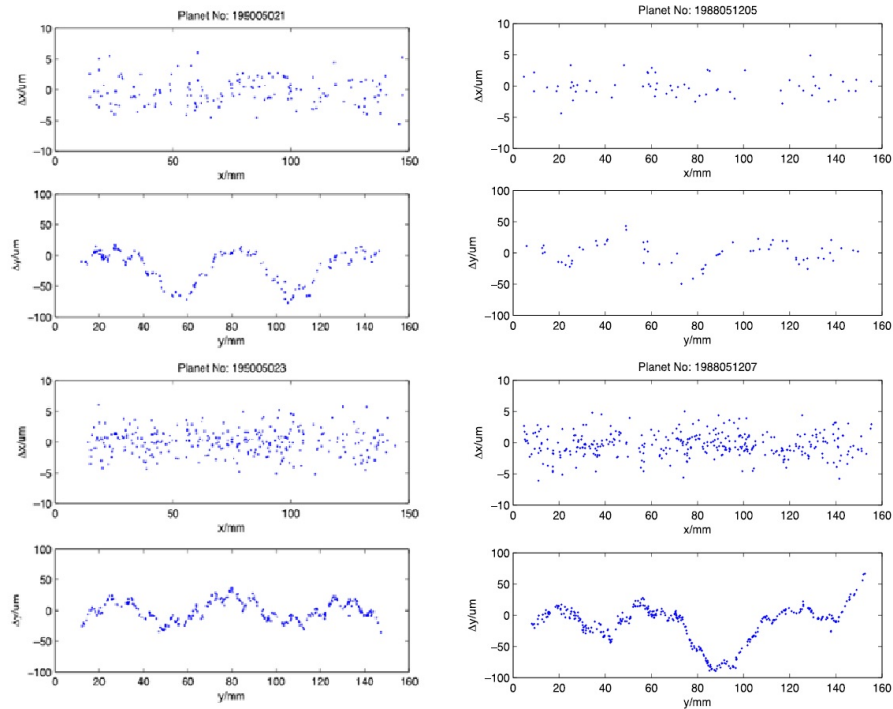


An accuracy as  $0.58 \mu\text{m}$  in the CCD direction is equivalent to the precision most photometric data system (PDS) measuring machines. For Telescope A, it corresponds like 8 mas system error, and same for Telescope B corresponding a value as 30 mas. While  $3.17 \mu\text{m}$  takes about 60 mas for

Telescope A and 200 mas for Telescope B.

Think of the accuracy of the catalogue UCAC4 used, which is 15 – 100 mas in position and about 1 to 10 mas/yr in proper motion depended on the magnitude of target (Zacharias et al. 2013 [20]), it means that the old observations which were taken 10 years earlier than the mean epoch of UCAC4, the derived accuracy of reference stars on plate is 30 – 100 mas in generally. Thus the scan precision in linear CCD direction (X) is equivalent to the catalogue accuracy, in other words, the scan precision in the scanning direction (Y) has an additional error as 60 mas for Telescope A and 200 mas for Telescope B.

Figure 8.2: Measured coordinate differences ( $\Delta X$ ,  $\Delta Y$ ), expressed in  $\mu m$ , versus star measured coordinates, expressed in millimetres, for four different plates. Differences are derived from the comparison of measured coordinates obtained at  $0^\circ$  and at  $180^\circ$  orientation of plates.



Moreover, in order to confirm this systematic errors, we take other 4 plates into experiments (2 of Saturnian satellites and 2 of Uranian satellites), both obtained with 1.0 meters telescope(A). The scanning result at  $0^\circ$  and at  $180^\circ$  orientation of plates, shows that the derived position of objects in X-axis, so-called  $\Delta X$  seems has an average arrangement and without any characteristic difference from one plate to another, in contrast, the  $\Delta Y$  ap-

pears a periodic changing in value without any consistency in all the plates. Figure (8.2) shows Measured coordinate differences ( $\Delta X$ ,  $\Delta Y$ ), expressed in  $\mu m$ , versus star measured coordinates, expressed in millimetres, for four different plates. And we also give the Standard deviations of residuals for the reference stars derived from measured coordinates obtained in the initial plate position  $A(XA_i, YA_i)$  and in the  $90^\circ$  rotated position  $B(XB_i, YB_i)$ .

Consequently, the system error comes from the non-linear movement of the camera that a significant error could influence our results very much. In order to avoid that, we prefer to measure both of each coordinate in the linear CCD direction, which means we will scan two times for every plate. In the first time we take a normal scan, and the second time the plates should be turning  $90^\circ$  in the horizontal direction to scan again. We could see the Table 8.3 of the standard deviations of residuals for the reference stars derived from measured coordinates obtained in the initial plate position  $A(XA_i, YA_i)$  and in the  $90^\circ$  position  $B(XB_i, YB_i)$ . Actually, it is in the next section. It proves that our method to deal with system non-linear movement error works well.

## 8.4 Reduction

As previously noted, each plate is scanned and measured in two orientations: first in an initial position A, and then, after being rotated by  $90^\circ$ , in position B. Hence for every object in same plate  $(XA_i, YA_i)$  and  $(XB_i, YB_i)$  are the raw measured coordinates obtained in positions A and B. And  $(Xm_i, Ym_i)$  is the final position used which takes  $XA_i$  as  $Xm_i$  and  $XB_i$  as  $Ym_i$ . We give the standard deviations of the residuals ( $\sigma_\alpha$ ,  $\sigma_\delta$ ) in Table 8.3 of the four plates which we mentioned in the section Scanner as an example.

Here, we take UCAC4 catalogue as the source of our reference stars that the number of the theoretical reference star on our astronomical plates is about 100. Normally we have more than 20 reference stars. We test different polynomial models, from 1-order to 4-order in our primary experiments, and chose the third-order polynomial model with 20 parameters for the astrometric reduction of our plates cause of its better in the standard deviations of residuals than lower order model and equivalent with 4-order model.

Our third-order polynomial model are:

$$\begin{cases} \xi = ax + by + c + dx^2 + exy + fy^2 + gx^3 + hx^2y + ixy^2 + jy^3 \\ \eta = a'x + b'y + c' + d'x^2 + e'xy + f'y^2 + g'x^3 + h'x^2y + i'xy^2 + j'y^3 \end{cases} \quad (8.4.1)$$

where,  $(x, y)$  is the coordinate measured in plate,  $(\xi, \eta)$  is the tangential coordinate. The parameters in Equation (8.4.1) are determined by a least squares method involved with each plate.

Table 8.3: Standard deviations of residuals for the reference stars derived from measured coordinates obtained in the initial plate position  $A(XA_i, YA_i)$  and in the  $90^\circ$  position  $B(XB_i, YB_i)$ . The final measured coordinates, both obtained in the linear CCD direction  $X$ , are  $Xm_i = XA_i$  and  $Ym_i = XB_i$ .

Planet	Plate No.	$XA_i$	$YA_i$	$XB_i$	$YB_i$	$Xm_i$	$Ym_i$
		$\sigma_\alpha$	$\sigma_\delta$	$\sigma_\alpha$	$\sigma_\delta$	$\sigma_\alpha$	$\sigma_\delta$
Saturn	1988051206	0.097	0.235	0.207	0.125	0.078	0.099
	1988051207	0.099	0.230	0.212	0.111	0.089	0.096
Uranus	199005041	0.150	0.265	0.229	0.179	0.149	0.165
	199005042	0.129	0.261	0.214	0.207	0.114	0.195

Table 8.4: An extract from the list of the observed equatorial coordinates of satellites obtained here. They are topocentric and referred to the J2000 ICRF reference frame. Satellite positions published for the first time are marked with an asterisk (\*).

Satellite	Date(UTC)	$\alpha$ (hour)	$\delta$ ( $^\circ$ )	Site code
$J_1^*$	1987 10 12.6524	1.6210670	8.4211902	286
$J_3^*$	1987 10 12.6524	1.6192411	8.4050179	286
$J_4^*$	1987 10 12.6524	1.6136393	8.3697619	286
$J_1^*$	1987 10 12.6667	1.6209710	8.4209216	286
$J_3^*$	1987 10 12.6667	1.6190649	8.4040104	286
$S_4^*$	1987 03 10.8574	17.3554323	-21.5912262	334
$S_5^*$	1987 03 10.8574	17.3534350	-21.5813007	334
$S_6^*$	1987 03 10.8574	17.3573388	-21.5826703	334
$S_7^*$	1987 03 10.8574	17.3545894	-21.6164870	334
$S_8^*$	1987 03 10.8574	17.3482055	-21.5444788	334
$S_3$	1988 05 11.7473	18.1412027	-22.2593249	286
$S_4$	1988 05 11.7473	18.1411854	-22.2690415	286
$S_5$	1988 05 11.7473	18.1411809	-22.2722384	286
$S_6$	1988 05 11.7473	18.1412198	-22.2418412	286
$S_3$	1990 05 1.7785	18.6963371	-23.3993310	286
$U_4$	1990 05 1.7785	18.6973951	-23.4114706	286
$U_2$	1990 05 1.8236	18.6971497	-23.4014725	286
$U_3$	1990 05 1.8236	18.6962945	-23.3991543	286
$U_4$	1990 05 1.8236	18.6973358	-23.4116925	286

## 8.5 New observed satellite astrometric positions

We present and renew 125 astrometric satellite positions from 27 plates, which were taken from 1987 to 1990, including 39 satellite positions that have never been published before, seems with some technique reason they did not be recognized at previously. <sup>1</sup>

We present part of the new observed positions in Table 8.4. The first column is the name of the satellites, in which for short we show them as the capital initial of the planet plus satellite number. Hence  $J_1$  means Io,  $S_6$  means Titan, and so on. The positions which are published for the first time have been marked with asterisk These data are topocentric and refer to the J2000.0 ICRF reference frame.

## 8.6 Comparison with theory

In following, we'd better compare all the position obtained from the old plates with their theory positions. We used planetary and satellite ephemerides available on the online server of the IMCCE, with DE431 planets ephemeris, for the Galilean satellites and Saturnian satellites with NOE (Lainey.V et al. 2004a, 2004b [3], and [4]), and Uranian satellites with ephemeris of Emelyanov (Emelyanov.NV and Nikonchuk.DV 2013 [24]).

We obtain the mean  $\mu$  and standard deviations  $\sigma$  of both coordinate for each mission with every satellite, that exhibit in Table 8.5. When the number of position is less than 2, it dose not exist Standard deviations. The mean residuals of major satellites of Saturn, Jupiter and Uranus in Table 7 appear to lower than 100 mas, except Mimas and Hyperion, which have a less accurate ephemerides than the other. And also we find that the mission obtained on Tsingtao Observatory (1987 March) show a less accuracy, up to 400 mas, cause of the smaller diameter and focal length (32 cm, 3.58 m) of Telescope B.

---

<sup>1</sup>The data are available as Supplementary Material to the online version of the paper on Blackwell Synergy, at the CDS via Anonymous FTP to cdsarc.u-strasbg.fr, or via <http://cdsweb.u-strasbg.fr/Abstract.html>.

Table 8.5: Mean residuals  $\mu$  and standard deviations  $\sigma$  of the residuals of “O-C”. N is the number of observed satellite positions.

Mission	Site code	Satellite	N	$\mu_\alpha(^{\circ})$	$\mu_\delta(^{\circ})$	$\sigma_\alpha(^{\circ})$	$\sigma_\delta(^{\circ})$
1987 Mar	334	S4	2	0.393	-0.009		
		S5	2	0.107	0.026		
		S6	2	-0.370	0.224		
		S7	2	0.430	-0.182		
		S8	2	-0.199	0.112		
		Total 1	10	0.072	0.034		
1987 May	286	S2	4	0.128	0.132	0.235	0.091
		S3	8	-0.027	0.088	0.138	0.080
		S4	8	-0.031	0.010	0.118	0.140
		S5	8	-0.098	0.105	0.149	0.091
		S6	8	-0.060	0.125	0.125	0.114
		S7	5	0.080	-0.091	0.144	0.214
		S8	8	-0.109	0.135	0.122	0.126
		Total 2	49	-0.035	0.077	0.133	0.116
1988 May	286	S1	1	0.475	0.066		
		S2	5	-0.069	-0.092	0.196	0.193
		S3	6	0.033	-0.001	0.076	0.109
		S4	6	0.055	-0.104	0.044	0.101
		S5	6	0.073	-0.037	0.053	0.125
		S6	6	0.039	-0.085	0.033	0.101
		S7	1	0.047	-0.152		
		S8	2	0.024	0.128		
		Total 3	33	0.043	-0.050	0.113	0.121
1987 Oct	286	J1	2	-0.060	-0.175		
		J2	1	0.158	0.092		
		J3	3	0.084	0.100	0.330	0.199
		J4	3	-0.133	-0.026	0.182	0.195
		Total 4	9	-0.012	-0.013	0.211	0.193
1990 May	286	U1	4	0.058	-0.094	0.244	0.180
		U2	4	-0.048	0.020	0.330	0.516
		U3	8	-0.081	-0.008	0.226	0.155
		U4	8	0.019	-0.016	0.280	0.237
		Total 5	24	-0.019	-0.020	0.248	0.251



## 8.7 Conclusion

In total, the new observed satellite positions present a good accuracy much better than previous, even though it is same as the accuracy of recent CCD observations of natural satellites. In the other word, the old observations digitization and remeasurement could improve the precision of satellites position that with the modern catalogue, there exist more reference stars in same plate field. It should explain why it is so important to reduce old plates of natural satellites again, either from original measurements when available, which is very rare or from new measurements, as those presented here.

We are glad to propose a reliable method for the measurement and reduction of astrophotographic plates. Moreover, we will go on our digital work with a special science scanner equipped in Shangai, Sheshan station. We would like to contribute to the ambitious project of the new measurement and reduction of all old Chinese plates.



## Chapter 9

# Conclusion

In my thesis, I attempted to establish a connection between theoretical ephemerides and ephemerides resulting from numerical integration. If we manage to avoid the shortcoming of the limited interval, we obtain the characteristics of the system like the proper frequencies. This task is very useful for theoretical studies, e.g. the study of the rotation of the natural satellites.

In the case of orbital motion, we can expand the perturbing function as a function of the osculating elements, in order to use the Lagrange equations or their equivalent in Hamiltonian form. Moreover, from Laskar's work, the proper frequencies for a complex system can be obtained with an approximate motion. Therefore it is possible to obtain the proper frequencies and the representation of a numerical ephemeris. We use both the frequency analysis and the least squares methods in our calculations.

We can compare the JPL and TASS ephemerides from the understanding of the analytical theory and the proper frequencies. We take the ephemeris of Titan as a reference example. We compare two types of Titan ephemerides, in osculating Keplerian elements and positions, over 1,000 years. Moreover, we focus on the 200 years interval around the J2000.0 epoch, during which the ephemerides have the highest precision. It is clear that in the 1900-2100 interval these differences remain stable.

Varying the ephemeris timespan has no effect on the determination of the mean mean motion. However, it influences the values of the constant term  $\lambda_0$  in the mean longitude such as  $\lambda_{T10} = 5.71887846$  rad and  $\lambda_{J1}$  equals to 5.71749214 rad. After a careful analysis, in the goal of obtaining the remaining periodic part  $r$  in the JPL ephemeris, we use  $\lambda_{T10}$  from TASS as the mean longitude at the J2000,0 epoch  $\lambda_0$ , which is obtained from TASS-t.

To get a test representation of the mean longitude of Titan, we use TASS ephemeris on a limited interval of 1,000 years.

The limited interval influences the proper frequency values. In summary, long period terms such as  $-\Omega_6^*$ ,  $-\Omega_8^*$ ,  $-\varpi_8^*$  and  $-\varpi_6^*$ , are more affected, while

short period terms like  $\lambda_s, \lambda_6$  and  $\lambda_5$  are almost unaffected. So, we choose the corresponding values obtained for the least squares procedure to get TASS-s the representation of the mean longitude of Titan of TASS over 1,000 years only.

Finally, we repeat our work with the JPL ephemeris which is limited to 1,000 years. We obtain the proper frequencies and the representation of the corresponding mean longitude of Titan. The difference between our representation and the JPL ephemeris is less than 100 kilometers over 1,000 years. Therefore, in practice, our formula can be used to get an accurate estimate of the value of the mean longitude of Titan, for example, for the study of the rotation of Titan.

Our work will be completed by a similar analysis of the other orbital elements from JPL ephemerides (semi-major axis, longitude of the pericenter, longitude of the ascending node..) in order to have a complete ephemeris of Titan. Our method could also be applied to other Saturnian satellites, and moreover, using other numerical ephemerides like NOE.

# Chapter 10

## Appendix

The solution of TASS is taken as reference all along the manuscript. So we give here the solution for Titan. As the short period terms in TASS have not the form of series with the exact proper frequencies, we do not give the original form. We give the result of the frequency analysis of TASS version 1.6 over 10,000 years. The elements used are in the ring plane. It is named **TASS-t** (template of TASS). So TASS-t corresponds to TASS concerning the precision, but the representation uses the proper frequencies.

We give also the series for the elements of Iapetus  $z_8$  and  $\zeta_8$ .

### 10.1 Appendix 1

Table 10.1: Mean motion of Titan  $p_6$ . The series is in cosine, and  $N$  in use in TASS.

$n^\circ$	Frequency (rad/year)	Amplitude (rad)	(km)	Phase (rad)	Period (year)	Id
1	-0.000000000000	0.0001348090	164.719073	3.14159265	**	**
2	364.085272884288	0.0000251406	30.718545	-2.36335826	0.02	$\lambda_5^* - \lambda_6^*$
3	694.586823068935	0.0000123408	15.078853	-0.18685101	0.01	$\lambda_4^* - \lambda_6^*$

Table 10.2: The mean longitude of Titan in the ring plane of Saturn,  $\lambda_6 = N \times t + \lambda_0 + r_6$ .  $N = 143.924047285569$  rad/y,  $\lambda_0 = 5.718878462$  rad. The series is in sine.

$n^\circ$	Frequency (radian/year)	Amplitude (radian)	(km)	Phase (radian)	Period (year)	Id
1	0.00192554369	0.0014891848	1819.590232	-1.76176914	3263.24	$-\Omega_8^*$
2	0.008931239596	0.0006277976	767.087054	0.34279510	638.38	$-\Omega_6^*$
3	0.4265982410156	0.0002064532	252.258971	-1.15851073	14.73	$2\lambda_s^*$
4	0.213299120062	0.0001839936	224.816260	2.41533633	7.37	$\lambda_s^*$
5	0.006867993783	0.0000320522	39.163622	2.55841019	914.85	$\Lambda_6^*$
6	0.639897360242	0.0000291064	35.5642370	-1.91809699	9.82	$3\lambda_s^*$
7	0.017867728608	0.0000278284	34.002687	2.44323143	351.65	$2\varpi_6^*$
8	364.085272881417	0.0000120882	15.740789	0.77823556	0.02	$\lambda_5^* - \lambda_6^*$
9	0.003851087124	0.0000098618	12.049836	-0.38528668	1629.82	$2\Omega_8^*$

Table 10.3: Eccentricity and the pericenter of Titan :  $e_6 \cdot e^{\sqrt{-1}\varpi_6}$ . The series is in complex exponential.

$n^\circ$	Frequency (radian/year)	Amplitude (radian)	(km)	Phase (radian)	Period (year)	Id
1	0.008933864289	0.0289265365	35344.467153	2.86627922	703.30	$\varpi_6^*$
2	-0.008933959907	0.0001921234	234.749826	0.42638138	-703.29	$-\varpi_6^*$
3	0.417664365570	0.0000744656	90.987283	-0.72852474	15.04	$-\varpi_6^* + 2\lambda^*$
4	143.924047290026	0.0000668787	81.717077	-0.56432198	0.04	$\lambda_6^*$
5	0.007008286694	0.0000242939	29.68398759	-1.64598798	896.54	$\varpi_6^* + \Omega_8^*$
6	0.010859401773	0.0000239166	29.222976	-2.06132503	578.59	$\varpi_6^* - \Omega_8^*$
7	0.001974774505	0.0000172066	21.024228	-2.82136616	3181.72	$\varpi_8^*$
8	508.009320171889	0.0000101008	12.341865	0.21391389	0.01	$\lambda_5^*$
9	0.630963495932	0.000096035	11.734229	-1.47873726	9.96	$-\varpi_6^* + 3\lambda^*$

Table 10.4: Inclination and the ascending node of Titan:  $\sin \frac{i_6}{2} \cdot e^{\sqrt{-1}\Omega_6}$ . The series is in complex exponential.

$n^\circ$	Frequency (radian/year)	Amplitude (radian)	(km)	Phase (radian)	Period (year)	Id
1	-0.000000000000	0.0056023641	**	-3.06168702	**	**
2	-0.008931239594	0.0027899429	3408.947531	-0.25711520	-703.51	$\Omega_6^*$
3	-0.001925543576	0.0001312363	160.3536979	-1.27742697	-3263.07	$\Omega_8^*$
4	0.426598241223	0.0001125670	137.542240	2.04979896	14.73	$2\lambda_s^*$
5	-0.213299120064	0.0000191667	23.419216	0.82899234	-29.46	$-\lambda_s^*$
6	0.639897360235	0.0000149794	18.302879	1.30207992	9.82	$3\lambda_s^*$
7	0.213299120067	0.0000114462	13.985768	2.28081791	29.46	$\lambda_s^*$
8	-0.006831187831	0.0000110589	13.512538	-2.60258392	-919.78	$2\lambda_j^* - 5\lambda_s^*$
9	-0.003851087191	0.000094698	11.570865	-2.63456161	-1631.54	$2\Omega_8^*$

Table 10.5: Eccentricity and the pericenter of Iapetus :  $e_8 \cdot e^{\sqrt{-1}\varpi_8}$ . The series is in complex exponential.

$n^\circ$	Frequency (radian/year)	Amplitude (radian)	(km)	Phase (radian)	Period (year)	Id
1	0.001974690829	0.0293564806	104533.143250	-2.88504171	3181.86	$\varpi_8^*$
2	0.00000000173	0.0010160948	**	-1.17634332	**	**
3	0.008933864351	0.0009953583	3544.291742	-0.27290481	703.30	$\varpi_6^*$
4	-0.001974690013	0.0007357199	2619.766134	-0.28684911	-3181.86	$-\varpi_8^*$
5	-0.003900230657	0.0006699057	2385.413615	-1.60817645	-1610.98	$-\varpi_8^* + \Omega_8^*$
6	143.924047287379	0.0005937571	2114.262157	-0.56432011	0.04	$\lambda_6^*$
7	0.003900234199	0.0004151871	1478.406529	-1.46121687	1610.98	$\varpi_8^* - \Omega_8^*$
8	0.424623422946	0.0003789230	1349.276597	-1.32845238	14.80	$\varpi_8^* + 2\lambda_s^*$
9	-86.067002634140	0.0002637298	939.094346	1.93136965	-0.07	$-\lambda_6^* + 2\lambda_8^{*??}$

Table 10.6: Inclination and the ascending node of Iapetus:  $\sin \frac{i_s}{2} \cdot e^{\sqrt{-1}\Omega_s}$ . The series is in complex exponential.

$n^\circ$	Frequency (radian/year)	Amplitude (radian)	(km)	Phase (radian)	Period (year)	Id
1	0.00000000013	0.1320165341	**	-3.06166175	**	**
2	-0.001925543543	0.0679455002	241941.696022	-1.27380978	-3263.07	$-\Omega_8^*$
3	0.001925548274	0.0006892422	2454.274532	1.43655002	3263.06	$\Omega_8^*$
4	-0.008931561444	0.0002730339	927.224572	2.895442360	-703.48	$\Omega_6^*$
5	0.426598229330	0.0002641112	940.452443	2.050845161	14.73	$2\lambda_s^*$
6	0.428523789410	0.0001816922	646.973220	-2.872882953	14.66	$-\Omega_8^* + 2\lambda_s^*$
7	-0.003850976252	0.0000457179	162.793213	-2.698421716	-1631.58	$2\Omega_8^*$
8	-0.213299120075	0.0000449442	160.038206	0.826999484	-29.46	$\lambda_s^*$
9	0.639897360224	0.0000337462	120.164144	1.303788709	9.82	$2\lambda_s^*$



# Bibliography

- [1] IMCCE. Imcce ephemeris web-interface, 2018.
- [2] JPL. Horizons web-interface, 2018.
- [3] V Lainey, L Duriez, and A Vienne. New accurate ephemerides for the galilean satellites of jupiter-i. numerical integration of elaborated equations of motion. *Astronomy & Astrophysics*, 420(3):1171–1183, 2004.
- [4] V Lainey, JE Arlot, and A Vienne. New accurate ephemerides for the galilean satellites of jupiter-ii. fitting the observations. *Astronomy & Astrophysics*, 427(1):371–376, 2004.
- [5] Planetary Science Communications team at JPL and GSFC of NASA. Radio science subsystem, 2018.
- [6] A Vienne and L Duriez. Tass1. 6: Ephemerides of the major saturnian satellites. *Astronomy and Astrophysics*, 297:588, 1995.
- [7] A Richard, N Rambaux, and B Charnay. Librational response of a deformed 3-layer titan perturbed by non-keplerian orbit and atmospheric couplings. *Planetary and Space Science*, 93:22–34, 2014.
- [8] R-M Baland, G Tobie, A Lefèvre, and T Van H. Titan’s internal structure inferred from its gravity field, shape, and rotation state. *Icarus*, 237:29–41, 2014.
- [9] J Laskar. Frequency analysis for multi-dimensional systems. global dynamics and diffusion. *Physica D: Nonlinear Phenomena*, 67(1-3):257–281, 1993.
- [10] CF Peters. Numerical integration of the satellites of the outer planets. *Astronomy and Astrophysics*, 104:37–41, 1981.
- [11] JD Giorgini, DK Yeomans, AB Chamberlin, PW Chodas, RA Jacobson, MS Keesey, JH Lieske, SJ Ostro, EM Standish, and RN Wimberly. Jpl’s on-line solar system data service. In *Bulletin of the American Astronomical Society*, volume 28, page 1158, 1996.

- [12] L Duriez. A general planetary theory in elliptical heliocentric variables. 1979.
- [13] J Laskar. Accurate methods in general planetary theory. *Astronomy and Astrophysics*, 144:133–146, 1985.
- [14] JL Simon and P Bretagnon. A motion theory for jupiter and saturn over a 6000 yr span solution jason84. *Astronomy and Astrophysics*, 138:169–178, 1984.
- [15] J Laskar, C Froeschlé, and A Celletti. The measure of chaos by the numerical analysis of the fundamental frequencies. application to the standard mapping. *Physica D: Nonlinear Phenomena*, 56(2-3):253–269, 1992.
- [16] Jacques Laskar. The chaotic motion of the solar system: A numerical estimate of the size of the chaotic zones. *Icarus*, 88(2):266–291, 1990.
- [17] M Saillenfest. Représentation synthétique du mouvement des satellites de saturn. 2014.
- [18] VI Arnol'd. *Mathematical methods of classical mechanics*, volume 60. Springer Science & Business Media, 2013.
- [19] L Duriez. General planetary theory in elliptic variables. I-Expansion of the equations. *Astronomy and Astrophysics*, 54:93–112, 1977.
- [20] Norbert Zacharias, CT Finch, TM Girard, Arne Henden, JL Bartlett, DG Monet, and MI Zacharias. The fourth us naval observatory ccd astrograph catalog (ucac4). *The Astronomical Journal*, 145(2):44, 2013.
- [21] Jie Wu and Yong Zhang. The observations of satellites of saturn in 1988 and a comparison of the theory of the motion. *Publications of the Shaanxi Astronomy Observatory*, 11:31–33, 1988.
- [22] Rongchuan Qiao, Kaixian Shen, and Xuefang Zhang. Astrometric observations of the uranian satellites and a comparison with the theory. *Publications of the Shaanxi Astronomy Observatory*, 18:1–4, 1995.
- [23] B Vicente, C Abad, and F Garzón. Astrometry with carte du ciel plates, san fernando zone-i. digitization and measurement using a flatbed scanner. *Astronomy & Astrophysics*, 471(3):1077–1089, 2007.
- [24] NV Emelyanov and DV Nikonchuk. Ephemerides of the main uranian satellites. *Monthly Notices of the Royal Astronomical Society*, 436(4):3668–3679, 2013.

## RÉSUMÉ

---

Les éphémérides issues d'intégrations numériques qui peuvent être facilement téléchargées des sites de l'IMCCE ou du JPL, ont une très bonne précision pour les observations récentes. En même temps, un autre type d'éphémérides, celles analytiques comme TASS, décrivent en détail le système dynamique par une représentation en combinaison de fréquences propres.

Notre but est d'associer ces deux types d'éphémérides pour l'utiliser dans les études de la rotation des satellites naturelles. Cela signifie qu'il faut reconstruire des éphémérides à long terme et de haute précision montrant les caractéristiques du système comme les fréquences propres à partir des intégrations numériques. La principale difficulté est d'éviter l'intervalle de temps limité des éphémérides numériques.

Dans notre travail, nous partons de la représentation des éléments d'orbite de Titan sur 10 000 ans issues de TASS comme exemple et comme standard. Nous expérimentons comment obtenir les fréquences propres sur 1000 ans d'éphémérides de TASS, et comment obtenir la représentation analytique de la longitude moyenne de Titan sur cet intervalle limité. A cause de cette durée de 1000 ans, au lieu de l'analyse en fréquence, nous utilisons la méthode des moindres carrées, en particulier pour les termes à longue période.

L'efficacité et l'exactitude de l'ensemble de la méthode sont vérifiées en comparant les représentations de la longitude moyenne de Titan issue de TASS par la méthode des moindres carrées et par la représentation standard de TASS sur 10 000 ans.

Finalement et c'est ce qui importe, nous obtenons une représentation du mouvement de Titan pour les 1000 ans d'éphémérides du JPL. Il existe une différence de 60 km dans l'amplitude du terme principal entre les représentations du JPL et de TASS. Cette différence est considérée comme issue du système. L'intervalle de temps limité des éphémérides influence les fréquences propres et induit des erreurs dans les termes à longues périodes comme contenant la longitude du noeud de Titan. Pour toutes les autres composantes ou presque, leurs amplitudes et phases sont similaires à celles de TASS. L'erreur de représentation est inférieure à 100 km sur 1000 ans et la déviation standard est de 26 km environ.

## MOTS CLÉS

---

Éphémérides, Titan, Mécanique Céleste, Analyse en fréquence

## ABSTRACT

---

The ephemerides resulting from numerical integration, which are convenient to download from online service of IMCCE or Horizons of the JPL, have a very good precision on the fitting to recent observations. Meanwhile, analytical ephemerides like TASS describe in detail the dynamical system by a representation based on a combination of the proper frequencies.

We plan to use these two types of ephemerides in order to study the rotation of the natural satellites. It requires to rebuild a long-lasting and high precision ephemeris with proper frequencies based on the numerical integration ephemeris. The main difficulty is to avoid the shortcoming of the limited interval of the numerical ephemeris.

In our work, we use the representation of the orbital elements of Titan from the TASS ephemeris analyzed over 10,000 years as a reference example. We experiment to obtain the proper frequencies with the TASS ephemeris over 1,000 years only, and then to get the analytical representation of the mean longitude of Titan in this limited interval. Due to this 1000 years time span, we use the least squares method instead of the frequency analysis, especially for the long period terms.

The efficiency and exactness of the whole method are verified by comparing TASS representation of the mean longitude of Titan obtained by the least squares method with the 10,000 years reference example.

Finally and most importantly, we get the representation of the mean longitude of Titan from JPL ephemeris over 1,000 years. Between the solution of JPL and the representation of TASS, it exists a 60 km difference in the amplitude of the major component. This difference is considered as a system difference. The limited interval of the ephemeris modifies the proper frequencies, which leads to the error in the long period terms such as the one from the node of Titan. For almost all other components, their amplitudes and phases are similar to the relative terms from TASS. The error in our representation is less than 100 kilometers over 1,000 years and the standard deviation is about 26 kilometers.

## KEYWORDS

---

Ephemeris, Titan, Celestial Mechanics, Frequency analysis

